



**This electronic thesis or dissertation has been
downloaded from Explore Bristol Research,
<http://research-information.bristol.ac.uk>**

Author:

Ward, Juma R R

Title:

Exploring the microclot-driven pre-metastatic niche

live imaging studies in zebrafish larvae

General rights

Access to the thesis is subject to the Creative Commons Attribution - NonCommercial-No Derivatives 4.0 International Public License. A copy of this may be found at <https://creativecommons.org/licenses/by-nc-nd/4.0/legalcode>. This license sets out your rights and the restrictions that apply to your access to the thesis so it is important you read this before proceeding.

Take down policy

Some pages of this thesis may have been removed for copyright restrictions prior to having it been deposited in Explore Bristol Research. However, if you have discovered material within the thesis that you consider to be unlawful e.g. breaches of copyright (either yours or that of a third party) or any other law, including but not limited to those relating to patent, trademark, confidentiality, data protection, obscenity, defamation, libel, then please contact collections-metadata@bristol.ac.uk and include the following information in your message:

- Your contact details
- Bibliographic details for the item, including a URL
- An outline nature of the complaint

Your claim will be investigated and, where appropriate, the item in question will be removed from public view as soon as possible.

Exploring the Microclot-Driven Pre-Metastatic Niche

Live Imaging Studies in Zebrafish Larvae

By

JUMA WARD



School of Biochemistry
UNIVERSITY OF BRISTOL

A dissertation submitted to the University of Bristol in accordance with the requirements of the degree of DOCTOR OF PHILOSOPHY in the Faculty of Life Sciences.

DECEMBER 2022

Word count: 33,734

Abstract

During metastasis, many tumour cells move into the blood vessels of the host, where they can rapidly disperse to multiple sites within the body, distant from the primary tumour. Once these cells have reached the capillaries of a distant organ that might be suitable for the establishment of a secondary tumour, they must arrest and extravasate. The site of this arrest is known as the pre-metastatic niche. As the pre-metastatic niche develops, tumour cells recruit a range of host cells, including platelets and innate immune cells, which may then support cancer survival, extravasation and metastasis. The drivers and dynamics of these recruitment events are still unclear. Here, I have used human and zebrafish cancer cell grafts to develop a larval zebrafish model of the pre-metastatic niche. Taking advantage of the optical translucency of zebrafish larvae I investigate the roles of platelets, coagulation, and innate immune cells in the pre-metastatic niche using confocal live imaging.

I find that the presence of activated thrombocytes and fibrin leads to the recruitment of macrophages and neutrophils to cancer cells within the larval vasculature, and that the presence of these innate immune cells appears essential for cancer cell extravasation. Further, I discovered a link between fibrin association with cancer cells and the polarisation state of macrophages. Loss of fibrin appears to drive a pro-inflammatory, M1-like phenotype which inhibits metastatic behaviour in grafted cancer cells. My data show the importance of haemostatic pathways in metastasis and implicate innate immune cell interactions with fibrin and platelets as fundamental in this process, and so worth of further study as potential targets for clinical interventions in cases of metastatic cancer.

Acknowledgements

I would like to express my deepest gratitude to my supervisor, Prof. Paul Martin for his guidance, persistence and help, without which I would not have been able to complete this work.

I would also like to thank my labmates, past and present, for their support, ideas and friendship throughout this work. Their thoughts and advice have been indispensable for shaping this work throughout the years, and their camaraderie and friendship have created a positive and enjoyable lab to work in. So thank you; Anne, David, Esther, Fran, Jake, Kaiming, Lucy, Mark, Oscar, Paco, Terrence, Tim and Luke.

I would like to thank the Wellcome Trust, for their funding. The program directors, for their organisation. And all of the other Wellcome students, particularly my cohort, for their friendship and kindness throughout.

Finally, my family for their love and belief in me, and I would especially like to thank my partner, Georgina, for her support, kindness, and patience with me, particularly in the final stages.

Author's declaration

I declare that the work in this dissertation was carried out in accordance with the requirements of the University's Regulations and Code of Practice for Research Degree Programmes and that it has not been submitted for any other academic award. Except where indicated by specific reference in the text, the work is the candidate's own work. Work done in collaboration with, or with the assistance of, others, is indicated as such. Any views expressed in the dissertation are those of the author.

SIGNED:..... DATE:.....

Table of Contents

	Page
List of Tables	vii
List of Figures	viii
1 Introduction	1
1.1 The Innate Immune System	1
1.1.1 Haematopoiesis	1
1.1.2 Neutrophils	3
1.1.3 Macrophages	4
1.2 Haemostasis and Platelets	6
1.2.1 The Platelet Plug	6
1.2.2 The Coagulation Cascade	8
1.2.3 Platelets as Inflammatory Cells	9
1.2.4 Zebrafish Thrombocytes and Haemostasis	10
1.3 Cancer	12
1.3.1 The Primary Tumour Microenvironment	13
1.3.2 Invasion and Metastasis	20
1.3.3 The Pre-Metastatic Niche	20
1.4 Modelling Disease in Zebrafish	23
1.4.1 Innate Immunity in Zebrafish Larvae	23
1.4.2 <i>De Novo</i> Models of Cancer	25

1.4.3	Grafting Models of Cancer	27
1.5	Project Aims and Objectives	29
2	Materials and Methods	32
2.1	Zebrafish Lines and Husbandry	32
2.2	Cell Culture and Cancer Microinjection	33
2.2.1	Generation and Maintenance of Cell Lines	33
2.2.2	Microinjection of Cancer Cells into Zebrafish Larvae	34
2.3	Cloning	35
2.3.1	Plasmids	35
2.3.2	gDNA Extraction and Promoter Sequence PCR	36
2.3.3	Gateway Recombination and Golden Gate Assembly of Plasmids	36
2.4	CRISPR/Cas9 Directed Mutagenesis	37
2.4.1	Guide RNA Design	37
2.4.2	Assembly and Microinjection of Ribonucleoprotein complexes	38
2.4.3	gDNA Extraction and F0 Screening by Heteroduplex Gel Electrophoresis	38
2.5	Imaging	39
2.5.1	Live Imaging	39
2.5.2	Correlative Light and Electron Microscopy (Collaborators Techniques)	40
2.6	Image Analysis	43
2.7	Statistical Analysis	43
3	Characterising the Pre-Metastatic Niche	44
3.1	Introduction	44
3.2	Results	46
3.2.1	Human Cancer Cells	46
3.2.2	Characterising ZMEL cancer cell behaviours in the absence of a clot	58
3.2.3	Innate Immune Cells are Essential for Cancer Cell Extravasation	68
3.3	Discussion	72
3.3.1	Human Cancer Cells	72

3.3.2	ZMEL Cancer Cells	75
3.3.3	Innate Immune Cells are Required for Extravasation	77
4	Investigating the Mechanics of the Platelet-Driven Pre-Metastatic Niche	80
4.1	Introduction	80
4.2	Results	81
4.2.1	The innate immune response to laser-induced clotting	81
4.2.2	The Role of the Thrombocytic Plug in Innate Immune Recruitment	84
4.2.3	Fibrin is a Member of the Pre-Metastatic Niche in Zebrafish Larvae	87
4.2.4	Fibrin is Necessary for Cancer Cell Extravasation	91
4.2.5	Loss of Fibrin Drives a Pro-Inflammatory Response to Cancer Cells	96
4.2.6	Induction of a Pro-Inflammatory Phenotype Using a TLR7/8 Agonist Reduces Extravasation	102
4.3	Discussion	104
4.3.1	The Innate Immune Response to a Laser-Induced Thrombus	104
4.3.2	Fibrin is Required for the Recruitment of Pro-Metastatic Innate Immune Cells to the Pre-Metastatic Niche	106
5	CRISPR-Cas9 Targeted Knockout of Thrombocyte-Driven Immune Cell Recruitment	112
5.1	Introduction	112
5.2	Methods and Results	113
5.2.1	Towards a Tissue-Specific CRISPR Knockout in Thrombocytes	113
5.3	Discussion	122
6	Final Conclusions	124
	Bibliography	129

List of Tables

TABLE	Page
2.1 Zebrafish transgenic lines used	33
2.2 Plasmid Acknowledgements	35
2.3 Annealing Protocol	39
2.4 Automatic processing of TEM samples	42

List of Figures

FIGURE	Page
1.1 Platelet Activation	8
1.2 Human and Zebrafish Coagulation Cascade	11
1.3 Primary Tumour Microenvironment	19
1.4 Methodology for Investigating the Microclot-Driven Pre-Metastatic Niche	31
3.1 Optimising Imaging of Extravasated Cancer Cells	47
3.2 Live Imaging the Dynamics of a Human Cancer Cell Extravasating from a Zebrafish Vessel	48
3.3 Innate Immune Cells Interact with Human Cancer Cells	50
3.4 Human Cancer Cells Associate with Zebrafish Thrombocytes	51
3.5 Cancer Cells May Undergo Vasculogenic Mimicry	53
3.6 CLEM Further Reveals Host:Cancer Cell Interactions	55
3.7 Human Cancer Cells Interact Closely with Thrombocytes	57
3.8 ZMEL Cancer Cells Form Extensions and Extravasate Into the Surrounding Tissues	59
3.9 Extravasated Cancer Cells Undergo Mitosis	60
3.10 Macrophages interact directly with extravasating cancer cells	61
3.11 Macrophages occasionally phagocytose cancer cells	62
3.12 Host Neutrophils Interact With ZMEL Cancer Cells	64
3.13 Cancer Cells Use Contractile Extensions to Cluster	65
3.14 Clustered Cancer Cells Have Increased Macrophage Interactions and Extravasate More Frequently	67

3.15	Macrophages Are Required for Cancer Cell Extravasation	69
3.16	Neutrophils Are Required for Extravasation	71
4.1	Visualising the Formation of a Thrombocytic Plug in Zebrafish Larvae Following Laser Insult	82
4.2	Describing the Resolution of a Clot in Zebrafish Larvae	83
4.3	Thrombocytic Plugs Recruit Macrophages to Cancer Cells	84
4.4	Reperfusion Leads to Increased Neutrophil Interactions with Cancer Cells	86
4.5	Grafted Cancer Cells Induce the Conversion of Human Fibrinogen to Fibrin	89
4.6	Drug Treatments Allow Modulation of Clotting	90
4.7	Warfarin Inhibits Cancer Cell Extravasation	92
4.8	Warfarin Reduces Macrophage Recruitment	93
4.9	Ponatinib Treatment Increases Cancer Cell Extravasation	95
4.10	Warfarin Induces a Shift to a More Pro-inflammatory Phenotype	97
4.11	Morpholino Knockdown of <i>fga</i> Causes Significant Reduction of Cancer Cell Extravasation	99
4.12	Morpholino Knockdown of <i>fga</i> Causes Increased <i>tnfa</i> Expression	101
4.13	Resiquimod Causes an Inflammatory Phenotype and Reduces Numbers of Extravasation Events	103
5.1	Workflow for CRISPR Validation	116
5.2	Assembly of a Vector for Ubiquitous Expression of Multiple sgRNAs	117
5.3	Assembly of a Thrombocyte-Specific Cas9 Expression Vector	119
5.4	Injection of Constructs Leads to GFP Reporting of Cas9 Expression	121
6.1	Proposed Model	128

Abbreviations

AVJ arterio-venous junction

BrdU bromodeoxyuridine

CAF cancer-associated fibroblast

csf1r macrophage colony stimulating factor receptor

CHT caudal haematopoietic tissue

CLEM correlative light and electron microscopy

CSC cancer stem cell

CTC circulating tumour cell

CTLA4 cytotoxic T-lymphocyte-associated protein 4

CVP caudal vein plexus

dH₂O deionised water

DoC Duct of Cuvier

dpf days post fertilisation

ECM extracellular matrix

EdU 5-ethynyl-2'-deoxyuridine

EGFP enhanced green fluorescent protein

EMT epithelial-mesenchymal transition

FACS fluorescence-activated cell sorting

GPCR G-protein coupled receptor

hpf hours post fertilisation

hpi hours post injection

HSC haematopoietic stem cell

IFN γ interferon gamma

ISV inter-segmental vessel

itga2b integrin alpha 2b

LPS lipopolysaccharide

lyz lysozyme C

MET mesenchymal-epithelial transition

MHC major histocompatibility complex

MS-222 tricaine

mpeg1.1 macrophage-expressed gene 1

mpx myeloperoxidase

NET neutrophil Extracellular Trap

NK natural killer cell

nfsB nitroreductase

OCS open canalicular system

PAR protease-activated receptor

PCR polymerase chain reaction

PD-1 programmed cell death protein 1

PD-L1 programmed death ligand 1

PMN pre-metastatic niche

PSGL-1 P-selectin glycoprotein ligand-1

R848 resiquimod

RAG1 recombination-activating gene 1

RNP ribonucleoprotein

ROS reactive oxygen species

selp P-selectin

SNAP soluble N-ethylmaleimide-sensitive factor attachment protein

SNARE soluble N-ethylmaleimide-sensitive factor attachment protein receptor

SNP single nucleotide polymorphism

TEM transmission electron microscopy

TCR T-cell receptor

TF tissue factor

TGF β transforming growth factor beta

TLR toll-like receptor

TME tumour microenvironment

tnf α tumour necrosis factor alpha

TUNEL terminal deoxynucleotidyl transferase dUTP nick end labeling

TxA₂ Thromboxane A₂

VEGFR vascular endothelial growth factor receptor

vWF von Willebrand Factor

Chapter 1

Introduction

1.1 The Innate Immune System

Innate immunity is largely mediated by motile immune cell lineages that are conserved across all jawed vertebrates and are capable of responding to a range of different stimuli such as wounds, infection or cancer. These cells, largely neutrophils and macrophages, are able to rapidly mount a protective response by reacting to general signs of damage or infection, such as the release of reactive oxygen species (ROS) (Weavers and Martin, 2020). To complement the innate immune response, cells of the adaptive immune system can develop specific responses to antigens produced by different pathogens and store this information. Upon re-exposure to the same antigens, adaptive immune cell populations can expand and quickly and efficiently neutralise the invader, often before it is able to cause any disease at all (Baumgarth, 2021; Muruganandah et al., 2018).

1.1.1 Haematopoiesis

Haematopoiesis is the process by which blood cells are formed. In mature mammals, multipotent haematopoietic stem cells (HSCs) reside within the bone marrow. These HSCs give rise to all of the cell types within the blood. To protect this essential niche from DNA damage, these cells are kept in a reversible quiescent state. Through a process of asymmetric cell division HSCs will produce myeloid and lymphoid progenitor cells, while maintaining a population of

stem cells within the niche (Loeffler and Schroeder, 2021). Myeloid and lymphoid progenitors are post-mitotic cells that are able to differentiate into many different cell types to maintain the various populations of blood cells within the body. Lymphoid progenitor cells give rise to the adaptive immune system, differentiating into natural killer cells (NKs), T cells and B cells (Kondo et al., 1997; Pellin et al., 2019; Velten et al., 2017). Myeloid derived cells include cells of the innate immune system, such as neutrophils and monocytes, which give rise to dendritic cells and macrophages (Akashi et al., 2000).

During development there are multiple conserved waves of haematopoiesis. Primitive haematopoiesis occurs early in development, before the stem cell niche has been established. This transient wave of embryonic haematopoiesis originates from the haemato-vascular mesoderm and gives rise to a range of primitive cell types, including early erythrocytes and a small population of monocytes (Ivanovs et al., 2017; Kennedy et al., 2007). In humans, primitive haematopoiesis occurs from 2 weeks post fertilisation until 8 weeks post fertilisation, at which time HSCs begin to seed the liver as an early haematopoietic niche (Tavian et al., 2001; Migliaccio et al., 1986).

1.1.1.1 Haematopoiesis in Zebrafish

Primitive haematopoiesis is conserved in zebrafish, occurring in 2 waves. As with humans, the first wave of primitive myeloid and erythroid cells are derived from the haemato-vascular mesoderm (Detrich et al., 1995). This occurs between 10 and 26 hours post fertilisation (hpf), with primitive macrophages found over the yolk sac around 17 hpf and the first erythroid cells entering the circulation at 24-26 hpf (Lieschke et al., 2002). A second wave of primitive haematopoiesis has been observed where erythromyeloid progenitor cells (EMPs), originating from the ventral wall of the haemogenic endothelium at 30 hpf, give rise to further erythroid and myeloid cells (Bertrand et al., 2007). EMP cells appear to give rise to erythroid cells, and to both macrophages and neutrophils (Bertrand et al., 2007). By 72 hpf, these transient EMPs can no longer be detected (Bertrand et al., 2007).

Definitive haematopoiesis in zebrafish, as in mammals, begins with a transient haematopoietic niche populated with HSCs (Kissa et al., 2008; Murayama et al., 2006). This is the liver in mammals and the caudal haematopoietic tissue (CHT) in zebrafish (Kissa et al., 2008; Murayama et al., 2006). These cells then migrate into a final niche where they persist until the end of development and through adulthood (Langenau et al., 2004; Bertrand et al., 2008). In zebrafish, the kidney is the equivalent of the bone marrow niche of mammals and gives rise to all further immune cells (Amatruda and Zon, 1999). The adaptive immunity of zebrafish is active from about 3 weeks post fertilisation, although T cells may be found within the thymus from about 4 days post fertilisation (dpf) (Hess and Boehm, 2012).

1.1.2 Neutrophils

Neutrophils are a highly abundant innate immune cell with important roles in infection, wound healing and cancer. The large number of neutrophils is maintained by a high rate of turnover, with around 10^{11} cells turned over each day (Dancey et al., 1976). These cells originate in the bone marrow of mammals and circulate within the blood vessels before extravasating to allow the tissues to be populated with neutrophils. Neutrophils are able to rapidly respond to signals of damage or infection and are the first immune cells to arrive at the site of inflammation (De Oliveira et al., 2016).

During an infection, neutrophils are able to contribute to the clearing of pathogens through phagocytosis, granule release and by use of neutrophil Extracellular Traps (NETs). Phagocytosis occurs when a neutrophil encounters a microorganism, recognises it using surface receptors and draws it intracellularly into a vacuole. Reduction of pH and release of digestive enzymes from granules into the phagocytic vacuole allow the neutrophil to eliminate its pathogenic cargo (Liew and Kubes, 2019). NETs are made up from the chromatin structures of neutrophil nuclei, forming a sticky network that can physically trap pathogens. This is especially important in the context of larger pathogens that are unable to be phagocytosed, NETs restrict the movement of the pathogen and bring it into close contact with antimicrobial produced by neutrophils (Mutua

and Gershwin, 2020). The process of NETosis is tightly regulated as it results in the death of neutrophils and NETs can cause thrombosis (Mutua and Gershwin, 2020).

Neutrophils also play important roles in wound healing, in part through their capacity to sterilise a wound after the breach of the barrier layer and invasion by opportunistic pathogens, but also as mediators of other immune cells. Neutrophils can release both pro- and anti-inflammatory molecules that may alter the response of macrophages and adaptive immune cells. When neutrophils are no longer required at the site of insult, they may apoptose. Macrophages in the region that phagocytose apoptotic neutrophils are pushed towards a less inflammatory phenotype, driving resolution of the wound (Voll et al., 1997; Marwick et al., 2018).

1.1.3 Macrophages

Macrophages are large, monocyte-derived cells present in much smaller numbers than neutrophils in most healthy adults. Macrophages have a diverse set of roles, ranging from protection from invading pathogens to orchestrating aspects of wound healing, to driving the proliferation of some blood cells (Kim and Nair, 2019; Pidwill et al., 2021; Li et al., 2021). For simplicity, macrophage phenotypes can be divided into two major categories; M1 classically activated, pro-inflammatory cells; and M2 alternatively activated, anti-inflammatory cells (Boutillier et al., 2021). A dynamic balance of these behaviours is necessary for normal immune responses and an over-abundance of either phenotype can lead to disease.

M1 macrophages are thought of as pro-inflammatory, expressing classic markers of inflammation such as $\text{TNF}\alpha$ and $\text{IL-1}\beta$ (Zhao et al., 2021). In this state, they may release inflammatory cytokines and ROS to help clear pathogens or destroy tumours (Cassetta and Kitamura, 2018; Beatty et al., 2011). They also act as the main phagocytic cells of the body; engulfing cell debris, micro-organisms or entire apoptotic or necrotic cells to prevent further damage during an inflammatory event (Hirayama et al., 2017). Overrecruitment and overstimulation of M1 macrophages can potentially lead to chronic inflammation and auto-immune disorders (Funes et al., 2018).

M2 macrophages play an anti-inflammatory role, tending to release factors that support tissues in the later stages of wound healing to allow proper re-epithelialisation (Gordon, 2003; Kim et al., 2019b). An inappropriate increase in M2 macrophages can prevent the effective clearance of infection or lead to macrophages supporting the growth of a tumour instead of recognising and attacking cancer cells (Tamura et al., 2018). Indeed, reprogramming macrophages to remain in a pro-inflammatory state may be a therapeutic strategy for killing cancer (López-Cuevas et al., 2022).

Further, plasticity of phenotype within macrophage populations appears important for proper control of wound healing. At early timepoints after an injury, an increase of tumour necrosis factor alpha (*tnf α*)-positive macrophages within the region is important for proper neoangiogenesis and vessel sprouting (Gurevich et al., 2018). However, if this population of pro-inflammatory macrophages persists then these nascent vessels are more leaky (Gurevich et al., 2018). Thus, precise timing of these phenotype switching events is essential for macrophage function.

Neutrophil-macrophage interplay is important in driving the development of an inflammatory event. Neutrophils are thought to respond to insult first, arriving quickly and using a wide range of factors to shape the landscape of the tissue, including releasing cytokines that attract macrophages (De Oliveira et al., 2016). The classical view of neutrophil behaviour is that once they have performed their functions within a wound site they will apoptose and be cleared by incoming macrophages however, neutrophils have also been observed migrating back to the vessels which appears to be mediated by macrophage arrival and signalling (Mathias et al., 2006).

1.2 Haemostasis and Platelets

Haemostasis is defined by the formation of a temporary clot that prevents bleeding from damaged blood vessels and protects tissues that might otherwise be exposed to the outside world. There are two main activation steps involved in haemostasis: primary haemostasis, the formation of a platelet plug; and secondary haemostasis, the coagulation cascade and formation of the fibrin clot (Gale, 2011).

1.2.1 The Platelet Plug

Platelets are the main haemostatic cell of the body. In the context of damage, there is a host of different stimuli that may cause the activation of platelets through their surface receptors, allowing them to respond in a variety of different damage scenarios (**Figure 1.1**). These stimuli can be split into two major pathways of activation, G-protein coupled receptors (GPCRs) and glycoproteins (Yun et al., 2016).

When blood vessels become damaged, the extracellular matrix (ECM) that supports the endothelial layer may be exposed to the blood. Platelet glycoproteins, especially GPVI, mediate binding to this ECM driving their activation through immunoreceptor tyrosine-based activation motif (ITAM) receptors (Perrella et al., 2021). Further, as the thrombus develops, shear force may increase in the region due to narrowing of the lumen space. This shear force may drive platelet activation through GPIb interactions with von Willebrand Factor (vWF), a very large multimeric protein released by platelets and endothelial cells upon damage (Goto et al., 1998).

Soluble factors are essential for driving platelet responses through GPCR signalling. P2Y purinergic receptors, such as P2Y₁ and P2Y₁₂, respond to nucleotides that may be released by immune cells, endothelial cells or other platelets (Gachet and Hechler, 2020). protease-activated receptor (PAR)1 and 4 are highly expressed GPCRs, activated by thrombin-mediated cleavage, allowing further linking of the coagulation cascade with platelet activation (Downes et al., 2022;

Jaberi et al., 2019). Thromboxane A₂ (TxA₂) is a member of the prostanoid lipid family, which also includes prostaglandins, released by a variety of cell lineages (Calde, 2020). Platelet production of TxA₂ is mediated by the aspirin responsive cyclooxygenase-1 (COX-1) enzyme (Mitchell et al., 2019; Lucotti et al., 2019).

Inactive platelets are small, cellular fragments with a discoid shape maintained by a marginal band of microtubules (Cuenca-Zamora et al., 2019). Upon activation, there is a rapid reorganisation of the cytoskeleton. First, platelets transition to a spherical shape, allowing easy access of granule contents to the plasma membrane (Seifert et al., 2017). Next, an irregular shape is generated by formation of dynamic, actin-based membrane extensions (Seifert et al., 2017). This extended shape aids in binding to key molecules in the formation of the plug. Once bound, platelets are able to generate contractile force, dramatically reducing the volume of a clot and creating a more stable structure (Sun et al., 2021). Platelet aggregation is mediated by cross-linking interactions between integrins on the surface of activated platelets and extracellular proteins, such as vWF and fibrinogen (McManama et al., 1986; Gralnick et al., 1985).

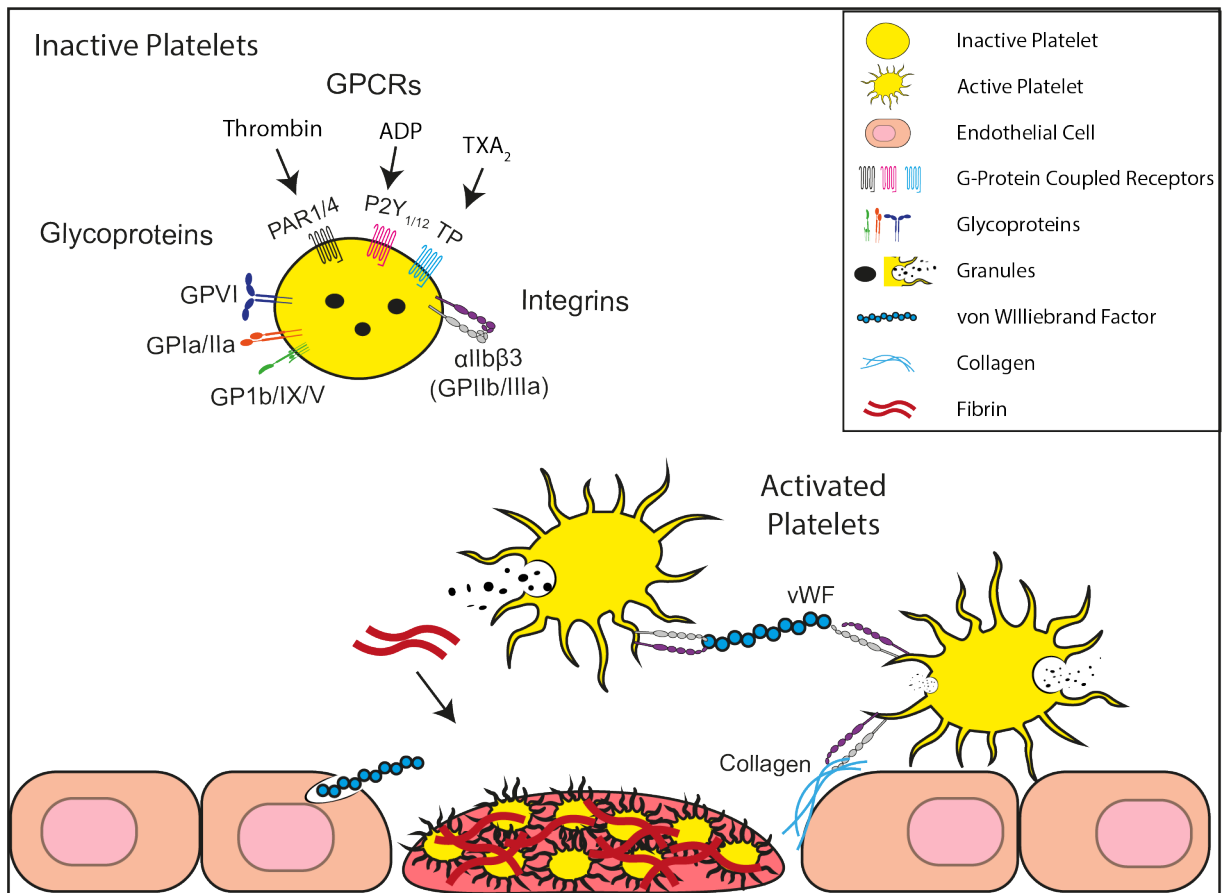


FIGURE 1.1. Platelet Activation Schematic representation of platelet activation. Surface receptors on platelets detect a range of signals for activation. Activated platelets undergo a dramatic shape change, release granule contents to signal to immune cells and propagate platelet activation. Damaged endothelial cells expose extracellular matrix and release von Willebrand factor allowing cross-linking of platelets and formation of the platelet plug.

1.2.2 The Coagulation Cascade

The coagulation cascade leads to the formation of fibrin from fibrinogen. Fibrin crosslinking causes the formation of a stiff gel that forms the bulk of a clot (Du et al., 2022). The coagulation cascade is made up of a series of clotting factors, found within blood plasma, ordinarily held in an inactive state by antithrombotic molecules expressed by endothelial cells (Neubauer and Zieger, 2022). The multi-stage cascade allows propagation, so that each factor may produce more of the next factor and allow the exponential increase of thrombin that is required for adequate

conversion of fibrinogen to fibrin (Macfarlane, 1964).

There are 3 classical pathways within the cascade: the extrinsic pathway, the intrinsic pathway, and the common pathway. The common pathway is the endpoint of the coagulation cascade, resulting in the conversion of fibrinogen (FI) to fibrin (FIa) by thrombin (FIIa) (Mackman et al., 2007). Thrombin is generated from prothrombin (FII) by FXa, which is activated by distinct forms of the tenase complex, resulting from either the extrinsic or the intrinsic pathway (Mackman et al., 2007).

The extrinsic pathway is initiated when circulating FVII is exposed to tissue factor (FIII), either released by damaged endothelial cells or exposed in stromal cells when the vessel is damaged. FVIIa and tissue factor form the extrinsic tenase complex and activate FX (Grover and Mackman, 2019). The intrinsic pathway begins with exposure of FXII to endothelial or stromal collagen, activating it (Grover and Mackman, 2019). From here, FXI is activated, which in turn activates FIX (Macfarlane, 1964; Davie and Ratnoff, 1964). FVIIIa, itself activated by thrombin, and FIXa form the intrinsic tenase complex (Grover and Mackman, 2019). As FV, FVIII and FXI are all activated by thrombin generated in the extrinsic pathway, the classical two-armed coagulation pathway has begun to be considered as a single, integrated pathway (O'Donnell et al., 2019).

1.2.3 Platelets as Inflammatory Cells

While platelets are most commonly associated with haemostasis, they also play important roles in inflammation. As previously mentioned, platelet granules contain cytokines, which recruit immune cells to the site of an injury (Ziegler et al., 2019). Platelet surface receptors, including P-selectin, also allow platelets and immune cells to interact (Evangelista et al., 1999). Platelet-neutrophil complexes form through P-selectin-PSGL1 interactions, recruiting neutrophils to sites of damage (Sreeramkumar et al., 2014). Subsequent release of the damage signal, HMGB1 from platelets can stimulate neutrophil NETosis, which, in turn, may further activate platelets (Maugeri et al., 2014).

Platelet activation has been recognised as an important pathological feature of severe acute respiratory syndrome coronavirus 2 (SARS-CoV-2) infection, with coronavirus disease 2019 (COVID-19) patients frequently exhibiting hyperinflammatory and hypercoagulable pathologies (Pavoni et al., 2020). Complexes between platelets and immune cells were seen more frequently in COVID-19 patients (Kanth Manne et al., 2020), and platelets from COVID-19 patients were seen to activate pathways associated with thromboinflammation in endothelial cells (Barrett et al., 2021).

Activated platelets have also been seen to induce anti-inflammatory phenotypes in innate immune cells. Platelet prostaglandin E₂ and CD40L may drive IL-10 expression and inhibit TNF α production in macrophages, leading to an M2-like phenotype (Linke et al., 2017; Gudbrandsdottir et al., 2013).

1.2.4 Zebrafish Thrombocytes and Haemostasis

Unlike mammals, zebrafish haemostasis is not characterised by anucleate, megakaryocyte-derived platelets. Instead, nucleated cells called thrombocytes are responsible for haemostatic plug formation and expression of the coagulation cascade (Jagadeeswaran et al., 1999). These thrombocytes are much larger than mammalian platelets, to accommodate their nucleus, and are derived directly from haematopoietic stem cells.

Extensive characterisation studies have been performed on zebrafish thrombocytes, revealing strong similarities with platelets in terms of functionality and expression patterns. Electron microscopy of zebrafish thrombocytes has, importantly, shown the presence of the open canalicular system (Jagadeeswaran et al., 1999). This system of channels through the membrane of platelets is thought to be important for the expansive shape changes that occur during activation, and for release of granule contents (Selvadurai and Hamilton, 2018; Behnke, 1967).

As a highly complex and essential process, coagulation has remained virtually unchanged

since the evolution of bony fish. The coagulation cascade in zebrafish has been shown to be highly conserved, with few apparent duplication events affecting the cascade (Hanumanthaiah et al., 2002). FIX, however, has 3 orthologues. Recently, the functions of these has been revealed, with *f9a* acting as the paralogue of FIX, while *fixl* appears to have activity more similar to human FX (Iyer et al., 2021).

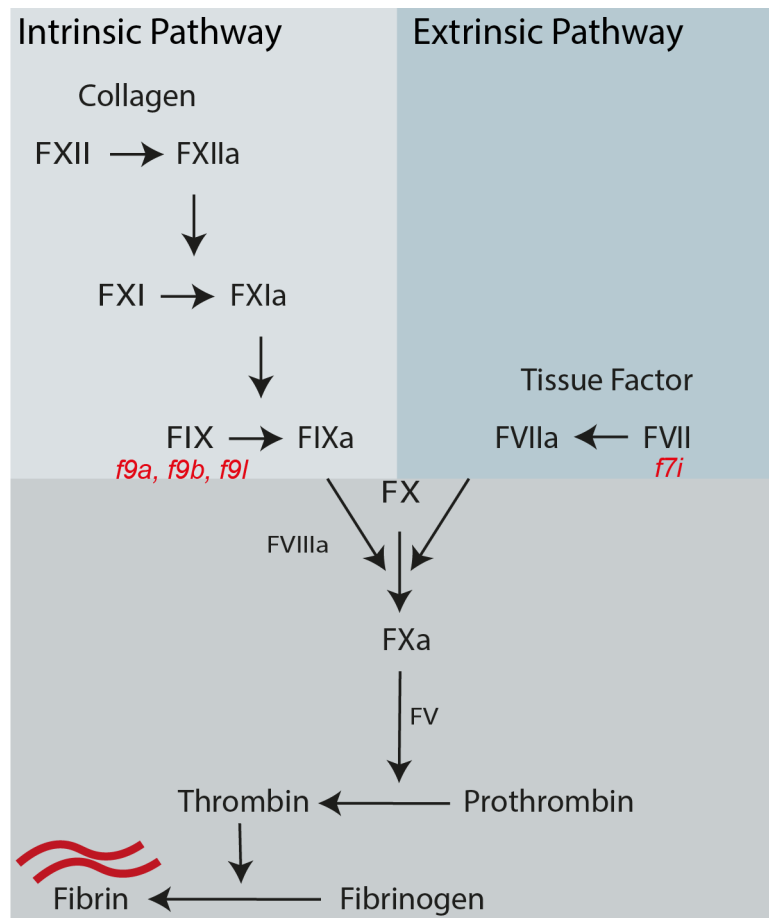


FIGURE 1.2. Human and Zebrafish Coagulation Cascade The extrinsic pathway initiates coagulation by exposure to tissue factor, generating a small amount of thrombin from prothrombin. This thrombin activity is sufficient to drive the Intrinsic pathway. Both pathways lead to formation of an active tenase complex with FX, which goes on to activate thrombin for the conversion of fibrinogen to fibrin. Zebrafish genes with known paralogues are highlighted in red.

Zebrafish respond to common antiplatelet drugs such as aspirin (Jagadeeswaran et al., 1999; Hortle et al., 2019). Coumadin derivatives, such as warfarin, have been shown to be effective at

preventing coagulation (Hanumanthaiah et al., 2001), as have heparins (Jagadeeswaran and Sheehan, 1999). Human fibrinogen has also been injected into zebrafish larvae and shown to be converted into fibrin that participates in zebrafish coagulation (Liu et al., 2014).

Early studies of zebrafish thrombocytes used DiI(C18) injections, which preferentially labels thrombocytes within the vasculature. These studies indicated two populations of thrombocytes: immature thrombocytes were not labelled with DiI at low concentrations, while mature thrombocytes were. Later, a fluorescent reporter line driven under integrin alpha 2b (*itga2b*) was generated, which also showed two populations, brighter and dimmer cells (Lin et al., 2005). Recently, these two populations have been characterised by comparative transcriptomics, revealing changes that occur during thrombocyte maturation. Additionally, this transcriptomic data has allowed comparisons with human megakaryocytes and platelets (Fallatah et al., 2022).

1.3 Cancer

Cancer is a disease of dysregulation. Cells acquire mutations within pathways that drive uncontrolled proliferation, leading to the acquisition of new mutations that further disrupt normal cellular behaviour (MacCarthy-Morrogh and Martin, 2020). Through selection pressures exerted by the surrounding environments, tumours trend towards increased proliferation and invasion. As the primary tumour grows, it must invade into the surrounding tissues to overcome the physical limits of its growth. Increased invasiveness generally comes with a shift towards more mesenchymal properties known as epithelial-mesenchymal transition (EMT) (Nieto et al., 2016). Eventually, some tumour cells break away from the primary tumour and use nearby blood and lymph vessels to travel to distant sites in a process known as metastasis (Bergers and Fendt, 2021). Here, they will undergo a mesenchymal-epithelial transition (MET) and establish a secondary tumour. Metastasis is responsible for more than 90% of all deaths attributed to cancer (Ribatti et al., 2020).

1.3.1 The Primary Tumour Microenvironment

1.3.1.1 Cancer Stem Cells

Tumour growth practically necessitates a developing and varied tumour microenvironment (TME) (Papanicolaou et al., 2022). As previously mentioned, newly acquired mutations lead to heterogeneity between cancer cells. These differences can lead to the development of multiple roles for cancer cells within a tumour. Some cells may be more pluripotent and take on the function of cancer stem cells (CSCs) (Al-Hajj et al., 2003). Early studies of CSCs indicated that only a small subpopulation of cells within a tumour could cause disease upon transplantation into a new mouse (Al-Hajj et al., 2003). This suggested that certain cells could be responsible for proliferation of the tumour, while others could be performing different roles, just like the difference between stem cells and differentiated cells within a healthy epithelium. More recently, lineage tracing in tumours has bolstered the evidence for these CSC behaviours, showing that expansion of a tumour comes from clones of stem-like cells (Maruno et al., 2021; Jia et al., 2022). Interestingly, cancer stem cells appear to show fewer neoantigens than other cancer cells within the tumour, allowing immune evasion and persistence of the niche within a tumour (Watanabe et al., 2022).

The identification of CSCs has also allowed markers of cancer stem-ness to be identified, allowing these cells to be specifically targeted (Watanabe et al., 2022). In murine tumours, depletion of CSCs often leads to a shrinkage of the tumour suggesting that CSCs may be a viable clinical target for anti-cancer therapies (Zhu et al., 2014). If removal of just the CSCs is sufficient to halt cancer progression, then removal of every mutant cell within a patient is not necessary for a cure; targeting CSCs more specifically could lead to improved outcomes in certain cases of cancer (Zhu et al., 2014).

Other cells within the tumour may be more adapted for invasion, allowing the tumour to extend beyond its boundaries or burrow through the basement membrane. This class of cell is one component of the microenvironment of a tumour and will change the signals that cells within

the tumour experience, influencing their behaviour.

1.3.1.2 Cancer-Associated Fibroblasts

Besides the influence of populations of cancer cells within the tumour itself, there are several host lineages that surround and support a tumour. Fibroblasts are cells that are situated close to an epithelial layer and are responsible for depositing ECM to provide structure and support for those cells. In recent years, it has been shown that fibroblasts are hijacked by tumours to become cancer-associated fibroblasts (CAFs) through signals including inflammatory cytokines and changes in ECM in the region (Sahai et al., 2020b). As CAFs, they can support the tumour metabolically through exchange of different amino acids and lactate (Bertero et al., 2019). Cancer cells frequently have a dysregulated metabolism, often relying on glycolysis for energy production in a process known as the Warburgh effect (Fu et al., 2017), and metabolite transfer with CAFs can help them to overcome some of the costs associated with these metabolic changes (Fu et al., 2017).

As fibroblasts are responsible for deposition of ECM in a healthy tissue, it is no surprise that CAFs can remodel ECM to benefit a tumour (Papanicolaou et al., 2022). Matrix composition and stiffness can alter the TME by changing immune infiltration, angiogenesis, and migration of cancer cells (Sahai et al., 2020a). Pancreatic cancer often leads to tumours with unusually high matrix stiffness, driven in part by CAFs in the stroma (Olive et al., 2009), which can reduce tumour infiltration by anti-tumour CD8+ T cells (Kuczek et al., 2019). The high matrix stiffness also increases mechanical forces acting on the tumour as it generates tension, these forces can stimulate mechanosignalling in tumour cells which have been associated with increased markers for stem-ness and EMT in tumours (Laklai et al., 2016). Furthermore, the unusual matrix composition of these tumours can reduce or change angiogenesis, resulting in poor perfusion within the tumour and preventing adequate drug delivery during chemotherapy (Annese et al., 2019; Provenzano et al., 2012).

CAFs are also known to secrete signalling factors that alter the tumour microenvironment. They may release **VEGF!** (**VEGF!**), leading to an increase of angiogenesis; and inflammatory cytokines such as IL-6 and transforming growth factor beta (TGF β), which can promote anti-inflammatory phenotypes in immune cells within the tumour (Philippeos et al., 2018; Koch et al., 2020).

1.3.1.3 Tumour Angiogenesis

As a tumour grows beyond 1-2 mm in size, it will require new vasculature to supply the abnormally large outgrowth of cells with oxygen and nutrients (Folkman, 1971; Lechertier et al., 2020). Cancer and host cells will detect the anoxic environment caused by increased metabolic load of the tissue and begin producing **VEGF!**, driving angiogenesis (Claffey et al., 1996). New vessels will sprout from existing vessels into the region of the tumour. Tumour vessels are known to be leakier than vessels in other tissues, meaning that cells inside the vessel have increased access to the tumour (Sweeney et al., 2019). This will lead to the microenvironment being more influenced by blood cells.

As an essential part of tumours expanding beyond a relatively small size, tumour angiogenesis has been targeted for anti-cancer therapies. Anti-**VEGF!** antibodies prevent cancer from signalling to endothelial cells to drive their growth and extension into the tumour microenvironment (Li et al., 2018). This treatment approach can slow tumour growth by limiting oxygen and nutrient delivery. However, it has been seen that this loss of angiogenesis increases necrosis within the core of a tumour, which can then lead to increased inflammation as immune cells respond to the necrosis, and potentially more aggressive invasion and metastasis (Wang et al., 2017).

Occasionally there are shortcomings in angiogenesis, potentially due to clinical treatment or other failures of the tumour. When this happens tumour cells themselves may undergo a process called vasculogenic mimicry (Maniotis et al., 1999; Silvestri et al., 2020). A subset of cancer cells within the tumour may overexpress VEGFR or VE-cadherin, allowing them to respond to the

need for more nutrient supply and form blood vessel-like structures (Hendrix et al., 2001; Xu et al., 2019). These structures can then invade and integrate into the existing, endothelial-derived vasculature and supply oxygen and nutrients to the tumour, as normal vessels would (Silvestri et al., 2020). The presence of vasculogenic mimicry within a tumour generally indicates a poor prognosis for patients (Cao et al., 2013).

1.3.1.4 Immune Landscape of the Primary Tumour

Inflammatory signals, such as TGF β and IL-6, released by CAFs and tumour cells recruit immune cells to the tumour. Immune infiltration can dramatically change the prognosis of a cancer, depending on the immune makeup of the niche (Mei et al., 2014; Denkert et al., 2018). CD8+ T cells can recognise and kill cancer cells (Raskov et al., 2021). CD8+ T cells are adapted to recognise cells carrying antigens and lyse those cells, these antigens can originate from a viral or bacterial infection and will bind to major histocompatibility complex (MHC) class I molecules before being transported to the plasma membrane to be presented. CD8+ T cells form a synapse with these cells, with a complex forming between the MHC, T cell receptor and CD8 (Mayya et al., 2019). This synapse brings the T cell close to the target cell so that it can use lytic granules to cause the death of the cell. The accumulation of mutations in cancer can lead to cancer cells expressing antigenic proteins, which may activate these cytotoxic T cells (Schumacher et al., 2019).

Cancer cells can subvert these killer T cells, leading to reduced cytotoxic activity and protecting the tumour (Lawson et al., 2020). One well studied method of immune evasion is the overexpression of programmed death ligand 1 (PD-L1). PD-L1 is the ligand for programmed cell death protein 1 (PD-1), which is expressed by T cells and B cells. Upon PD-1 signal activation, CD8+ T cells are driven towards apoptosis. This immune checkpoint is intended to prevent auto-immune diseases by essentially signalling to immune cells that another cell is "self". Cancer cells can overexpress PD-L1, overwhelming CD8+ T cells that may recognise cancer antigens and otherwise kill them (Diskin et al., 2020; Ambler et al., 2020). In recent years, antibodies

targeting PD-1 have entered the clinic as a cancer therapy. By blocking the receptor for PD-L1, cancer cells are less able to tailor the immune response to their benefit and are more likely to be killed by CD8+ T cells.

Other adaptive immune cells that may be found within the tumour microenvironment include CD4+ T cells. These can perform drastically different roles as T-helper cells, which facilitate the killing of tumour cells by activating T killer cells; or as regulatory T cells (Tregs), which suppress inflammation and are often associated with a poor prognosis in patients. CD4+ T-helper cells may be activated by antigen presenting cells or tumour cells directly, having been shown to recognise neopeptides produced by cancer cells (Linnemann et al., 2015). T-helper cell activation appears to be important for an effective and sustained immune responses from killer T cells, with cancer vaccines that target both CD4+ and CD8+ T cells having a marked benefit over those that only target CD8+ T cells (Bijker et al., 2007). This CD8+ activation by helper cells is mediated by release of IL-2 and IL-21 (Zander et al., 2019). T-helper cells can also have direct anti-tumour activity, releasing interferon- γ and other signalling molecules which can promote the death of cancer cells.

Tregs are a subset of Foxp3-expressing CD4+ T cells that are strongly anti-inflammatory (Sakaguchi et al., 2020). In recent years, Tregs have drawn focus in cancer research as a target for therapeutic intervention. Inhibition of Treg formation in animal models appears to have an anti-tumoural effect, allowing killer T cells to perform their proper functions in killing cancer cells (Shimizu et al., 1999; Maeda et al., 2019). Tregs have been shown to drive M2 phenotypes in macrophages, further exacerbating the anti-inflammatory effect within the tumour microenvironment (Hu et al., 2020).

Macrophages are often the most abundant immune cell within a tumour and have a range of activities that may influence the tumour microenvironment, including release of cytokines and growth factors, and matrix remodelling. Studies of patient tumours have frequently linked increased macrophage infiltration of a tumour with poor prognosis (Wang et al., 2019), and

blocking the recruitment of macrophages to the site of a tumour has been shown to reduce tumour growth (Lin et al., 2001).

As previously discussed, macrophages can have different behaviours depending on their polarisation (**Section 1.1.3**). M2 macrophages within the tumour microenvironment have been found to dampen the activity of CD8+ killer T cells (Peranzoni et al., 2018), and may also drive the differentiation of CD4+ T cells into Tregs, creating a positive feedback loop as Tregs also drive macrophages towards M2 phenotypes (Sun et al., 2017).

Macrophages are essential for proper angiogenesis through their secretion of VEGF and direct contacts with sprouting vessels (Salvesen and Akslen, 1999; Gurevich et al., 2018). Loss of macrophages within the tumour niche is associated with a reduction in neoangiogenesis and, subsequently, reduced tumour growth and progression (Lin et al., 2007). Further, direct contacts between cancer stem cells and macrophages, mediated by Eph-Ephrin interactions, activate NF- κ B in cancer stem cells and may help to maintain a stem-like niche within the tumour (Lu et al., 2014).

Conversely, M1 macrophages can perform anti-tumoural roles directly by release of cytotoxic ROS to kill tumour cells or by phagocytosis. Additionally, they can function indirectly by stimulation of lymphocytes to perform their own cytotoxic roles, through release of cytokines or presentation of antigens (Yin et al., 2021; Tang-Huau et al., 2018).

Similarly, neutrophils have multiple roles in the primary tumour, with N1 neutrophils having anti-tumour activity and N2 neutrophils having pro-tumour activity. High neutrophil to lymphocyte ratio within the circulation of patients is correlated with poor prognosis in the clinic (Shaul and Fridlender, 2019), and mice with carcinomas have increased N2 neutrophils, promoting an immunosuppressive state and pro-tumoural activity (Alshetaiwi et al., 2020; Casbon et al., 2015).

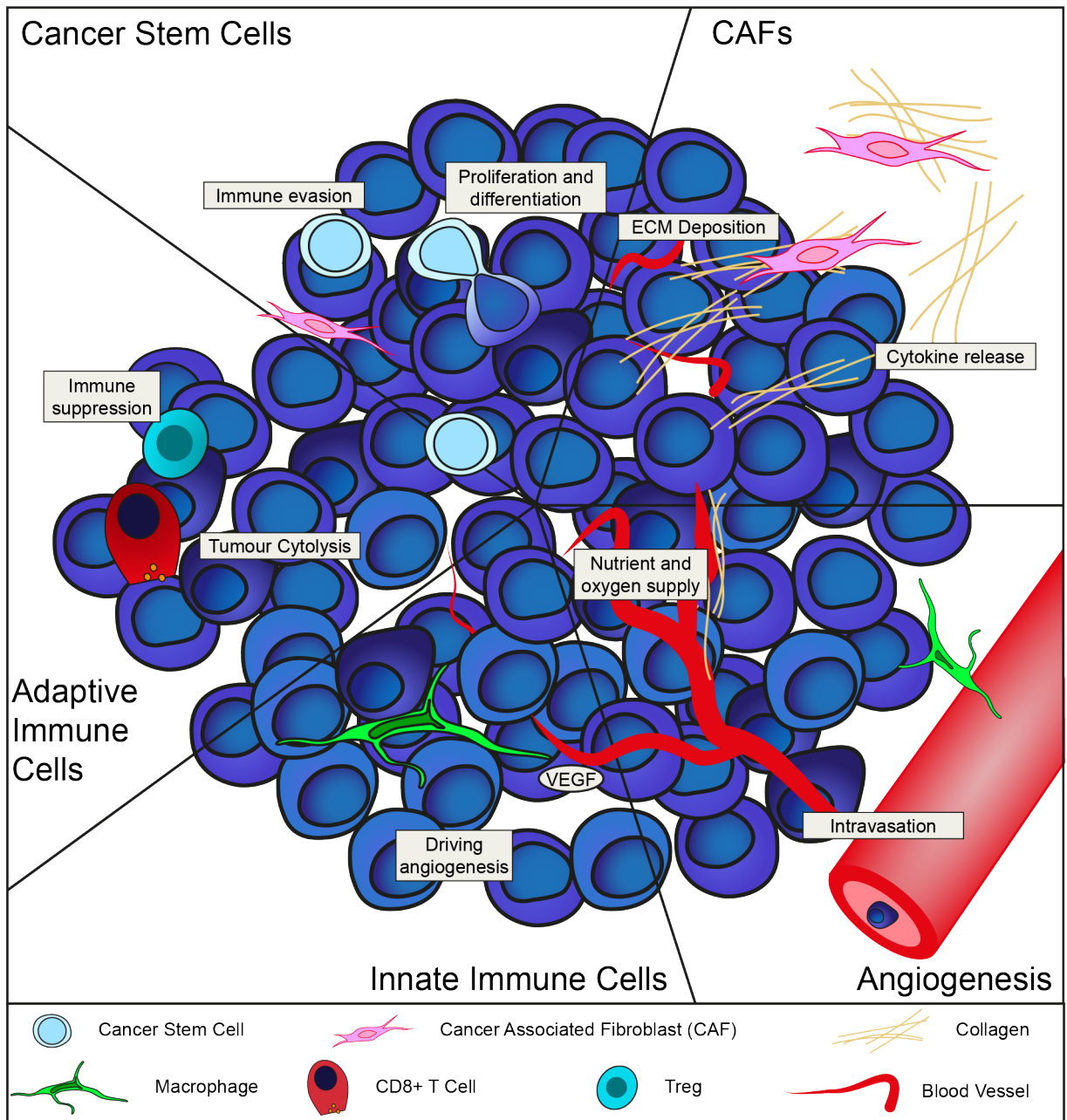


FIGURE 1.3. Primary Tumour Microenvironment

Cancer stem cells replenish the tumour by asymmetric divisions. Cancer associated fibroblasts (CAFs) alter the matrix composition. Angiogenesis provides nutrients to the tumour and gives access to the blood for cancer cells. Innate immune cells are recruited to the tumour by a variety of signals including ROS and cytokines. Within the TME, innate immune cells can provide growth factors to tumour cells and act as anti-inflammatory mediators to prevent immune attack of cancer cells. Adaptive immune cells may kill tumour cells. PD-L1 signalling dampens cytotoxic activity of T-cells. Tregs act as highly anti-inflammatory cells.

1.3.2 Invasion and Metastasis

Tumour progression in malignant tumours generally results in invasion of cancer cells beyond the basement membrane, entry of cancer cells into the blood vessels, arrest at distant sites and eventual formation of secondary tumours. Tumour cell migration into the tissues surrounding a tumour may be classically mesenchymal, with individual cell movement and invasion; or as only partially mesenchymal, recapitulating the collective migration of development and potentially allowing cells of differing roles to work together to seed a single tissue (Campbell et al., 2019).

Macrophages mediate cancer cell migration towards blood vessels by improving their ability to bind ECM and migrate. At the endothelium, macrophages have been seen to interact with cancer cells and endothelial cells (Sharma et al., 2021). These interactions are associated with poor prognosis in patient biopsies (Entenberg et al., 2020).

1.3.3 The Pre-Metastatic Niche

The pre-metastatic niche (PMN) is a microenvironment formed close to the site where a secondary tumour will be formed, before this metastatic event has fully occurred and reflects the "soil" of the "seed and soil" theory (Paget, 1889). In the early stages of PMN formation, cancer cells from the primary tumour release extracellular vesicles into the vessels which begin to signal to cells in secondary sites (Chen et al., 2022). These signals prime the tissues of distant organs, so that arriving cancer cells are better able to survive and form metastases. As the niche develops, circulating tumour cells (CTCs) will arrest within the site and further manipulate the microenvironment with surface signalling factors. Mirroring the microenvironment of a primary tumour, many host cell types may be recruited and taken advantage of by cancer cells.

1.3.3.1 Platelet Activation, Coagulation and Metastasis

Cancer cells target platelets in the region in a number of ways. They may release extracellular vesicles containing ADP or tissue factor, which activate platelets (Hisada and Mackman, 2021).

Once activated, these platelets form microclots in the PMN and degranulate, signalling to other cell types. The formation of microclots slows the rate of blood flow in the vessels of the PMN, giving cancer cells a mechanical advantage in rolling on the endothelium and arresting at the niche (Anvari et al., 2021). As cancer cells may express surface tissue factor, platelets may be activated and stick to the surface of cancer cells. This platelet coating may protect cancer cells from shear forces as they flow through the blood vessels, that can otherwise cause the lysis of cancer cells that don't have the same adaptations to the stressful environment as blood cells (Egan et al., 2014). Increased binding of platelets to cancer cells also increases the shear stress experienced by the walls of the vessel the cancer cell passes through. This wall shear stress is essential for the initiation of adhesion, meaning cancer cells with bound platelets are more likely to arrest and adhere to vessel walls, which precedes the process of extravasation into the surrounding tissues (Anvari et al., 2021).

Platelet coating of cancer cells also plays a role in immune evasion, with natural killer cells appearing less likely to recognise and lyse cancer cells with platelets on their surface (Strilic and Offermanns, 2017). Surface bound platelets stimulate the expression of PD-L1 by cancer cells, further mediating immune escape (Asgari et al., 2021).

Platelets and clotting have been shown to be important within the PMN for the recruitment of innate immune cells to cancer cells (Labelle et al., 2014; Gil-Bernabé et al., 2012). Gil-Bernabé *et al.* found that a larger volume of clots found within the PMN was associated with better cancer cell survival and formation of metastases in a murine xenograft model (Gil-Bernabé et al., 2012). Additionally, it was shown that blocking clotting led to a reduction in the number of macrophages being recruited to cancer cells and that knocking down total macrophages within the mouse led to a similar reduction of cancer cell survival (Gil-Bernabé et al., 2012). Taken together, this suggested that expression of tissue factor (TF) allows cancer cells to induce coagulation, which is essential for the recruitment of macrophages to the PMN and, ultimately, for metastasis (Gil-Bernabé et al., 2012).

Similarly, Labelle et al. (2014) depleted platelets within xenografted mice and showed a marked decrease in innate immune cell recruitment to the site of arrest of these cancer cells. Blocking communication between platelets and neutrophils also led to a loss of innate immune cell recruitment to the niche and, subsequently, to reduction of metastasis. From this, they asserted that platelets within the early PMN signal to recruit neutrophils which then act pro-metastatically to support tumour cells (Labelle et al., 2014).

1.3.3.2 Metastasis Associated Innate Immune Cells

As with other stages of cancer progression, macrophages in the pre-metastatic niche have been seen to exhibit a range of behaviours that may nurture cancer cells and aid their metastasis. Tumours may signal through extracellular vesicles to macrophages, upregulating PD-L1 and driving macrophage metabolism towards the glycolytic pathway (Morrissey et al., 2021). Increased glycolytic metabolism results in NF- κ B pathway activation which then further increases PD-L1 expression, further dampening the immune response to cancer (Morrissey et al., 2021). Additionally, macrophage-derived TGF β may shape the pre-metastatic niche by driving T cells towards less cytotoxic phenotypes, reducing mature dendritic cells, and reducing the number of activated natural killer cells within the niche (Sharma et al., 2015; Brownlie et al., 2021).

Macrophages are important for remodelling of both the ECM and the vessels of the pre-metastatic niche. Several *in vitro* models have suggested Macrophages appear to facilitate cancer cell extravasation by weakening endothelial tight junctions and producing pathways through the stromal ECM that enhance cancer cell migration (Kim et al., 2019a).

Neutrophils have also been linked to the promotion of metastasis. They have been found to be abundant within the pre-metastatic niche and genetically induced neutropenia, or inhibition of neutrophil leukotriene production, was seen to reduce the formation of metastases in mice (Wculek and Malanchi, 2015). Neutrophils are also able to dampen the immune response of CD8+ T cells. This has been linked the production of nitrous oxide, which may reduce proliferation of

naive CD8+ T cells, and prevent T cell activation (Coffelt et al., 2015). Interestingly, neutrophils also appear to have roles in re-activating dormant cancer cells, which have become senescent after dissemination. This activating function is driven by the breakdown of ECM components after NET formation, leading to the release of integrin-activating epitopes that stimulate cancer cells to re-awaken (Albregues et al., 2018).

1.4 Modelling Disease in Zebrafish

Zebrafish have become increasingly popular as a model organism in recent years owing, in part, to their genetic tractability, high fecundity and small size, while retaining homologous genes to 84% of all known human disease-causing genes (Patton et al., 2021). Additionally, larval zebrafish develop externally and are optically translucent, which enables high resolution live imaging to be performed on a vertebrate model. This has led to their use in studies of development, infection, wound healing and other human diseases (Dooley and Zon, 2000). The development of the casper mutant, lacking most pigment, means that live imaging is not restricted only to the larvae (White et al., 2008).

1.4.1 Innate Immunity in Zebrafish Larvae

As described in (**Section 1.1.1**), zebrafish and humans share a highly conserved immune system. However, in larval zebrafish, the adaptive immune system is not fully developed. Small numbers of T-cell receptor (TCR) positive cells may be seen in the thymus as early as 3 dpf, but adaptive immunity is not thought to be fully matured until they are 3-4 weeks old (Hess and Boehm, 2012). This allows the study of the actions of innate immune cells in the absence of immune cells such as T cells and B cells, thus reducing the complexity of the model. This can be highly desirable; in fact, mice and zebrafish lacking their respective orthologues of recombination-activating gene 1 (RAG1) have been generated to study phenomena such as the metastasis of xenografted cells in adult models. These knockout models are unable to perform V(D)J recombination, so do not produce functional TCRs or antibodies, and thus have no functional adaptive

immunity (Wienholds et al., 2002; Tokunaga et al., 2017).

Several fluorescent reporter lines have been generated in order to allow live imaging of the innate immune cells of zebrafish. Neutrophil-specific promoters for genes like myeloperoxidase (*mpx*) and lysozyme C (*lyz*) have been generated to drive expression of fluorescent proteins in the neutrophil lineage (Renshaw et al., 2006; Hall et al., 2007; Mathias et al., 2006). Using these lines, it was shown that inflammatory recruitment of neutrophils and the subsequent resolution of inflammation is highly comparable between zebrafish and mammals (Renshaw et al., 2006). Further, neutrophil-labelling reporter lines have allowed new phenomena to be identified such as reverse migration, whereby neutrophils can respond to signals from macrophages and migrate back into the circulation after responding to inflammation (Mathias et al., 2006). Prior to this study the prevailing thought was that resolution of inflammation was largely due to neutrophil apoptosis, with those spent cells then cleared by macrophage phagocytosis.

Likewise, macrophage reporter lines have been generated using a number of promoter regions such as those for macrophage colony stimulating factor receptor (*csf1r*) and macrophage-expressed gene 1 (*mpeg1.1*) (Gray et al., 2011; Ellett et al., 2011) and these, alongside other genetic techniques, have made more complex studies possible. To investigate functions of both neutrophils and macrophages, for example, selective ablation of macrophages by expression of the *E. coli* nitroreductase (*nfsB*) gene under the *mpeg1.1* promoter revealed their importance in adult tail regeneration (Petrie et al., 2015). There, the macrophage-expressed *nfsB* converts the prodrug metronidazole into a cytotoxic drug, leading to a significant loss of macrophages within the fish (Petrie et al., 2015). Additionally, recent advancements in CRISPR/Cas9 techniques have made the generation of specific knockout lines relatively straightforward and have created opportunities for more complex systems such as tissue-specific knockouts (Ablain et al., 2015).

Prior to these techniques, function testing studies on immune cells could be performed using morpholino knockdowns. Injection of morpholinos against *pu.1* and *gcsf* simultaneously causes the loss of both macrophages and neutrophils within the larval zebrafish. Using this approach,

our lab was able to show a link between the innate immune system and hyperpigmentation, following chronic inflammation (Lévesque et al., 2013), and to show that immune recruitment to pre-neoplastic cells is essential for the earliest stages of cancer development (Antonio et al., 2015; Feng et al., 2012).

More recent, zebrafish studies have shown the importance of macrophages and neutrophils in a range of different processes and disorders. Wound healing and regeneration have generated interest, as zebrafish have the ability to fully regenerate excised fins and appear resistant to scarring, which may allow insights into how we may prevent scarring in the future (Morris et al., 2018). Specific cellular nuclei may be isolated after *in vivo* biotagging, allowing transcriptomic analysis of nascent RNAs without the need for FACS (Trinh et al., 2017). Using this methodology, Simões *et al.* were able to show the contribution of macrophage collagen deposition to scarring in myocardial infarction (Simões et al., 2020). Neutrophil swarming, involving the co-ordinated migration of many neutrophils in infections and injury, was shown to be conserved in zebrafish (Isles et al., 2021). Additionally, by photoconversion and tracking of pioneers, it was revealed that they undergo NETosis to initiate these swarms (Isles et al., 2021).

1.4.2 *De Novo* Models of Cancer

1.4.2.1 Mammalian Models

Mammalian models of primary tumours include genetic manipulation and chemical induction of malignancies. Use of genetic tools can allow specific mutations, known to be associated with different human cancers, to be investigated specifically. This specificity can allow the development of powerful tools against specific drivers of cancer found in humans (Frese and Tuveson, 2007).

Chemically induced tumours may more faithfully model the mechanisms by which oncogenic mutations develop in human cancers upon exposure to mutagens, generating greater mutational burden and giving insights into the mutational signatures of tumours (Riva et al., 2020). Additionally, the increased mutational burden is well correlated with neoantigen expression, making

these tumours more responsive to immune therapies (Matsushita et al., 2012).

1.4.2.2 Zebrafish Models

Zebrafish models of cancer are a relatively recent development of the field. Their amenability to live imaging allows single cell tracking to describe the behaviour of both cancer cells and host cells within the cancer microenvironment (Feng and Martin, 2015). This opens the study of much more of the complete cancer progression than would be possible in an opaque model. Furthermore, complete sequencing of the zebrafish genome has revealed the close similarities in disease-causing genes between man and zebrafish. This has led to the creation of zebrafish lines overexpressing human oncogenes. For example, BRAF^{V600E} is a constitutively active mutant form of a serine/threonine kinase in the MAPK/ERK pathway. Ordinarily, BRAF is a member of a signalling cascade that upregulates cell growth and proliferation in response to external signals such as growth factors. However, the V600E mutation causes this kinase to inappropriately signal, leading to uncontrolled proliferation. In human melanoma, half of all lesions contain a mutation within the BRAF gene, with the vast majority of these being V600E. Patton et al. (2005) found that driving BRAF^{V600E} under a melanocyte promoter, in p53 null zebrafish, induced the formation of invasive melanomas on the skin of the fish.

Subsequently, other models for cancer have been generated using a range of human oncogenes. These different cancer models have allowed a range of studies. Translucent larvae allow the imaging of the earliest stages of cancer formation. Fluorescently labelled *kita*:HRAS^{G12V} cells can be identified as singlet and doublet pre-neoplastic cells as early as 48 hpf. Feng et al. (2010, 2012) showed that, even at these initial stages, preneoplastic cells are capable of recruiting innate immune cells to them, and their survival and growth is dependent on immune-derived factors such as prostaglandin-E2 and H₂O₂ .

However, one feature that these genetic models of cancer all appear to share is that they tend not to metastasise. To overcome this lack of metastatic activity, cancer cells may be implanted

into zebrafish from exogenous sources.

1.4.3 Grafting Models of Cancer

1.4.3.1 Mammalian Models

Although *de novo* tumours in mammalian models metastasise more commonly than those in zebrafish, cancer cell grafting is still a well-established model for the study of cancer metastasis. Cancer cells may be tracked with a range of fluorescent labels and can derive from different sources, including different cell lines through to patient derived tumours, makes grafting a versatile model. The ease of genetic manipulation of cell lines means that specific genes related to metastasis can be easily altered in their expression prior to engrafting without necessarily having to breed a new line of animals. Additionally, using exogenous cancer cells can allow the use of entirely wildtype animals which may allow refinement of the experiment.

Tumours generally undergo a series of mutations that change the tumour landscape over time and, as some cells become more mesenchymal and motile, eventually some cells may break away from the main tumour and undergo metastasis. Different graft sites can facilitate the study of different stages of the cancer metastatic journey. Cancer cells may be directly grafted into the blood vessels of the fish, which may be advantageous for studying the intravascular stages of metastasis without requiring a tumour to acquire metastatic activity. Alternatively, cancer cells can be injected subcutaneously, intravenously or peritoneally to mimic the growth and metastasis of different types of tumours (Taibi et al., 2019). This strategy can also reduce the amount of time an animal is exposed to cancer, as cancer grafts can be tailored to the stage of interest.

1.4.3.2 Zebrafish Models

Unlike in mammalian models, to study the metastatic invasion of cancer cells in zebrafish, it appears to be necessary to use grafted cancer cells because, as described above, *de novo* cancers appear not to metastasise. Again, grafted cells can be derived from cell culture or can even be

taken directly from patients to allow personalised medicine screening (Hua et al., 2022).

Xenografts are the engraftment of cancer cells from a different species (e.g. human or murine) to zebrafish. These have the advantage of allowing human cancer cells to be studied, which may allow a familiar cell line to be investigated *in vivo* to complement prior research, or may even allow the fish to act as "avatars" for patients (Hua et al., 2022). These "avatars" are a concept in personalised medicine whereby a biopsy of a tumour may be implanted into multiple fish, which will then be treated with different cancer therapies to rapidly identify and optimise treatment options to which the tumour might be sensitive. The high fecundity, and optical translucency of zebrafish larvae, make high throughput screens like these a possibility. As tumours from different patients may have vastly different mutations, leading to different dependencies and drug sensitivities, this approach is an exciting step towards giving patients more tailored "personalised medicine" treatments to their own disease.

Allografts describe the grafting zebrafish cancer cells into a zebrafish host. The ZMEL1 cell line was created by the White lab for this purpose (Heilmann et al., 2015) and will be used in my studies. ZMEL1 cells were initially isolated from transgenically generated zebrafish melanomas, driven by the BRAF^{V600E} oncogene, and immortalised to produce a stable cell line. The main advantages of allografts over xenografts are twofold. First, the cancer cells are of the same species, so there will be a reduced immunogenic response to a "foreign body" and secondly, the conditions of growth for both the cancer cells and the host are more closely matched. With mammalian cell xenografts, the injected fish must be kept at a compromise temperature between 32-35°C to allow the cancer cells to survive, whilst being within the survivable range of the zebrafish. This compromise temperature means that neither host nor graft is at their optimal temperature for survival and growth.

1.5 Project Aims and Objectives

Aim 1: To establish and optimise a live imaging model for microclot-driven pre-metastatic niche formation and cancer cell extravasation in zebrafish larvae

Objectives:

- First, describe naturally occurring extravasation events without experimental modulation of clotting.
- Determine appropriate timescales for live imaging of cancer cell extravasation.
- Identify which cancer cell lines are most appropriate for studies of metastasis and extravasation in zebrafish larvae.

Aim 2: To characterise innate immune cell behaviour in the formation of the pre-metastatic niche and during cancer cell extravasation.

Objectives:

- Show that innate immune cells interact with cancer cells in the vasculature of zebrafish larvae by live-imaging.
- Determine the importance of innate immune cells in cancer cell extravasation by cell-specific ablation.
- Explore what factors may influence innate immune cell interactions with cancer cells.

Aim 3: To use correlative light and electron microscopy to gain a more detailed view of host:cancer cell interactions in the pre-metastatic niche.

Objectives:

- Investigate whether innate immune cells interact directly with cancer cells
- Determine other host cells and factors that may be found within the pre-metastatic niche

Aim 4: To investigate the role of platelet- and fibrin-microclots in recruiting innate immune cells to cancer cells in the pre-metastatic niche.

Objectives:

- Establish a laser-driven microclot model to determine the effects of thrombocytes on the pre-metastatic niche
- Use drug treatments to modulate coagulation and measure changes to immune cell interactions with cancer cells

Aim 5: To determine the effects of microclots on innate immune cell inflammatory phenotypes.

Objectives:

- Use reporter lines for genes associated with the inflammatory status of immune cells to show changes in immune phenotype in response to microclots.
- Investigate how an increase in pro-inflammatory phenotypes in innate immune cells might alter metastatic potential in cancer cells by using drugs that drive inflammation.

Aim 6: To develop genetic tools for tissue-specific gene knockout in zebrafish thrombocytes.

Objectives:

- Create a zebrafish line expressing Cas9 specifically in thrombocytes to allow tissue-specific CRISPR gene editing.
- Design and characterise guide RNA sequences for knockout of genes related to thrombocyte signalling to immune cells, and create zebrafish lines expressing these guides.
- Determine the mechanisms of thrombocyte signalling to innate immune cells by knockout of potentially critical genes in thrombocytes.

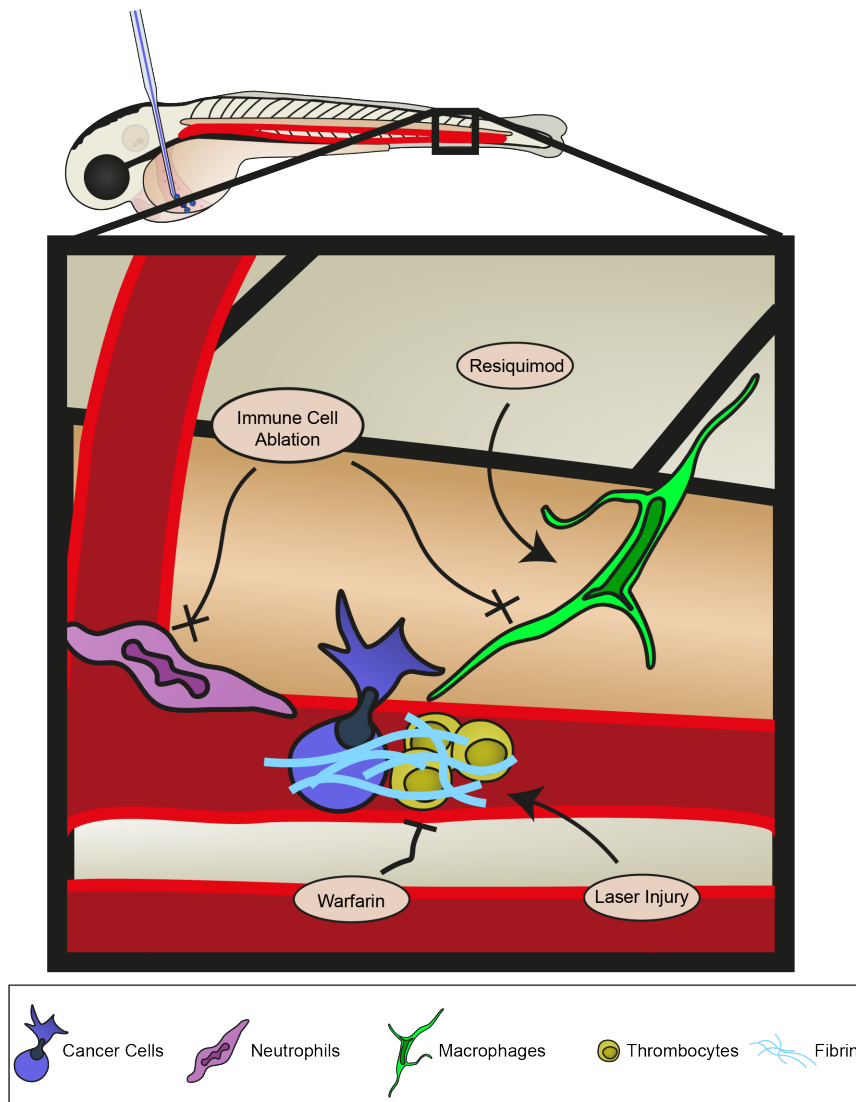


FIGURE 1.4. Methodology for Investigating the Microclot-Driven Pre-Metastatic Niche. Cancer cells of different origins may be injected directly into the vasculature of zebrafish larvae. Downstream of this, clotting may be modulated using drugs, laser-injury or morpholino-knockdown. Innate immune cell activity can be tracked, and/or altered using drugs or the nitroreductase ablation system.

Chapter 2

Materials and Methods

2.1 Zebrafish Lines and Husbandry

All animal experiments were conducted in accordance with the Animals Scientific Procedures Act 1986 (ASPA), the Animal Welfare Act 2006 and were ethically approved by the University of Bristol Animal Welfare and Ethical Review Body (AWERB).

Breeding lines were maintained in tanks of 18-22 fish, at 25 °C. Embryo experiments were performed by placing male and female zebrafish into 6 L mating tanks overnight to allow spawning. Mating tanks generally contained 3 female fish and 2 male fish. For CRISPR experiments, a divider was placed in the tank to separate male and female fish overnight and was removed in the morning to allow collection immediately after spawning so that injections could be performed on the one-cell stage. Larvae were kept in embryo water (Danieau's solution plus 0.025% methylene blue) at 28 °C.

Line Name	Line Description	Referred to as	Citation
Tg(<i>itga2b</i> :GFP)	Green labelled thrombocytes	<i>itga2b</i> :GFP	(Lin et al., 2005)
Tg(<i>csf1ra</i> :GFP)	Green labelled macrophages	<i>csf1ra</i> :GFP	(Dee et al., 2016)
Tg(<i>fli1</i> :EGFP)	Green labelled endothelial cells	<i>fli</i> :GFP	(Lawson and Weinstein, 2002)
Tg(<i>lyz</i> :dsRed)	Red labelled neutrophils	<i>lyz</i> :dsRed	(Hall et al., 2007)
Tg(<i>mpeg</i> :mCherry)	Red labelled macrophages	<i>mpeg</i> :mCherry	(Ellett et al., 2011)
Tg(<i>mpx</i> :GFP)	Green labelled neutrophils	<i>mpx</i> :GFP	(Renshaw et al., 2006)
Tg(<i>mpx</i> :Gal4)	Gal4 expression in neutrophils	<i>mpx</i> :Gal4	(Robertson et al., 2014)
Tg(<i>mpeg</i> :Gal4)	Gal4 expression in macrophages	<i>mpeg</i> :Gal4	(Ellett et al., 2011)
Tg(UAS: <i>nfsB</i> -mCherry)	Gal4-driven expression of nitroreductase enzyme and mCherry	UAS: <i>nfsB</i> -mCherry	(Davison et al., 2007)

Table 2.1: Zebrafish transgenic lines used

2.2 Cell Culture and Cancer Microinjection

2.2.1 Generation and Maintenance of Cell Lines

Human cancer cell lines, MDA-MB-231 and PC3, were maintained at 37 °C, 5% CO₂, 10% humidity in DMEM with sodium bicarbonate and phenol red (Sigma Aldrich), supplemented with 10% FBS, 0.3 g/L L-glutamine, penicillin and streptomycin.

ZMEL-1 cells were a kind gift from Jacky Goetz (Centre de Recherche en Biomédecine de Strasbourg, France). These are zebrafish melanoma cells generated into a stable cell line from transgenic *mitfa* BRAF^{V600E}, p53^{-/-} fish (Heilmann et al., 2015). ZMEL-1 cells were maintained in DMEM/F12 supplemented with 10% FBS, 1% pen/strep, 1% L-glutamate, 1% amphotericin B, 1% non essential amino acids and HEPES. ZMEL cells were maintained at 28 °C, 5 % CO₂, 10% humidity.

2.2.2 Microinjection of Cancer Cells into Zebrafish Larvae

Highly metastatic cancer cell lines were chosen for xenograft experiments. MDA-MB-231 cells are metastatic lung cancer cells, originally isolated from the lung fluid of a patient. PC3 cells are a prostate cancer line isolated from a patient's bone marrow. These cells were seeded with around 10^6 cells in a T75 flask 2 days before injection. On the day of injection, cells were roughly 70% confluent. Cells were washed with PBS before the addition of 0.25% (w/v) Trypsin - 0.53 mM EDTA solution and incubation at 37 °C for 5 minutes. Once cells were no longer adherent, trypsinisation was quenched using complete media before centrifuging the cells at 800 G for 2:30 minutes. Cells were then washed 3 times in PBS, with the same centrifugation protocol, before being resuspended in PBS at 5×10^7 cells/mL.

Zebrafish cancer cells were seeded 3 days before injection. Immediately prior to trypsinisation, ZMEL cells were labelled with Vybrant DiI (ThermoFisher) and Hoechst for 15 minutes in serum-free media. Cells were then washed in the dish; 3 x 2 minutes before trypsinisation at 28 °C for 10 minutes. Once cells were no longer adherent, they were washed using the same protocol as human cells.

Polyvinylpyrrolidone (PVP) (Sigma-Aldrich) was added to the cell suspension to a final concentration of 2%. PVP was used to retain single cell suspension, without it cancer cells were found to be more adherent to one another during injections. 10 μ L of the suspension mix was loaded into borosilicate glass capillary needles (1 mm O.D., 0.58 mm I.D., Harvard Apparatus G100-4. Pulled using a Stutter Model P-97 needle puller). Needles were affixed to a Parker Picospritzer®III microinjector, their tips were broken to approximately a 15 μ m bevel length and pump time was adjusted until an approximately 1 nL bolus was released per pump, measured using a graticule. 2 dpf Zebrafish larvae were anaesthetised in 0.1 mg/mL tricaine in E3 and arranged on an agarose filled 10 cm petri dish (50 mL of 1% agarose in E3, poured into a 10 cm petri dish and allowed to cool) with their yolk sacs facing the same direction. Using a micromanipulator, the needle was inserted into the Duct of Cuvier, close to the pericardial vessel, and approximately 200 cells were injected into the blood vessel. Larvae were then rinsed with fresh E3 and placed in E3 at 33 °C (for human cancer cells) or 28 °C (for zebrafish cancer cells) for up to 24 hours before imaging.

2.3 Cloning

2.3.1 Plasmids

Plasmid Acknowledgements:

pGGDestTol2LC-1sgRNA was a gift from Wenbiao Chen (Addgene plasmid #64239; http://n2t.net/addgene:64239 ; RRID:Addgene_64239)
pGGDestTol2LC-2sgRNA was a gift from Wenbiao Chen (Addgene plasmid #64240; http://n2t.net/addgene:64240 ; RRID:Addgene_64240)
pGGDestTol2LC-3sgRNA was a gift from Wenbiao Chen (Addgene plasmid #64241; http://n2t.net/addgene:64241 ; RRID:Addgene_64241)
pGGDestTol2LC-4sgRNA was a gift from Wenbiao Chen (Addgene plasmid #64242; http://n2t.net/addgene:64242 ; RRID:Addgene_64242)
pGGDestTol2LC-5sgRNA was a gift from Wenbiao Chen (Addgene plasmid #64243; http://n2t.net/addgene:64243 ; RRID:Addgene_64243)
pU6a:sgRNA#1 was a gift from Wenbiao Chen (Addgene plasmid #64245; http://n2t.net/addgene:64245 ; RRID:Addgene_64245)
pU6a:sgRNA#2 was a gift from Wenbiao Chen (Addgene plasmid #64246; http://n2t.net/addgene:64246 ; RRID:Addgene_64246)
pU6b:sgRNA#3 was a gift from Wenbiao Chen (Addgene plasmid #64247; http://n2t.net/addgene:64247 ; RRID:Addgene_64247)
pU6c:sgRNA#4 was a gift from Wenbiao Chen (Addgene plasmid #64248; http://n2t.net/addgene:64248 ; RRID:Addgene_64248)
pU6d:sgRNA#5 was a gift from Wenbiao Chen (Addgene plasmid #64249; http://n2t.net/addgene:64249 ; RRID:Addgene_64249)
pDONRP4-P1R, Tol2Kit (Kwan et al., 2007)
p5E-mpl, Generated from pDONRP4-P1R
pME-Cas9-T2A-GFP was a gift from Leonard Zon (Addgene plasmid #63155; http://n2t.net/addgene:63155 ; RRID:Addgene_63155)
p3E-polyA, Tol2Kit (Kwan et al., 2007)
pGGDestTol2LC-U6xsgRNA-mpl-Cas9-T2A-GFP, Generated using plasmids above
mTagBFP2-Farnesyl-5 was a gift from Michael Davidson (Addgene plasmid #55295; http://n2t.net/addgene:55295 ; RRID:Addgene_55295)

Table 2.2: Plasmid Acknowledgements

Gateway recombination was used to generate the tissue-specific expression vector for Cas9, with Golden Gate assembly used for the inclusion of the U6xsgRNAs. The mpl promoter sequence was cloned out of zebrafish gDNA, using the primers attB4-mpl-fwd:

5'-GGGGACAACCTTTGTATAGAAAAGTTGCGCTCCTTCGCTACGCA-3'

and attB1R-mpl-rev:

5'-GGGGACTGCTTTTTTTGTACAAACTTGTGTTGATGGGGGTCCATACACAA-3'.

This fragment was then introduced into the pDONRP4-P1R plasmid using BP Clonase II mix (Thermo-Fischer) incubated at 4 °C overnight to generate p5E-mpl. The 5', Middle and 3' Entry Vectors were then combined into the destination vector, pGGDestTol2LC, with LR Clonase II mix overnight at 4°C. Guide RNA sequences were entered into their respective U6 plasmids using BSmBI digestion. The U6xsgRNA sequences were then entered into the destination vector using Golden Gate assembly. All plasmids were incubated together with BsaI overnight at 4°C.

2.3.2 gDNA Extraction and Promoter Sequence PCR

gDNA (genomic DNA) was extracted from wildtype zebrafish larvae. 5 larvae were anaesthetised in an overdose of tricaine and suspended in 100 μ L 50 mM NaOH and heated to 95 °C for 10 minutes. This mixture was then placed at 4 °C for 10 minutes to cool, before addition of 3 μ L 1 M Tris-Hcl pH 8.0 to neutralise. The mixture was then centrifuged at 13,000 G for 60 seconds and supernatant was used for subsequent PCR reactions.

Platinum SuperFi II polymerase (Invitrogen) was used to amplify the mpl promoter sequence, following manufacturer's instructions. 100 ng gDNA was added to a 50 μ L final volume. *att* site containing primers were used at a final concentration of 500 nM. The PCR product was run on an agarose/ethidium bromide gel and purified using gel extraction kit (IDT).

2.3.3 Gateway Recombination and Golden Gate Assembly of Plasmids

The expression vector was assembled using Gateway Recombination as described by Kwan *et al.* (Kwan *et al.*, 2007). Purified promoter sequence, flanked by *att* sequences, was inserted into pDONRP4-P1R by a BP recombination reaction. The promoter fragment was incubated with the

DONR plasmid along with BP Clonase II mix (Thermo-Fischer) at room temperature overnight to generate p5E-mpl. The 5', Middle and 3' Entry Vectors were then combined into the destination vector, pDestTol2pA2 (Kwan et al., 2007), with LR Clonase II mix overnight at room temperature.

Guide RNA sequences were entered into their respective U6x plasmids using BsmBI digestion. The U6xsgRNA sequences were then entered into the golden gate destination vector, pGGDestTol2 (Yin et al., 2015) using Golden Gate assembly. All U6xsgRNA plasmids were incubated together with the destination vector with BsaI and T4 DNA ligase, 3x(37°C for 20 min, 16°C for 15 min) followed by 80°C for 15 min.

Plasmids containing the mpl:Cas9 expression construct and the U6xsgRNAs were constructed using Gibson assembly. Overlapping primers were designed for both pEC-mpl-Cas9-T2E-EGFP and pEC-U6xsgRNA using NEBuilder (NEB). Platinum SuperFi II polymerase (Invitrogen) was used to produce PCR products from the 2 plasmids. PCR products were run on a 1% agarose gel and gel extraction kit (IDT) was used to purify them. PCR products were then incubated with Gibson Assembly Master Mix (New England Biolabs, USA) at 50°C for 15 minutes.

2.4 CRISPR/Cas9 Directed Mutagenesis

2.4.1 Guide RNA Design

Open access softwares, Benchling and Crispor, were used to generate guide RNA sequences with appropriate on-target and off-target scores. Potential guide sequences were then ranked by their mean score across the available tests and chosen based on highest scores located in exons that were deemed likely to cause non-functional proteins.

Ensemble was used to find exons within target proteins that are most likely to cause loss of function when disrupted. Exons early in the genes were prioritised with the hopes that an early frame-shift mutation would be more likely to produce a non-functional protein.

2.4.2 Assembly and Microinjection of Ribonucleoprotein complexes

On ice, 1.5 μL of 30 μM sgRNA in RNase-free Tris buffer (pH 7.4) was mixed with 1.5 μL of 30 μM Cas9 protein in resuspension buffer. This mix was incubated for 5 minutes at room temperature to allow the formation of ribonucleoprotein (RNP) complexes and returned to ice. The RNP mix was then backloaded into a borosilicate glass capillary needle (1 mm O.D., 0.58 mm I.D., Harvard Apparatus G100-4. Pulled using a Stutter Model P-97 needle puller). Eggs were collected from breeding tanks and immediately used for injections, so that they were injected during the one-cell stage. Approximately 1 nL RNP mix was injected directly into the yolk of each egg.

2.4.3 gDNA Extraction and F0 Screening by Heteroduplex Gel

Electrophoresis

A sample of between 8 and 12 fish from each round of injections was taken to gauge the rate of mutations. These fish were culled with excess tricaine (MS-222) and rinsed in dH₂O before separating them into PCR tubes and adding NaOH to a final concentration of 50 mM. They were then heated to 95 °C for 10 minutes, agitated to break apart the samples and cooled to 4 °C before neutralising with a 1/10 volume of 1 M Tris-HCL (pH 8.0).

1 μL of this extraction was added directly to Qiagen Fast-cycling PCR master mix, which was then run according to primer annealing temperatures and manufacturer's instructions for 30 cycles in a PTC-200 Thermal Cycler (MJ Research), followed by an annealing step with the following conditions:

Annealed PCR products were then run on a 4% agarose gel in TAE buffer for 60 minutes at 80 V. Secondary, larger bands were identified as heterodimer DNA, indicating the presence of mutant DNA within the sample.

Temperature (°C)	Time (min)	Ramp Rate (°C/sec)
95	10	
↓		2
85	1	
↓		0.3
75	1	
↓		0.3
65	1	
↓		0.3
55	1	
↓		0.3
45	1	
↓		0.3
35	1	
↓		0.3
25	1	
↓		(full speed)
4	hold ∞	

Table 2.3: Annealing Protocol

2.5 Imaging

2.5.1 Live Imaging

Zebrafish larvae were prepared for imaging by anaesthetising in 0.1 mg/mL MS-222 before mounting larvae on a 35 mm glass bottomed imaging dish (MatTek) in 1 % low-gelling agarose (Thermo-Fisher) in E3 with 0.1 mg/mL MS-222 added.

Drug treatments were added to the larval media for 24 hours prior to imaging, and throughout the duration of imaging experiments. In experiments using drug treatments, larvae were mounted in glass bottomed 8 well chambers (Ibidi) to allow treatment with different drugs.

Images were collected using a Leica TCS SP8 AOBS confocal laser scanning microscope attached to a Leica DMI8 inverted epifluorescence microscope with a 20X glycerol lens maintained at 35 °C. Imaging intervals were determined for different experimental contexts. In experiments where neutrophil movements were tracked, stacks were taken with 3 minute intervals. When tracking macrophages, 5 minute intervals were used between stacks, as macrophages tend to

move at a lower speed than neutrophils.

2.5.2 Correlative Light and Electron Microscopy (Collaborators Techniques)

All correlative light and electron microscopy (CLEM) presented with this thesis was performed as part of a collaboration with Dr Lorna Hodgson (Wolfson Bioimaging Facility, University of Bristol). My contributions to this work are as follows: I designed and performed zebrafish experiments, including xenografting of cancer cells and live fluorescent imaging of larvae; I analysed data from these live imaging experiments and identified samples to go forward for transmission electron microscopy (TEM); I received incremental electron micrographs from Dr Lorna Hodgson during cutting of samples and analysed these myself, giving advice on where particular regions of interest could be located and helping to choose new depths to cut and when to stop cutting; I analysed the final micrographs for cells of interest and interactions and performed post-hoc image editing, including false colouring to highlight different cell types. The contributions of Dr Hodgson have been clearly indicated throughout the text and figure legends of this thesis, including in the methods section associated with TEM. Briefly, Dr Hodgson received larval zebrafish samples that had been pre-imaged using confocal microscopy by myself, fixed and stained these samples for TEM before embedding in resin, cutting samples, mounting on TEM support grids, imaging by electron microscopy and creating stitched together montages of micrographs to show a larger field of view. Dr Hodgson also provided advice pertaining to sample preparation, to ensure good outcomes for EM, and on cutting and orienting samples to give the best view of the region of interest.

Following confocal microscopy, zebrafish larvae were de-embedded from agarose by washing vigorously with Danieau's solution containing 0.1 mg/ml MS-222. Larvae were then placed in a drop of 4 °C primary fixative containing 2.5 % glutaraldehyde and 0.1 M sodium cacodylate in H₂O. With the larvae inside a drop of fixative, a scalpel blade was used to harvest the tissues of the tail dorsal to the cloaca. These were then placed in excess primary fixative with gentle agitation overnight at 4 °C. Samples were then washed in cold 0.1 M cacodylate buffer; 3 x 10

min with gentle agitation at 4 °C. Samples were then added to secondary fixative containing 1 % OsO₄, 1.5 % Potassium ferrocyanide, 0.1 M sodium cacodylate in water, and fixed for 2 hours at 4 °C. Samples were washed in 0.1 M sodium cacodylate on a rotator; 3 x 10 min. And washed in H₂O; 1 x 10 min.

Samples were then placed on a glass slide and excess liquid was removed using filter paper. A bovine serum albumin (BSA)/gluteraldehyde solution was made up, containing 6.75 % BSA, 2.5 % gluteraldehyde in 0.1 M cacodylate buffer, and quickly added to samples on glass slides, dropwise until the tails were covered, and left to set for 10 min. The gel encased specimens were then placed in water.

Next, samples were processed using an automatic tissue processor using the program outlined in **table 2.4**. Samples were removed from the processor and transferred to fresh EPON for 2-3 hours, before transferring to coffin molds. Samples were oriented in molds and polymerised at 60 °C for 24-48 hours.

The blocks were then removed from the oven and block faces were trimmed using a razor blade. 300 nm sections were cut using a UC6 Leica ultramicrotome with diamond knife (Diatome). Sections were stained with methylene blue and imaged using a stereomicroscope. 70 nm sections were collected onto pioloform-coated copper slot grids. These sections were then imaged using a Tecnai 12 BioTwin Spirit TEM (tungsten filament, 120 kV) and a FEI Eagle 4k x 4k CCD camera.

Treatment	Time	Repeats
Deionised water 4 °C	10 min	x7
3 % Uranyl acetate 4 °C	12 hours	x1
Deionised water 4-60 °C	10 min	x5
0.03 M aspartic acid solution, pH 5.5 60 °C	30 min	x1
Waltons lead aspartate, pH 5.5 60 °C	30 min	x1
0.03 M aspartic acid solution, pH 5.5 50 °C	10 min	x1
Deionised water 35 °C and 15 °C	10 min	x2
Deionised water 4 °C	12 hours (remove from processor)	x1
30 % ethanol 10 °C	10 min	x1
50 % ethanol 10 °C	10 min	x1
70 % ethanol 10 °C	10 min	x1
90 % ethanol 20 °C	10 min	x1
100 % ethanol 20 °C	10 min	x5
100 % ethanol 20 °C	20 min	x3
Propylene oxide 20 °C	10 min	x3
Propylene oxide:EPON (1:1) 20 °C	60 min	x1
Propylene oxide:EPON (1:2) 20 °C	60 min	x1
Propylene oxide:EPON (1:9) 20 °C	120 min	x1
EPON 20 °C	60 min	x1
EPON 20 °C	120 min	x3

Table 2.4: Automatic processing of TEM samples

2.6 Image Analysis

Images were exported to Fiji for processing and analysis. Cell tracking was automated using scripting for the Fiji Trackmate plugin (Tinevez et al., 2017) written using the Python programming language (Python Software Foundation, <https://www.python.org/>) using the pyimagej wrapper (Reuden et al., 2020). Briefly, trackmate parameters were decided upon by comparing a manual count of cells with the trackmate output. These parameters were fed into the Python script, which then iterates through all imaging sets. The trackmate output XML files were then used to generate coordinates for all cells at all timepoints, allowing position and velocity to be tracked. Comparing cell coordinates between separate channels gave the proximity of different cell types to one another. Cells within 30 μm were arbitrarily selected as closely interacting.

2.7 Statistical Analysis

Statistical analyses were performed using Graphpad Prism 9. Details of specific statistical tests used are indicated in the respective figure legends. Shapiro-Wilk test of normality was used to determine whether data was normally distributed. Welch's corrections were used if the variance between samples was significantly different by F test.

Chapter 3

Characterising the Pre-Metastatic Niche

3.1 Introduction

Circulating tumour cells (CTCs) have been found even at the early stages of cancer progression, at a stage when the tumour would previously have been considered to be "localised" (Stott et al., 2010) (**Section 1.3.1**). This suggests that the capacity for invasion and migration are not necessarily rate limiting factors in the formation of metastases and that a process downstream of this might prevent these cells from forming secondary tumours. The pre-metastatic niche (PMN) is the site where CTCs arrest and eventually extravasate into the surrounding tissues. A variety of other host cells are recruited to this site to nurture cancer cells and aid their movement out of the vessel (**Section 1.3.3**). For these reasons, the PMN is clearly rate limiting in the formation of metastases and so is a target for therapeutic intervention.

Previous studies of the PMN have revealed key roles for innate immune cells in the survival of cancer cells and their extravasation from the vessel (Qian et al., 2011). Further studies have shown the presence of platelets within the niche, and these may be interacting with both cancer cells and immune cells (Ablain et al., 2015; Labelle et al., 2014). The interaction between activated platelets and cancer cells has also been posited to aid the arrest of CTCs, allowing them the

opportunity to bind tightly to the endothelium and subsequently move through it (Kim et al., 1998).

Most studies of the PMN thus far have used models with opaque tissues, such as mouse and rat. These rodent studies have led to the discovery of many of the cell types and factors that are required for the formation of the secondary tumour, but since these models are not readily amenable to live imaging they cannot fully reveal the dynamics of these cellular interactions (**Section 1.3.3**). I have established the use of a larval Zebrafish model to study the formation and development of the PMN, allowing high spatial, and temporal, resolution imaging of individual cancer cells and the host cells that they interact with to drive their extravasation.

3.2 Results

3.2.1 Human Cancer Cells

3.2.1.1 Cancer Cell Behaviour

Initial experiments used to develop a model of platelet and immune involvement in the pre-metastatic niche were performed using highly metastatic human cancer cells lines. First, to establish the activity of these cells in the absence of any intervention, cancer cells were injected into larval zebrafish and their behaviour was assessed using live imaging.

Human PC3 prostate cancer cells or MDA-MB-231 breast cancer cells were injected directly into the Duct of Cuvier (DoC) of 2 dpf zebrafish larvae. Cancer cells are subsequently seen spread throughout the vasculature of the zebrafish as early as 2 hours post injection (hpi). Because cancer cells are injected directly into the DoC of the fish, they have immediate access to the dorsal aorta. Immediately post injection, cells are generally found exclusively within this major artery and may cause disruption to the blood flow of the fish, due to their large size of up to 20 μm . As some of these cells arrest, normal blood flow appears to be restored, perhaps due to endothelial remodelling. Occasionally, cancer cells could be seen freely circulating within the vessels of larvae, though this appeared rare.

Using a fluorescent reporter line for endothelial cells provides the best opportunity to observe when cancer cells have extravasated. Human cancer cells were observed outside of the vessel lumen from around 6 hpi (**Figure 3.1**). Some cancer cells can be seen invading the tissues surrounding vessels. Additional to these invasive extravasation events, some cancer cells appeared to have extravasated by endothelial remodelling. This phenomenon, described by Follain et al. (2018), occurs when cancer cells interact with endothelial cells, causing them to form a new endothelial layer that excludes cancer cells from the vessel lumen. In the current studies, cancer cells could be seen apparently surrounded by endothelial cells, below the lumen of the caudal vein (**Figure 3.1**).

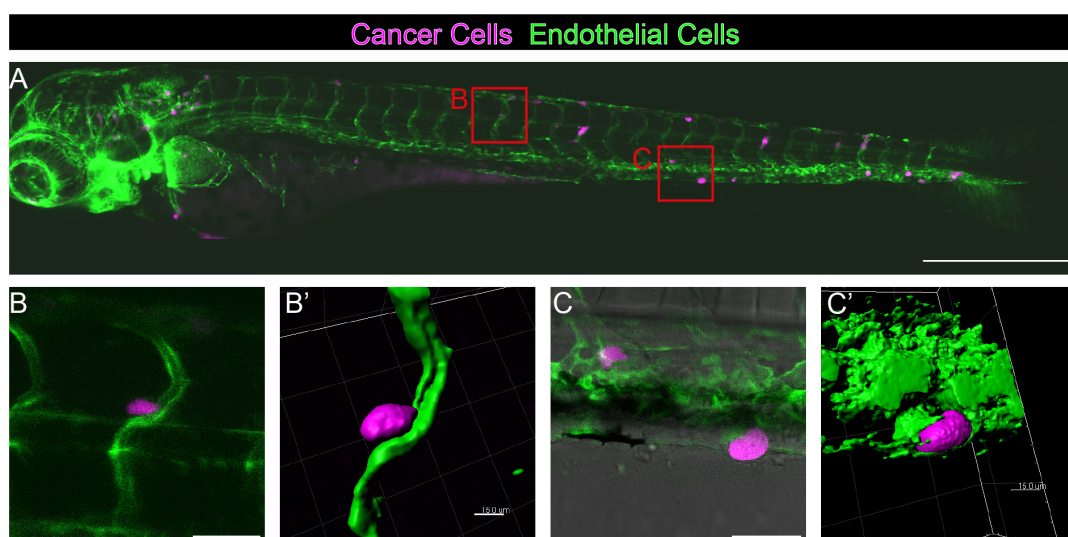


FIGURE 3.1. Optimising Imaging of Extravasated Cancer Cells. **A** Shows PC3-RFP cells (magenta) spread throughout the vessels (green) of a larva, 24 hpi. Red boxes denote areas which show closeups. **B-B'** Show closeup imaging and rendering of an invasive extravasated cancer cell. **C-C'** Shows a closeup and rendering of a human cancer cell with endothelial marker surrounding. Scale bars: A = 500 μm ; B & C = 50 μm ; B' & C' = 15 μm .

To capture the extravasation process in detail, live imaging was performed over a 14 hour period. Human cancer cells could be observed moving from inside the lumen of the vessel into the stroma (**Figure 3.2**). A range of morphological changes were observed during this process. Initially, cancer cells appear rounded up within the vessel, before beginning to extend parts of their membrane beyond the endothelial wall. These invadopodia-like structures appear highly dynamic, forming new branches and retracting repeatedly. During transendothelial migration, cancer cells adopted a highly restricted morphology, narrowing their cytoplasm and apparently squeezing through a small gap created within the endothelial layer. Once extravasated from the vessel, cancer cells appear to readopt their original, rounded morphology.

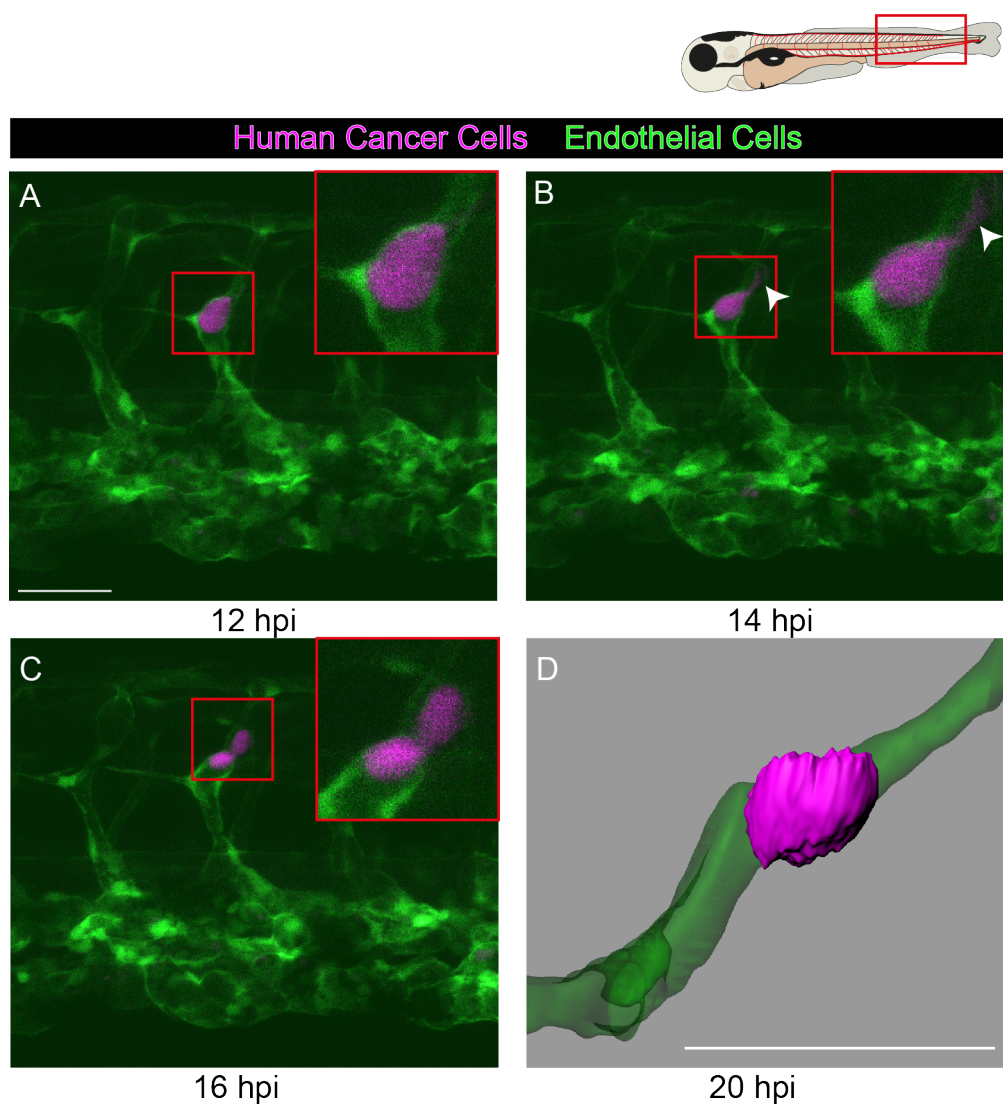


FIGURE 3.2. Live Imaging the Dynamics of a Human Cancer Cell Extravasating from a Zebrafish Vessel. **A-C** Are snapshots from live imaging of a human PC3 cancer cell (magenta) during the period of extravasation from a vessel (green) in the tail of a 3 dpf larva, injected 12 hours prior. High magnification view in red boxes. Invadopodia (arrow heads) extend into the surrounding tissue, preceding the moment of extravasation. Cancer cell morphology changes over time. **D** Imaris 3D rendering to show the cell outside of the vessel after extravasation. Scale bars = 50 μm .

3.2.1.2 Human Cancer Cell Interactions with Host Cells

It is well established that a range of host cells play key roles in each of the constitutive processes contributing to cancer metastasis. To investigate how zebrafish host cells interact with grafted human cancer cells, live imaging of each of a number of the different host cell lineages with human cancer cells was performed. The genetic tractability of zebrafish has led to the generation of many fluorescent reporter lines, including some of those believed to be important in the pre-metastatic niche. Of particular relevance here, the innate immune cell lineages, neutrophils and macrophages (Renshaw et al., 2006; Ellett et al., 2011), and the thrombocyte lineage (Lin et al., 2005). These reporter lines allow the observation of host cells interacting with cancer cells.

Importantly, innate immune cell interactions with human cancer cells appeared quite frequent, with all observed cancer cells experiencing close interactions throughout the duration of a 14 hour imaging time frame. Some macrophage interactions with cancer cells in the vessels of larvae resulted in an extended, flattened broad face of interaction, and these individual interactions last upwards of an hour. This morphological change suggests cytoskeletal changes associated with a direct interaction. Neutrophils were also frequently observed closely interacting with human cancer cells, although these interactions appeared briefer and did not appear to involve such close contact as macrophage:cancer cell interactions (**Figure 3.3**).

Further, human cancer cells can occasionally be seen closely interacting with thrombocytes within the lumen of the caudal plexus. Thrombocytes appear clustered with one another, potentially indicating cancer-driven activation. On occasions, thrombocytes were seen tightly associated with cancer cells, wrapped over the surface of the cell membrane (**Figure 3.4**). These interactions did not appear common, which might be explained by a lack of compatibility between human and zebrafish factors.

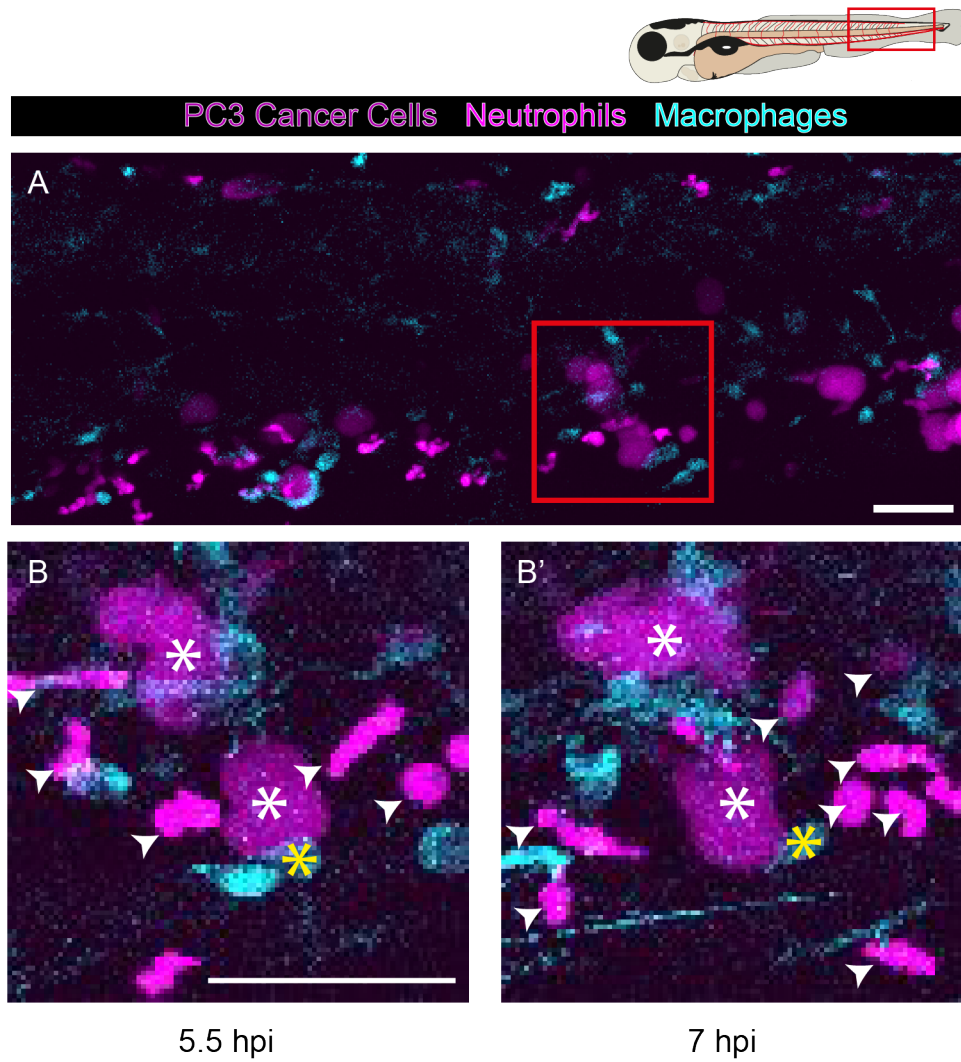


FIGURE 3.3. Innate Immune Cells Interact with Human Cancer Cells. **A** Shows human cancer cells within the tail vessels of a 3 dpf larval zebrafish. **B-B'** The same view at two different time points. Neutrophils (small, bright magenta cells, marked with arrowheads) and macrophages (Cyan cells) interact with Human PC3-RFP cells (large, rounded magenta cells marked with asterisks) within the caudal vein plexus of a zebrafish. Yellow asterisks indicate a long term, direct interfacing of a macrophage with a cancer cell. Scale bars = 50 μm .

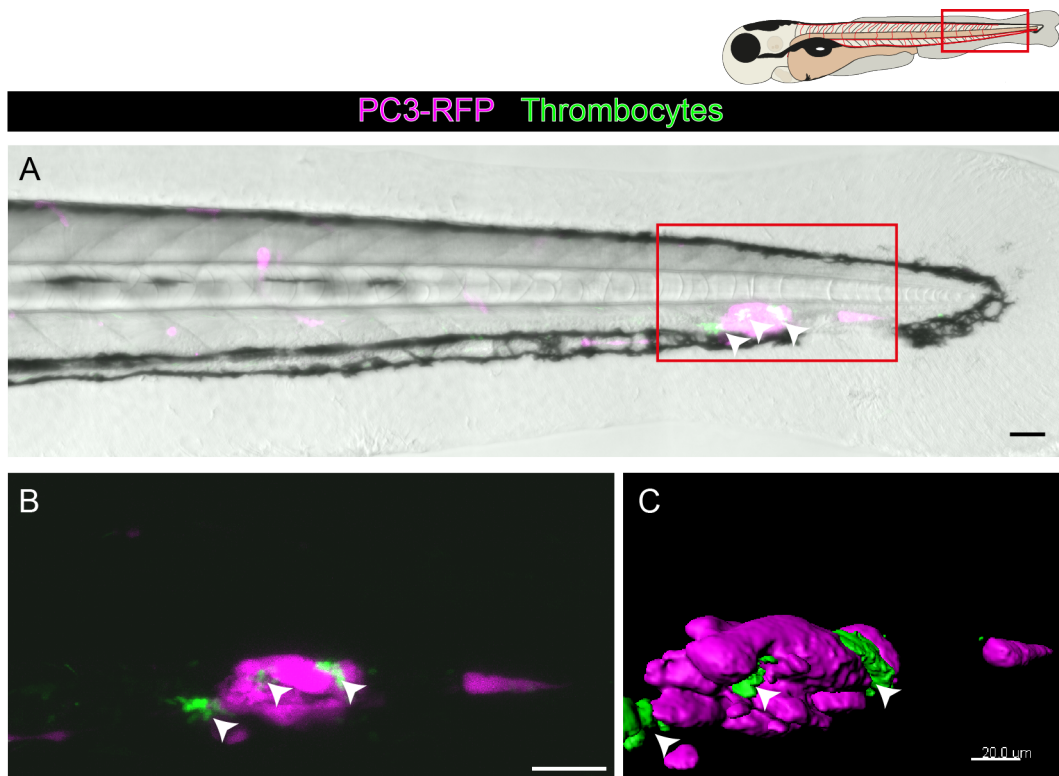


FIGURE 3.4. Human Cancer Cells Associate with Zebrafish Thrombocytes. **A-B** Show a tilescan and high magnification view of the tail of a 3 dpf zebrafish larva, 24 hours after injection of human PC3 cancer cells (magenta). Thrombocytes (green) are associated with these cancer cells within the lumen of the vessels. Arrow heads indicate groups of thrombocytes associating with cancer cells. **C** Shows an imaris 3D render of these thrombocytes and cancer cells to more clearly reveal the direct interactions between cells. Scale bars: A & B = 50 μm ; C = 20 μm .

Due to the relative infrequency of these close interactions between cancer cells and thrombocytes, laser injury of the endothelial wall was used to cause thrombosis, as described later in **(Section 4.2.1)**. Serendipitously, during optimisation of this technique, an intersegmental vessel was ablated close to the site of arrest of a cancer cell, in the flank of a larval zebrafish. Upon laser destruction of the intersegmental vessel, human cancer cells appear able to respond to the damage signals and potentially integrate with the host larval vessels **(Figure 3.5)**.

Human PC3 cancer cells were observed to form a vessel-like structure in the place of the original vessel. This cancer cell vessel structure appears to have a much larger diameter than the host inter-segmental vessels (ISVs). Live imaging captured extensions from cancer cells, moving towards nearby undamaged host vessels, appearing to integrate with the existing vasculature. The passage of host blood cells through the structure was observed, confirming the presence of a functional lumen **(Figure 3.5)**.

Macrophages were also seen within the stroma, closely interacting with these blood vessel-like structures **(Figure 3.5)**. This may mirror the angiogenic response following wounding, where macrophages have previously been shown to "hug" growing vessels and drive wound neoangiogenesis (Gurevich et al., 2018). This phenomenon may be an example of the vasculogenic mimicry of cancer cells, as previously described by others (Maniotis et al., 1999; Silvestri et al., 2020) and so perhaps zebrafish might be a good model in which to further study this using live cell imaging.

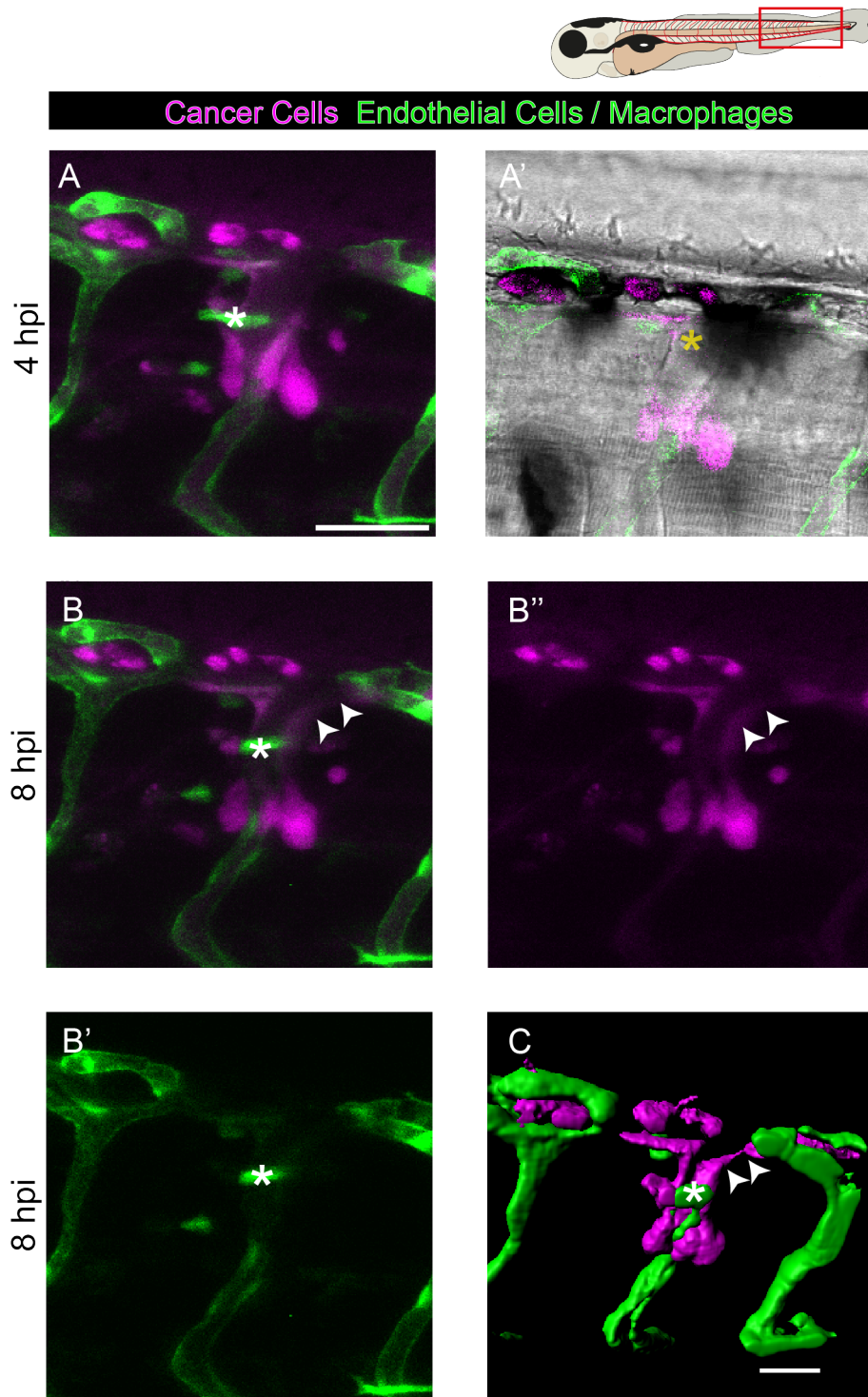



FIGURE 3.5. **Cancer Cells May Undergo Vasculogenic Mimicry.** (Legend continues on next page)

Figure 3.5: (Continued) **A-C** Shows live imaging of human PC3 cancer cells (magenta) injected directly into 2 dpf larval vessels (green). **A** Shows cancer cells (4 hpi) interacting with a macrophage (green, white asterisk) . **A'** Shows a single plane of this confocal stack, in which a blood cell can be seen passing through the lumen (yellow asterisk). **B-B''** Show cancer cells at 8 hpi, with an extension reaching to the zebrafish vasculature (arrows). A macrophage (white asterisk) is interacting with these cancer cells. **C** Imaris rendering reveals details of the 3D structure of these cellular interactions. Scale bars = 50 μm .



3.2.1.3 Correlative Light and Electron Microscopy of the Pre-Metastatic Niche

To further investigate host cell interactions with human cancer cells, TEM was used to gain sub-cellular resolution of the niche. In collaboration with Dr Lorna Hodgson (Wolfson Bioimaging Facility, University of Bristol), confocal light microscopy of cancer cells within the tail vessels was matched to TEM of the same region. Arrested human cancer cells and a range of host cell types were identified within close proximity of one another.

Using this approach, cancer cells within the caudal vein plexus (CVP) could be seen making close contact with endothelial cells (**Figure 3.6**). The proximity of the plasma membranes of these human cancer cells and zebrafish endothelial cells is, at times, below the limit of resolution in these experiments, on the nanometre scale. This may represent "pocketing", which has been described as a precursor to extravasation events (Follain et al., 2018).

Innate immune cells can be identified by a number of distinct morphologies. Macrophages can be identified by their large size, large lysosomes and relatively regularly shaped nuclei. In comparison, neutrophils appear smaller, contain electron-dense "cigar shaped" granules and have polymorphic nuclei. Broad, flattened faces of interaction between macrophages and cancer cells are occasionally observed. Interdigititation of short membrane extensions between cancer cells and macrophages were seen at these fronts of interaction (**Figure 3.6**), revealing just how intimate these interactions are.

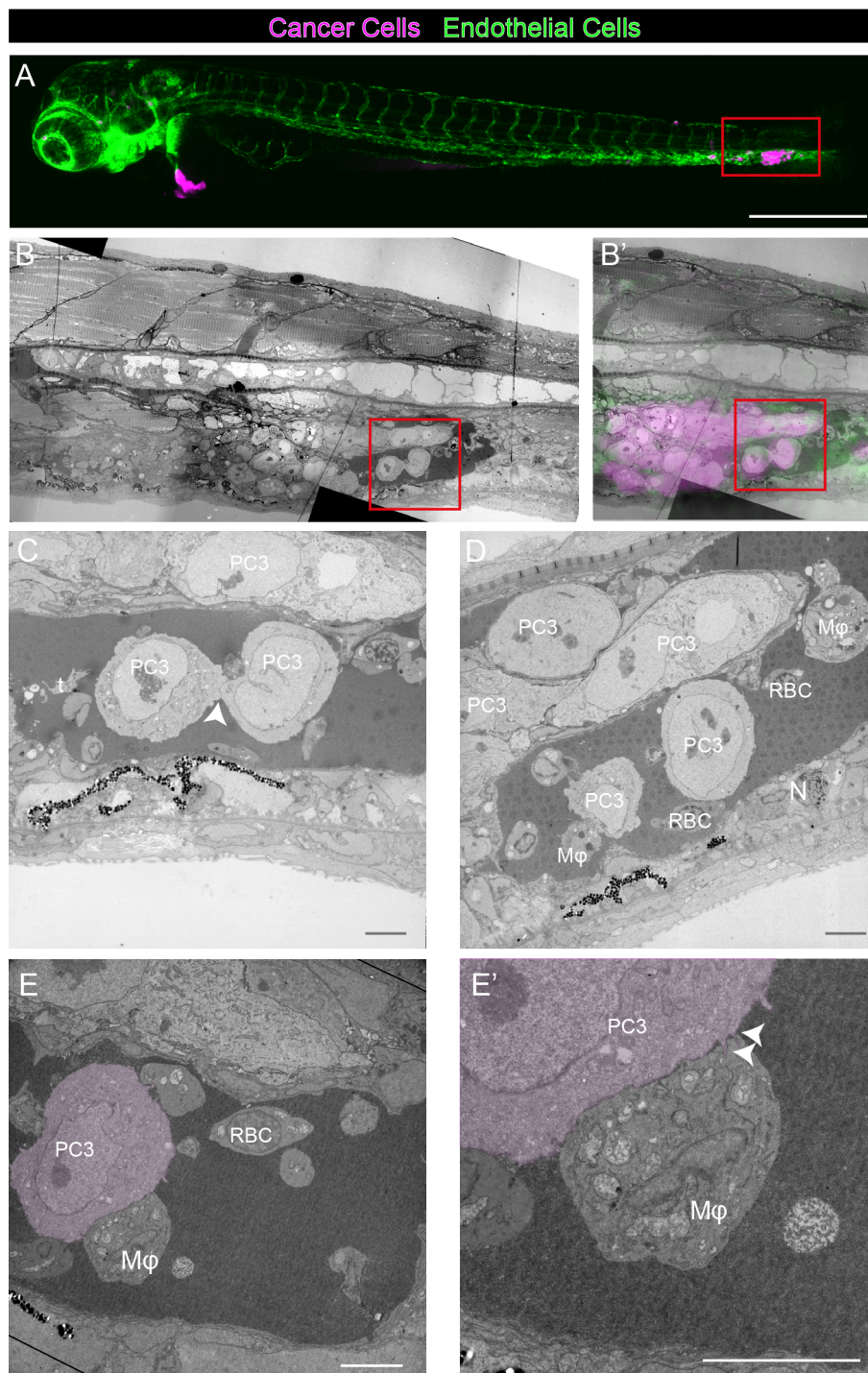


FIGURE 3.6. CLEM Further Reveals Host:Cancer Cell Interactions. (Legend continues on next page)

Figure 3.6: (Continued) **A** Shows a confocal tilescan of a 3dpf larva injected with human PC3-RFP (magenta) cancer cells 24 hours prior to imaging. **B** Shows a transmission electron microscopy (TEM) montage of a region of the tail of the same fish **B'** Shows an overlay of light microscopy and TEM. **C** High magnification view of two cancer cells within the caudal vein. t indicates an activated thrombocyte. Cancer cells make direct contact with one another (white arrowhead). **D** Another TEM view of the same cells, macrophages ($M\phi$) seen close to, and interacting with, cancer cells (PC3). **E-E'** A macrophage makes a broad interface with a cancer cell. Cancer cell membrane extensions can be observed interdigitating with the macrophage plasma membrane (white arrowheads). Macrophage mitochondria (green) are positioned close to the face of interaction. Scale bars: A = 500 μm , C-E' = 10 μm .

Inactive thrombocytes can be identified by their open canalicular system (OCS), a conserved surface membrane structure that permeates the plasma membrane of zebrafish thrombocytes and mammalian platelets (Jagadeeswaran et al., 1999), whereas activated thrombocytes exhibit an extended, highly stellate morphology. In TEM sections, both inactive and activated thrombocytes are seen close to tumour cells within the lumen of the vessel (**Figure 3.6**).

Further, cancer cells could be observed directly interacting with thrombocytes within the pre-metastatic niche and, occasionally, cancer cells appeared to partially engulf thrombocytes, surrounding their surface. It is unclear whether these interactions would lead to the phagocytosis of thrombocytes but, clearly, close interactions between human cancer cells and thrombocytes were present within the vasculature (**Figure 3.7**).

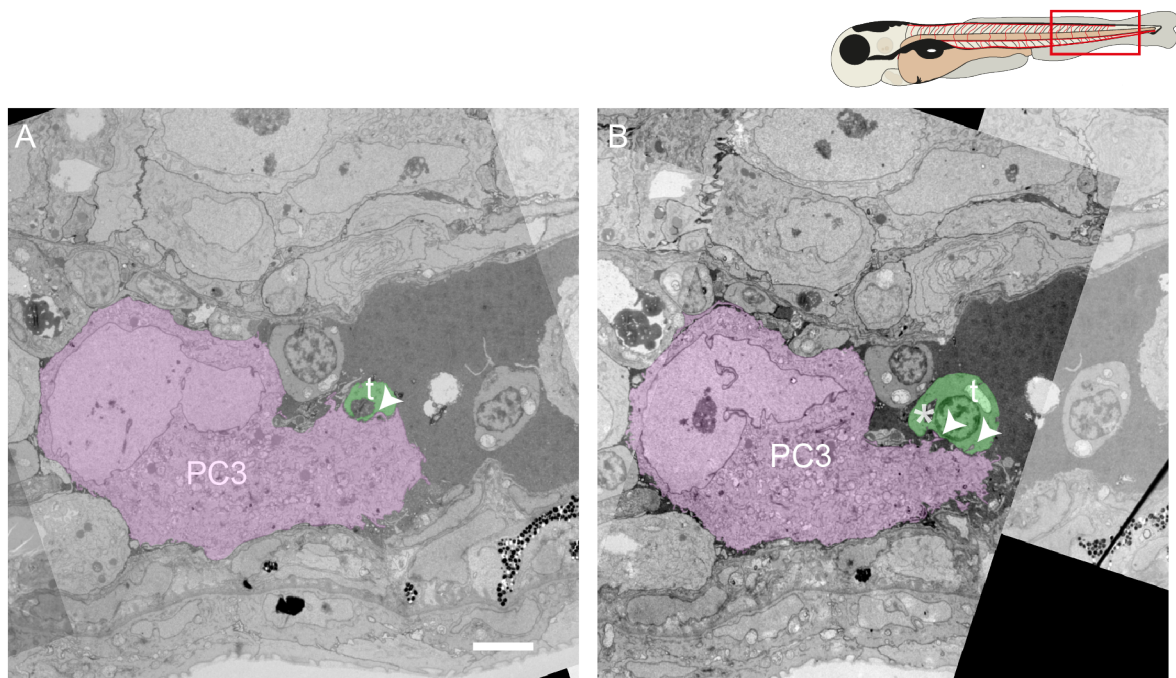


FIGURE 3.7. Human Cancer Cells Interact Closely with Thrombocytes. Transmission electron microscopy (TEM) of serial sections through a larval zebrafish tail containing human PC3 cells injected 24 hours prior. **A** Shows a cancer cell (Magenta, PC3) making close, engulfing interactions with a thrombocyte (green, t). Arrow heads show possible membrane exchange. **B** A further section showing the same cells. More of the thrombocyte is revealed, showing its open canalicular system (asterisk). Scale bar = 5 μm .

In order to perform human cancer cell xenografts in zebrafish, a compromise temperature was used to allow both host and cancer cells to operate within an acceptable temperature range. However, lower temperatures from 30-32 °C appeared to limit the activity of cancer cells, leading to few extravasation events occurring and rather little migration. Conversely, increased temperatures from 33-35 °C tended to lead to increased mortality in zebrafish larvae. This was most apparent during live imaging, where the addition of phototoxicity and anaesthesia may further contribute to larval death. This made experiments using human cancer cells inconsistent and rather low throughput. For these reasons a zebrafish-derived melanoma cell line, ZMEL, was used for further experiments within this work.

3.2.2 Characterising ZMEL cancer cell behaviours in the absence of a clot

The zebrafish melanoma cell line, ZMEL, was chosen as a highly metastatic zebrafish cell line, suitable for allografts into larval zebrafish. ZMEL cancer cells have been widely used for a range of studies on the behaviour of metastatic cancer (Heilmann et al., 2015; Follain et al., 2018). First, the behaviour of cancer cells in the absence of a generated thrombotic plug, or other interventions, was examined to establish a baseline for the activity of grafted cancer cells and the host response to these cells.

As with human cancer cells, ZMEL cells were seen to spread throughout the vasculature as early as 2 hpi. ZMEL have a much smaller diameter than human cancer cells, at roughly 5-10 µm across compared to the human cancer cells diameter of around 15-20 µm. Despite this difference in size, there appeared only minimal differences in their dispersal within the vasculature. ZMEL cells appeared slightly less likely to arrest within the ISVs than human cancer cells, but otherwise appeared to arrest most frequently in the same locations, these 'hotspots' have previously been shown to be where the flow-rate is more conducive to arrest, in the arterio-venous junction (AVJ) and CVP (Follain et al., 2018).

Allografted cancer cells were observed to extravasate relatively frequently, compared to

human cancer cells. During live imaging of human cancer cells, cancer cell extravasation was only observed in 2-3 larvae, while ZMEL cancer cells were seen to extravasate in almost all allografted larvae. ZMEL cancer cells within the vessels tended to have a highly rounded morphology, whereas cells found outside of the vessels were more extended (**Figure 3.8**). This elongation is likely due to the external forces of the surrounding cells and tissues that are clearly not present within the lumen of a vessel. Clustered groups of cancer cells appear to initiate metastatic processes at roughly the same time as one another, extending protrusions beyond the vessel of the lumen, though these extensions do not always lead to extravasation of the cell (**Figure 3.8**).

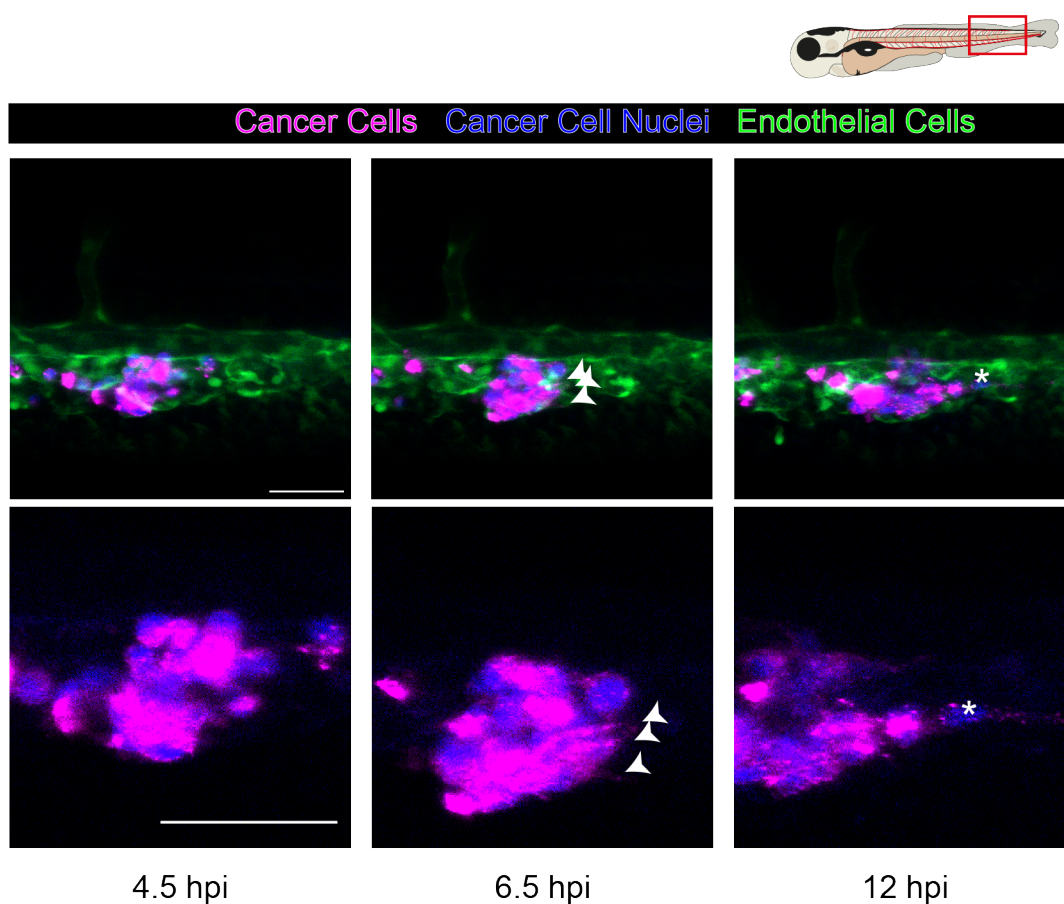


FIGURE 3.8. ZMEL Cancer Cells Form Extensions and Extravasate Into the Surrounding Tissues. ZMEL cancer cells (magenta with blue nuclei) in the caudal vein (green) of a zebrafish larva. Cancer cells begin by extending protrusions beyond the vessels (arrow heads). Some extravasated cancer cells migrate further from the initial point of exit from the blood vessel (asterisk). Scale bar = 50 μm .



Live imaging allows capture of events that might be rapid or rare. For example, occasionally cancer cells could be seen dividing (**Figure 3.9**). This was an infrequent event seen only 3-4 times throughout these studies, but was observed exclusively after the cancer cell had exited the vessel, after a brief period within the stroma. The first indication of a division nuclear shape change, presumably coinciding with DNA condensation. Within 10 minutes of this nuclear shape change, two daughter cells are apparent (**Figure 3.9**).

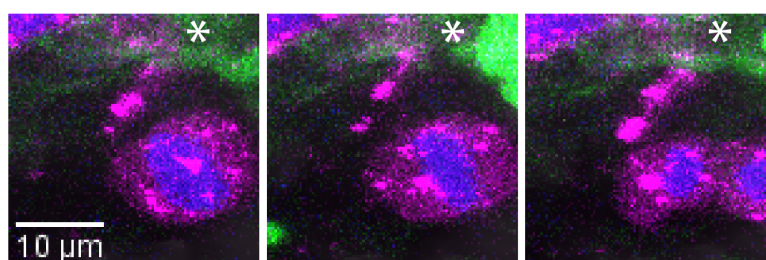


FIGURE 3.9. Extravasated Cancer Cells Undergo Mitosis. A ZMEL cancer cell (magenta with blue nucleus) divides 90 min after extravasation from adjacent vessel (green and arrow head). Asterisks indicate the nuclei of the extravasated cell. Frames are 10 minutes apart. Scale bar = 10 μm .



3.2.2.1 Cancer cell:Host cell interactions

Interactions between grafted zebrafish cancer cells and host cells were then characterised by live imaging. As cancer cells injected directly into the vessels of larvae generally arrest within the CVP and AVJ, innate immune cells residing in the nearby caudal haematopoietic tissue (CHT) appeared to have closest access to cancer cells and were recruited rapidly. Macrophages were observed to interact with ZMEL cancer cells both inside and outside of the vessel lumen (**Figure 3.10**). These interactions appeared close and could persist for extended time periods, over several hours.

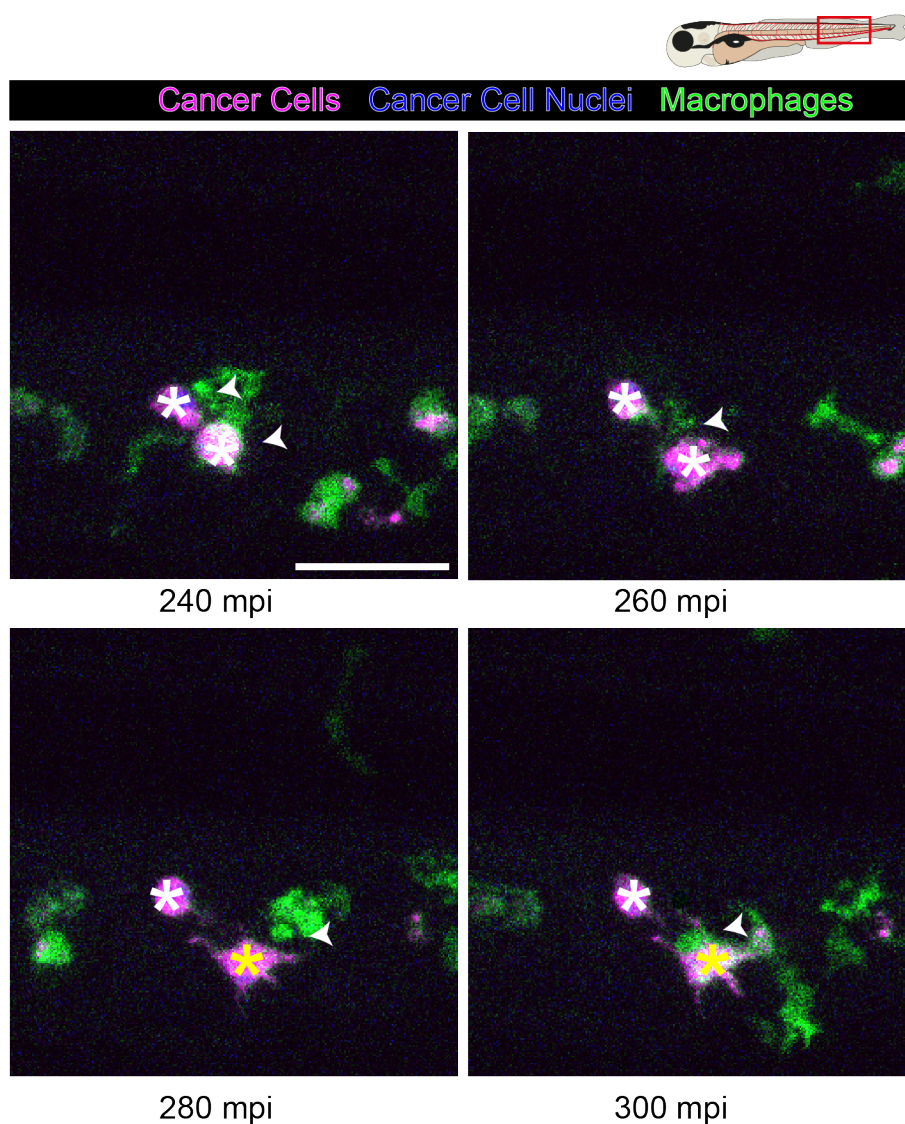


FIGURE 3.10. Macrophages interact directly with extravasating cancer cells. Timecourse imaging showing ZMEL cancer cells (magenta with blue nuclei) and macrophages (green) within the tail of zebrafish larvae. Macrophage:cancer cell interactions (arrows) occur while cancer cells are intravascular (white asterisks) and extravascular (yellow asterisks). Scale bar = 50 μm .



Occasionally, macrophages can be seen engulfing cancer cells (**Figure 3.11**). In these cases, nuclear labelling with hoechst shows that cancer cells die shortly after they are phagocytosed, with their nucleus condensing and becoming brighter, before fading. After having engulfed a cancer cell, these macrophages tended to adopt a rounded morphology and the fluorescent membrane

label of cancer cells was retained for up to 12 hours later. Phagocytosis by macrophages already containing cancer cell fluorescence appeared more common than for "unprimed" macrophages, perhaps indicating a separate population of pro-phagocyte macrophages (**Figure 3.11**).

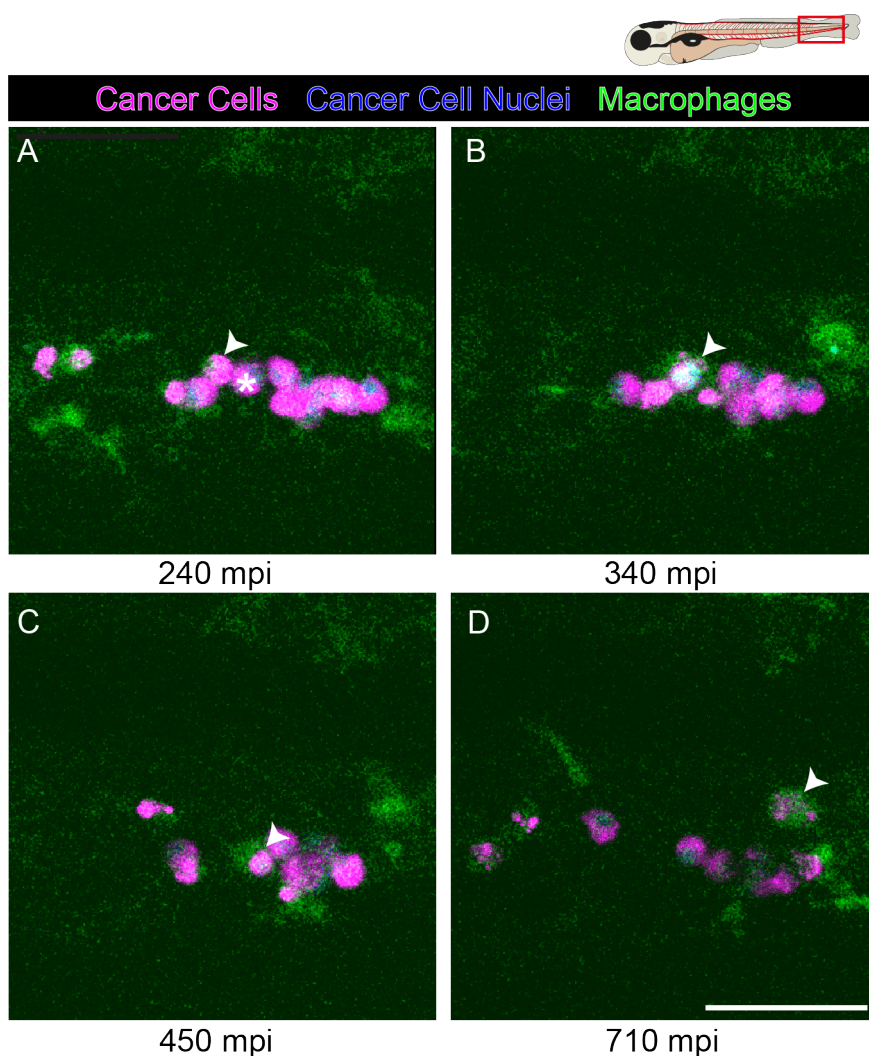


FIGURE 3.11. Macrophages occasionally phagocytose cancer cells. Timecourse imaging of ZMEL cancer cells (magenta, blue nuclei) and macrophages (green) in the tail of zebrafish larvae following a phagocytic event. A macrophage containing cancer cell fluorescence (arrow head) engulfs another cancer cell (asterisk) resulting in a burst of bright nuclear fluorescent. Some cancer cell fluorescence is retained within this macrophage. Scale bar = 50 μm .

Neutrophils, like macrophages, can be seen interacting with cancer cells in unwounded zebrafish larvae for the duration of all live imaging experiments. Although there appeared to be slightly fewer neutrophils recruited to cancer cells than macrophages, neutrophils were also observed to interact directly with cancer cells, occasionally appearing to crawl over the surface of an arrested cancer cell (**Figure 3.12**).

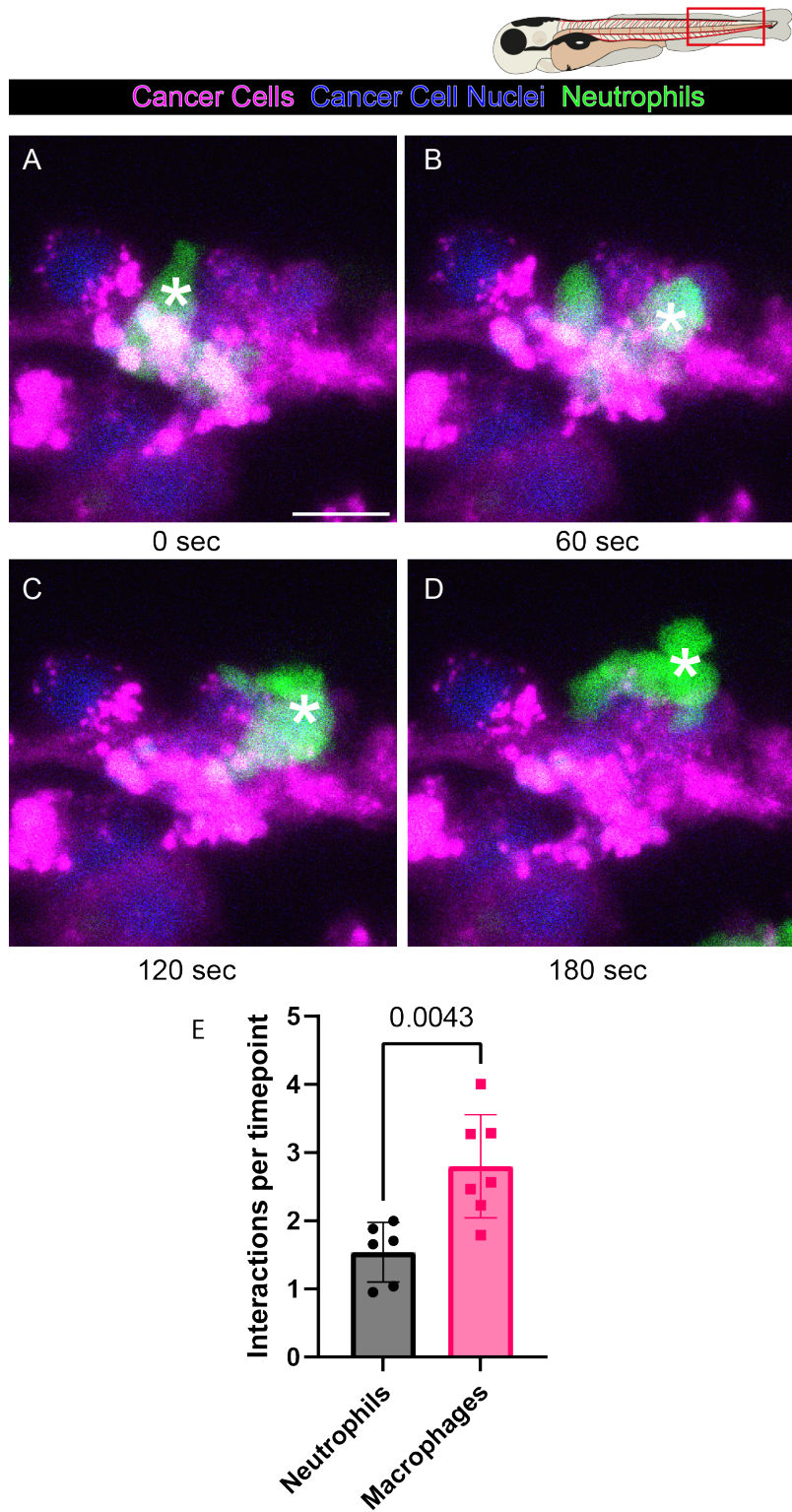


FIGURE 3.12. **Host Neutrophils Interact With ZMEL Cancer Cells.**(Legend continues on next page.)

Figure 3.12: (Continued) **A-D** Show timelapse imaging of ZMEL cancer cells (magenta with blue nuclei) and neutrophils (green) in the tail of a 2.5 dpf zebrafish larval tail, 16 hpi. A neutrophil (asterisk) appears to crawl over the surface of a cancer cell. **E** Shows quantification of the number of macrophage vs neutrophil interactions with cancer cells per timepoint. Scale bar = 10 μm .



Clusters of multiple ZMEL cancer cells could often be found, particularly in the AVJ. These clusters range from 2-20 cells. Cancer cells appeared to favour these clusters. Occasionally, cancer cells may break away from these clusters, but remain attached through long membrane extensions (Figure 3.13). These extensions could sometimes be observed to contract and drag cancer cells back to the cluster (Figure 3.13). This, apparently active, behaviour in retaining clustering may suggest a benefit to cancer cells from this clustering.

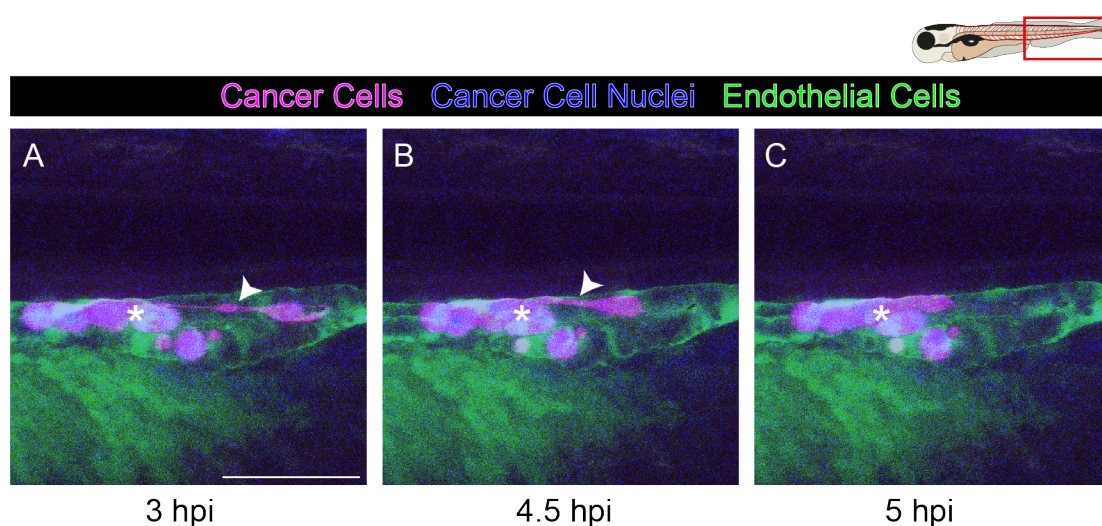


FIGURE 3.13. Cancer Cells Use Contractile Extensions to Cluster. **A-C** Show timelapse imaging of ZMEL cancer cells (magenta with blue nuclei) in the tail vessels (green) of a zebrafish larva, injected 3 hours prior. A cancer cell is linked to a cluster of cancer cells (asterisk) by a long membrane extension (arrow). This extension returns the singlet cancer cell to the cluster. Scale bar = 50 μm .



To investigate the importance of these clusters, live imaging was used to observe clustered and singlet cells over time. The distance between nuclei of cancer cells was measured at each timepoint, and cells that were within 30 μm of one another were defined as "neighbours". It

was observed that the extravasate, perhaps suggesting a cumulative attractive signal release. Furthermore, extravasated cancer cells had, on average, twice as many neighbours as those that did not extravasate (**Figure 3.14**).

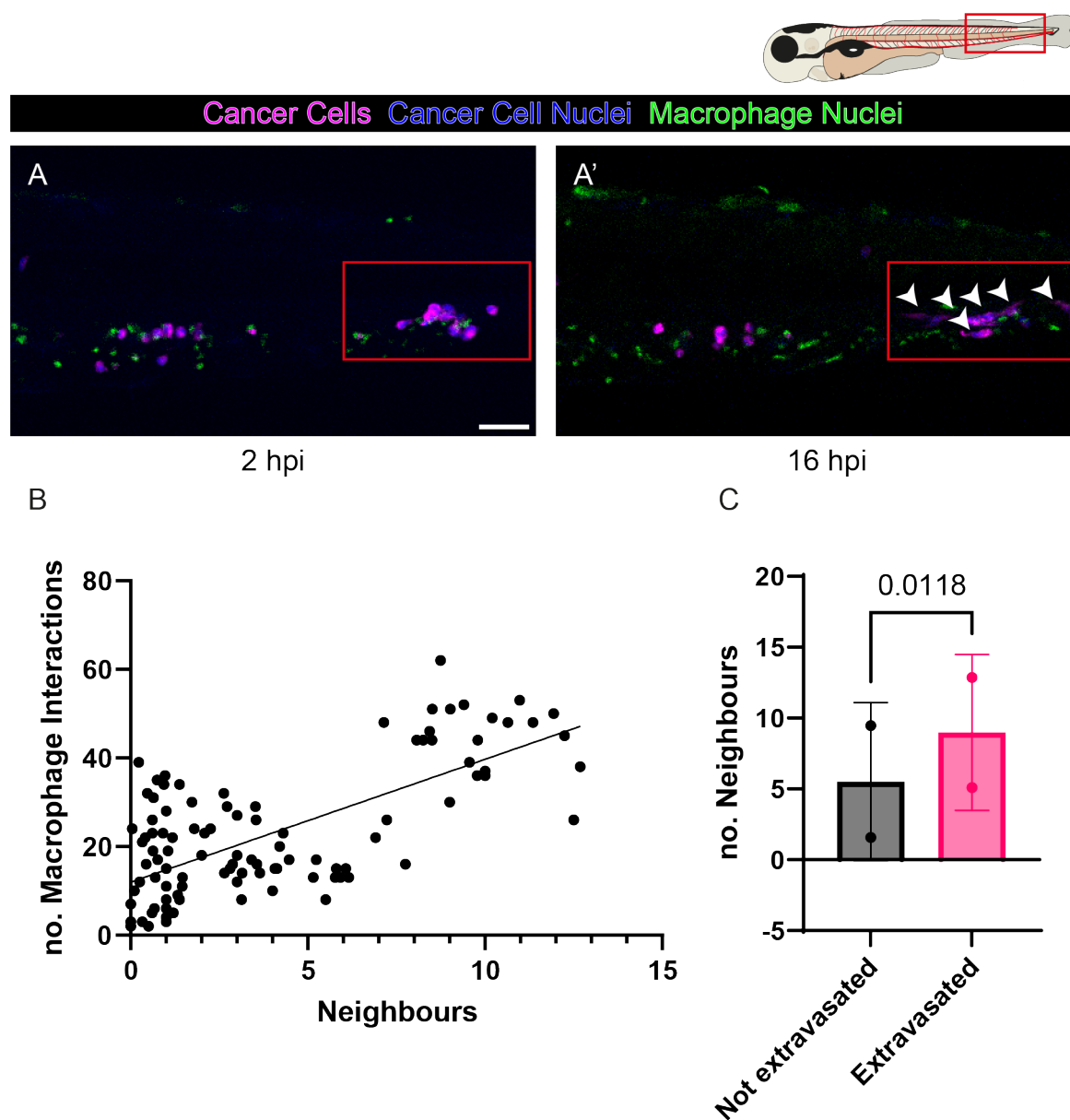


FIGURE 3.14. Clustered Cancer Cells Have Increased Macrophage Interactions and Extravasate More Frequently. **A-A'** Show ZMEL cancer cells at two time-point after injection into the tail of a zebrafish larva. Red box indicates clustered cancer cells. Arrowheads indicate extravasated cancer cells. **C** Shows simple linear regression of the number of neighbours vs the number of macrophage interactions experienced by a cancer cell. Slope = 2.772, Deviation from zero $p < 0.0001$. **D** Quantification of average number of neighbours throughout the timecourse for extravasated vs vascular cells. Analysed by Student's t-test. Scale bar = 50 μm .

3.2.3 Innate Immune Cells are Essential for Cancer Cell Extravasation

To investigate the importance of macrophages in driving cancer cell extravasation, macrophages were ablated by treating Tg(*mpeg:Gal4*; UAS:*nfsB-mCherry*) larvae with the pro-drug nifurpirinol (NFP). NFP treatment was optimised to cause significant reduction of macrophages without causing any observable toxicity to treated larvae (**Figure 3.15**).

Ablation of macrophages in 2 dpf larvae prior to injection of ZMEL cancer cells led to a reduction in extravasation of cancer cells, as observed by live imaging. Extravasation efficiency was assessed by measuring the percentage of cells observed within the trunk of the zebrafish larvae that were outside of the vasculature (henceforth referred to as percentage extravasated cancer cells). Using this readout as a means of quantification, extravasation appeared to be reduced by roughly half in macrophage-ablated larvae (**Figure 3.15**).

To ensure the observed reduction in cancer cell extravasation was due to the loss of macrophages, Tg(*mpeg:Gal4*; UAS:*nfsB-mCherry*) siblings were screened against red fluorescence to find larvae that were not expressing *nfsB*. These *nfsB*-negative larvae were similarly tested for percentage extravasated cancer cells. No significant difference in percentage extravasated cancer cells was observed when Tg(*mpeg:Gal4*; UAS:*nfsB-mCherry*) negative larvae were treated with NFP, compared to those treated with DMSO (**Figure 3.15**).

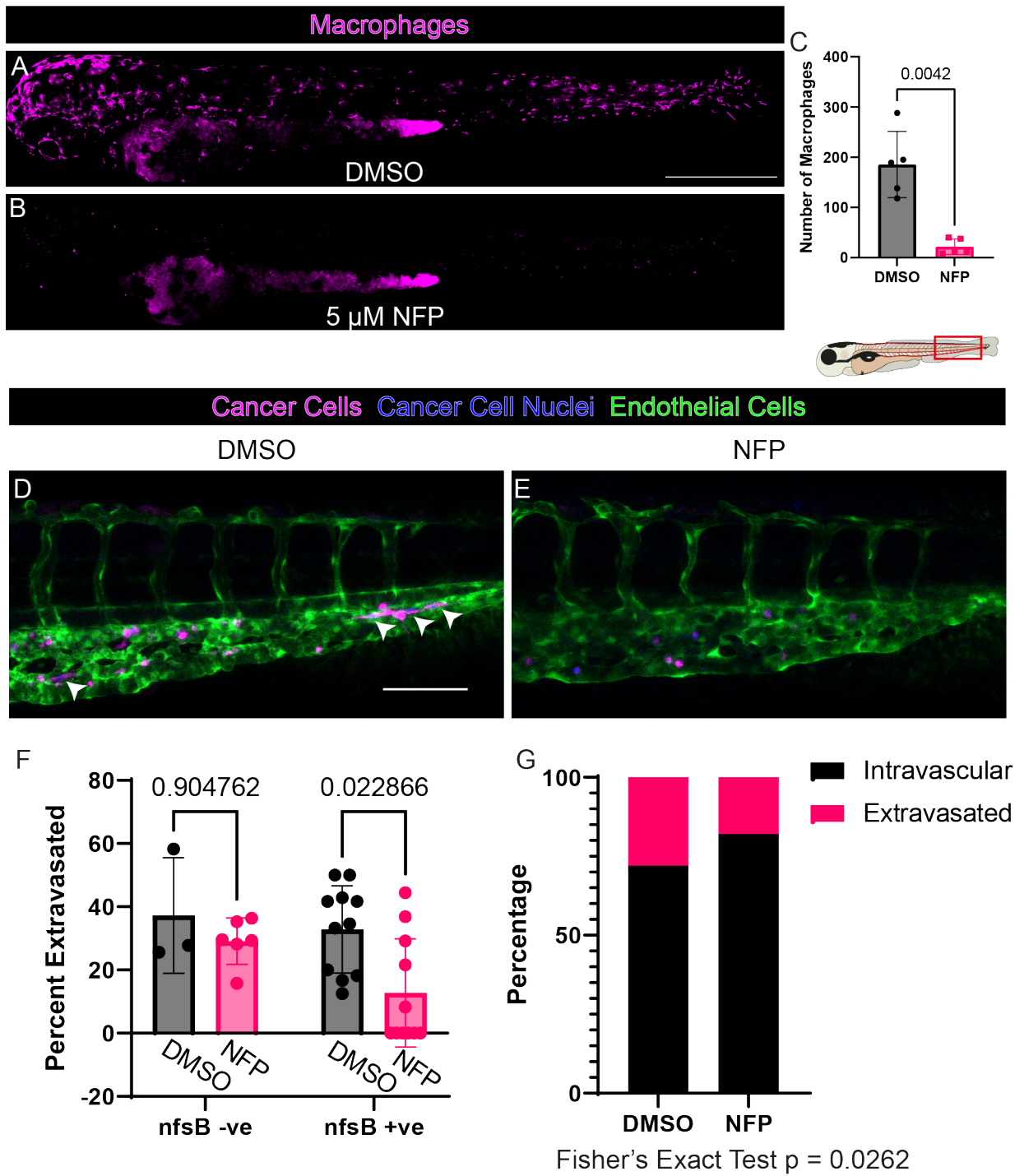


FIGURE 3.15. **Macrophages Are Required for Cancer Cell Extravasation.** (Legend continues on next page)

Figure 3.15: (Continued) **A-B** Show tilescans of nifurpirinol (NFP)-treated versus control DMSO-treated 3 dpf larvae expressing *nfsB*-mCherry specifically in macrophages (magenta). **C** shows quantification of the number of macrophages detected in larvae treated with DMSO versus NFP. Analysed by Student's t test. **D-E** Representative images of ZMEL cancer cells (magenta, blue nuclei) in control versus NFP-treated, 3dpf, *Tg(mpeg:Gal4; UAS:nfsB-mCherry; fli:EGFP;)* larvae. Cancer cells (magenta, blue nuclei) can be seen inside the vessels of the trunk, and extravasated into the surrounding tissues (arrow heads). **F** Quantification of the number of extravasated cells in *nfsB* positive and negative larvae treated with NFP. Multiple Mann-Whitney U tests with Šidák correction used for analysis and P values are presented above these graphs. **G** Contingency analysis of cancer cell extravasation in *nfsB* positive larvae using Fisher's exact test. Scale bar = 50 μ m.

Work from Richard Hynes' lab has identified how CXCR2 is an important receptor for recruitment of a subset of neutrophils to the site of cancer cells arrested in early metastatic niches within mouse lungs (Labelle et al., 2014). These neutrophils appear to be pro-metastatic in this context (Labelle et al., 2014). To examine such pro-metastatic effects further in our larval zebrafish model, fluorescent reporter lines for neutrophils were used to allow live imaging of their behaviours.

To further investigate the effect of neutrophils in the pre-metastatic niche, neutrophil-specific ablation was performed using NFP treatment of larvae expressing nitroreductase enzyme specifically within their neutrophils. Ablation of neutrophils in 2 dpf larvae, prior to injection of ZMEL cancer cells, led to a reduction in the percentage of extravasated cancer cells. In DMSO-treated larvae, about 35% of cells arrested within the tail were seen to have extravasated by 16 hpi, while only 20% of cancer cells extravasated in NFP-treated larvae expressing *nsfB* in their neutrophils (**Figure 3.16**). These data suggest an important role for innate immune cells within the pre-metastatic niche.

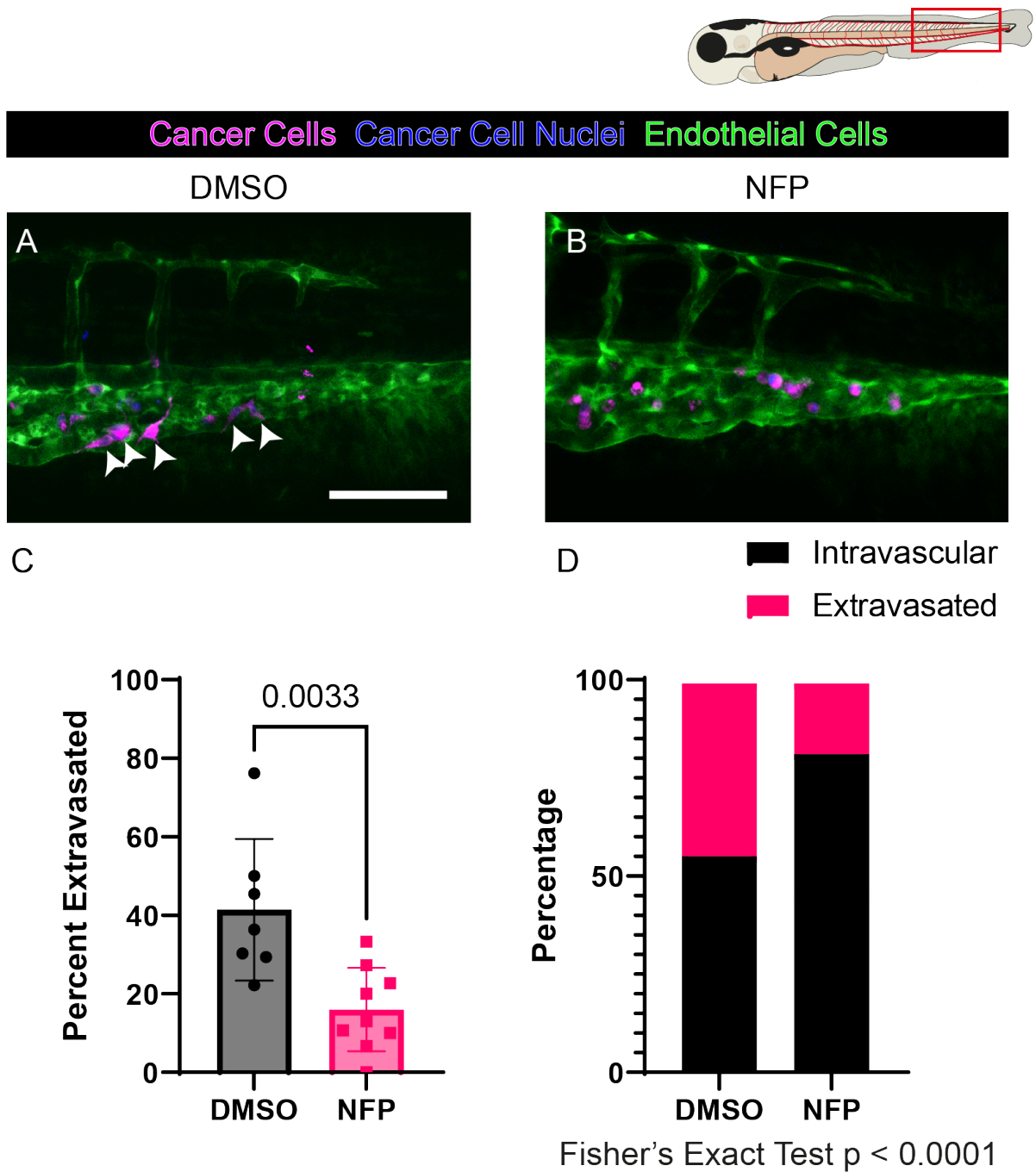


FIGURE 3.16. Neutrophils Are Required for Extravasation. A-B Show 3 dpf larvae injected with ZMEL cancer cells (magenta, blue nuclei) 16 hours prior to imaging. Cancer cells can be seen inside the vessels (green), and extravasated (arrow heads). C-D Quantification of the number of extravasated cells in the context of neutrophil ablation using Student's and Fisher's exact test. Scale bar = 50 μm .

3.3 Discussion

3.3.1 Human Cancer Cells

As discussed, the use of human cancer cells in a zebrafish model may have some advantages over the use of zebrafish cells, including the potential for "personalised medicine" approaches, and allowing continuity with other models (**Section 1.4.3**). Moreover, human cancer cell lines are widely used and their culture is commonplace making them easily accessible for xenograft experiments.

Previous research using human cancer cell xenografts in zebrafish has used a range of temperatures to allow host larvae and cancer cells to co-exist. However, here I found that this temperature compromise appeared prohibitive, leading to mortality in larvae or loss of activity in human cancer cells. It is not clear why I was unable to replicate prior research, though future experiments could be performed to further optimise human cancer cell experiments to take advantage of some of the benefits that these may offer.

Vasculogenic mimicry is a phenomenon where cancer cells may take the place of endothelial cells to produce a vessel-like structure with a functional lumen, which may integrate with the network of host vessels (Maniotis et al., 1999). Here, in my zebrafish studies, I observed cancer cells appearing to replace damaged vessels within the trunk of the larvae, it is possible that these cancer cells are able to recognise the angiogenic signals produced in response to vessel damage. This observation might allow the development of an *in vivo* model for live imaging of the process of vasculogenic mimicry, a process that has been historically difficult to study in animal models. Zebrafish, clearly, would offer the opportunity to live image this phenomenon. Vasculogenic mimicry has been linked to poor prognosis within the clinic, so an understanding of the mechanisms of this process could allow the development of potential treatments.

3.3.1.1 CLEM

Light microscopy allows the observation of the dynamic processes that might drive cancer metastasis, and may reveal close cellular interactions between host cells and cancer cells. However, the nature of these interactions can be difficult to resolve. Electron microscopy is able to resolve subcellular detail, down to the nanometre scale. Here, CLEM was used to gain insights into the composition of the pre-metastatic niche.

Resolution of the internal structures of cells may reveal interesting behaviour of cancer cells and host cells. For example, the increased resolution afforded by TEM in my larval zebrafish model appears to corroborate my observations, using light microscopy, that macrophages may interact with cancer cells with a broad front, similar to that of a T cell immune synapse (Ambler et al., 2020). Further to this, it also reveals the apparent alignment of the organelles during these interactions. Mitochondrial positioning close to immune synapses has previously been described as an essential process for proper signalling and activation of T cells (Baixauli et al., 2011). Here, I have observed the mitochondria of macrophages clustering close to an interface with a cancer cell, which may indicate a complex or energy intensive process.

Macrophages have previously been described to form tight interactions, even synapses with a range of cell types and may exhibit different behaviours dependent on the context of these interactions (Kasproicz et al., 2018). Phagocytic synapses are important for the clearance of apoptotic cells, and might allow macrophages to phagocytose and kill cancer cells, although cancer cells have developed strategies to escape this engulfment by expression of "dont-eat-me" signals (Barclay and Van Den Berg, 2014). Interestingly, I also observed what appears to be transfer of material between cancer cells and macrophages within the pre-metastatic niche. Direct transfer of macrophage material to cancer cells has been shown stimulate their migration another zebrafish model (Roh-Johnson et al., 2017).

Cancer cells are often seen within the caudal plexus. This is a region of blood vessels that forms an irregular structure around the CHT, allowing nascent blood cells access to the vascu-

lature of the fish. Due to the complexity of this region, it can be difficult to determine whether a cancer cell has undergone transendothelial migration. Use of CLEM allowed me to elucidate some of the complexities of the endothelium, showing potential remodelling due to the presence of cancer cells in the vessels. Though this remodelling is partially visible using confocal microscopy, as the endothelial layer is so thin, it can be difficult to appreciate the extent of these changes without the use of electron microscopy.

As with their interactions with endothelial cells, interactions between neighbouring cancer cells were extremely tight, suggesting an importance for cancer to cancer interactions within this model. Prior research has described collective migration in metastasis (Campbell et al., 2019). Although individual mesenchymal behaviour may allow more efficient movement, cancer cells have been observed to make contacts with one another and exhibit some partially epithelial behaviour (Campbell et al., 2019). It has been speculated that these contacts might cause polyclonal populations of cancer cells to move together, allowing the more migratory cells to drive the movement of less migratory cells that may be more suited to the establishment of a secondary tumour (Campbell et al., 2019).

Activation of platelets is known to stimulate the release of their granule contents which may drive immune cell recruitment to cancer cells (Labelle et al., 2014). Studies in mammalian models have previously established that cancer cells may overexpress tissue factor, causing the activation of platelets, and coagulation, within the pre-metastatic niche (Gil-Bernabé et al., 2012). Here, I observed few instances of activated thrombocytes close to cancer cells. This could be caused by a lack of cross-species affinity in the activating factors expressed by human cancer cells. Although human cancer cell interactions with thrombocytes may not commonly cause thrombocyte activation, these interactions appeared to include the transfer of material from one cell to another. Previous research has shown how transfer of platelet material to cancer cells might drive plasticity and aggression in circulating tumour cells (Rodriguez-Martinez et al., 2022), while tumour "education" of platelets has been noted in a clinical setting as a biomarker for disease progression (Best et al., 2017).

Through a combination of light microscopy and transmission electron microscopy (TEM), I was able to observe human cancer cells interacting with a range of host, zebrafish cell lineages which have previously been reported to have pro-metastatic effects in other models (Labelle et al., 2014; Gil-Bernabé et al., 2012; Qian et al., 2011). Although I did observe human cancer cell extravasation using this model, it appeared relatively infrequent and slow in comparison to the allograft model using zebrafish cancer cells. I speculate that the metastatic potential of these cancer cells is affected by the reduced temperature that must be used to allow zebrafish and cancer cells to simultaneously survive over a period of days.

3.3.2 ZMEL Cancer Cells

3.3.2.1 Allografted Cancer Cell Behaviour

It is important to determine the behaviour of grafted cancer cells under normal conditions and to establish the health of the cancer cells in their new environment. Here, I have detailed a number of cancer cell behaviours seen in untreated larvae. Previous studies have shown the importance of flow dynamics for tumour cell arrest, with lower flow rates preferentially initiating arrest (Follain et al., 2018). Similarly, in my own studies I have seen greater incidence of cell arrest within the AVJ and CVP, where blood flow is attenuated by directional changes and entrance into smaller vessels.

Cell division is clearly a good indicator of cell viability within a population. Although rare, I was able to observe ZMEL cells dividing during my experiments, thus indicating that the health of cells had not been significantly compromised. Hoechst labelling was used to visualise the nuclei of these ZMEL cells, which may have diminished their ability to divide to some extent, too. Interestingly, cell division appeared more likely after cancer cell extravasation. Studies of cell division in different contexts have shown that mechanical tension may stimulate and facilitate division events (CURTIS and SEEHAR, 1978). This could suggest that cancer cells within the vessels are less likely to divide due to a lack of mechanical tension, as they are not surrounded

by cells and ECM. Reporters of cell division, such as incorporation of modified nucleotides 5-ethynyl-2'-deoxyuridine (EdU) and bromodeoxyuridine (BrdU), would allow for further study of the proliferative behaviour of these grafted cancer cells in the future.

Interestingly, cell death by apoptosis was not observed as it had been when using human cancer cells. However, there were occasionally phagocytic events, whereby macrophages engulfed entire cancer cells. This could be due to the size difference observed between human cancer cells and ZMEL, making phagocytic events difficult or impossible with human cancer cells. To more specifically test for apoptotic events in the future, terminal deoxynucleotidyl transferase dUTP nick end labeling (TUNEL) staining could be used. This may reveal additional details about the health of grafted cancer cells within zebrafish larvae. A lipophilic membrane dye was used to visualise ZMEL cancer cells. After a phagocytic event, this fluorescence was retained for some time in macrophages, and it appeared that "virgin" macrophages were less likely to phagocytose cancer cells than those containing ZMEL fluorescence, suggesting a priming effect. The retained cancer fluorescence within these cells could be used to allow fluorescence-activated cell sorting (FACS). First selecting for macrophages by their expression of enhanced green fluorescent protein (EGFP) under the *cfms* promoter and, subsequently, separating out macrophages that contained the DiI cancer label. This would allow further characterisation of the phenotypic differences between these cells and might reveal a differential activation state among macrophages that have phagocytosed these cancer cells.

Although macrophages may occasionally clear grafted cancer cells, innate immune cell interactions have been shown to drive cancer progression at virtually all stages of the disease (Güç and Pollard, 2021). Work from our lab has shown the importance of macrophages and neutrophils at the early stages of cancer development in zebrafish, where they provide trophic support and enhance clonal growth (Feng et al., 2010; Feng, 2012; Antonio et al., 2015). To determine whether immune cells interacting with ZMEL cells could play similar supporting roles in this zebrafish model of metastasis, fluorescent reporter lines for macrophages and neutrophils were used to track their recruitment to vascular cancer cells. As with genetic models of cancer, innate immune

cells are indeed seen interacting with grafted cells.

Previous studies using *de novo* genetic models of cancer observed that, as clones of pre-neoplastic cells proliferated and became larger, there was an increase in the number of innate immune cells recruited to the clone (Feng et al., 2010). Here, some early, low repeat, data suggests that larger clusters of cancer cells appear to recruit greater numbers of macrophages, perhaps suggesting a cumulative, attractive signal released or induced by these cancer cells. Furthermore, cancer cells in these clusters also appeared more likely to extravasate, suggesting a possible selective advantage to these clusters in capacity for metastasis, perhaps due to increased innate immune cell recruitment. To further investigate this phenomenon, extravasation and clustering could be measured after immune cell ablation experiments. If cancer cell clustering and extravasation were no longer correlated in the absence of innate immune cells, this would suggest clustering behaviours drive metastasis through increased immune cell recruitment.

3.3.3 Innate Immune Cells are Required for Extravasation

Previous data from murine models implicated innate immune cell recruitment to tumour cells as essential for many processes in metastasis. These interactions range from guiding tumour cells from the primary tumour to vessels and driving intravasation (Sharma et al., 2021), to increasing cancer cell survival in the tissues of distant organs to allow the formation of secondary tumours (Gil-Bernabé et al., 2012). However, many of these studies were undertaken in murine models that are often limited in their ability to follow the actions of cells over time because of tissue opacity. Translucent larval zebrafish offer a model of the pre-metastatic niche that is highly amenable to live imaging, allowing the dynamic behaviours of these cells to be observed and quantified.

It is clear from the data presented in this work, that macrophages frequently interact with cancer cells and, since increased interactions between cancer cells and macrophages appeared to be associated with increased likelihood of extravasation, these interactions may be important for

cancer cell survival and perhaps drive cancer extravasation events. One approach to test this dependency on macrophage:cancer cell interactions would be to diminish macrophage numbers. This can be achieved in a number of ways, including the use of *panther* mutants, or morpholino injections to knock down macrophage lineages (Liongue et al., 2009), but here I have used an *E. coli* nitroreductase enzyme, specifically expressed by macrophages, to convert a pro-drug into a toxic product, leading to the specific death of macrophages.

Although ablation significantly diminished the number of macrophages, some reporter fluorescence remained visible after treatment. However, my live imaging studies revealed that this was likely a combination of immobile, dying macrophages, other apoptotic material left over after macrophage death, and neutrophils that had taken up macrophage material. There appears to be increased fluorescent material remaining after macrophage ablation when compared to other published ablation lines, and even the other lines used here. As macrophages are the 'professional' phagocytes, it is possible that their loss leaves only less effective phagocytic cells, such as neutrophils, to clear up remaining cell debris.

As anticipated, macrophage ablation led to a significant reduction of cancer cell extravasation, likely indicating a key role for macrophages in cancer cell metastatic potential. Previous studies have offered a number of mechanistic insights into the roles of macrophages in the pre-metastatic niche, including increasing vessel permeability, remodelling of the surrounding ECM, and suppressing the lymphocyte response to cancer cells (Kim et al., 2019a; Kaplan et al., 2005; Brownlie et al., 2021).

As with macrophages, I was able to use a nitroreductase line to ablate the neutrophil population. Here, neutrophil numbers dropped significantly and remaining neutrophils were observed to be largely stationary. Following this neutrophil ablation, I was able to show a reduction in extravasation events by almost 50%, suggesting that neutrophil presence within the larva might also be important in facilitating cancer metastasis, potentially due to direct interactions with cancer cells. To study this further, it would be valuable to reduce neutrophil numbers or their

interactions with cancer cells, separately.

As prostaglandin-E2 (PGE2) has been previously implicated as a trophic signal, delivered by leukocytes to support early pre-neoplastic cells in their growth (Feng et al., 2012), it would be interesting to study whether it is also an important factor within the pre-metastatic niche. Chemical inhibitors and genetic targeting of prostaglandin synthesis have been previously used to diminish PGE2 in the larval zebrafish, offering multiple possibilities to investigate its potential effects on the pre-metastatic niche and cancer cell extravasation (Feng et al., 2012; Loynes et al., 2018).

Chapter 4

Investigating the Mechanics of the Platelet-Driven Pre-Metastatic Niche

4.1 Introduction

Having established a model that allows the study of the pre-metastatic niche in zebrafish larvae, I wanted to investigate the role of innate immune cells in cancer cell extravasation from blood vessels. Previous studies have indicated that the presence of innate immune cells in the pre-metastatic niche might be required for the formation of secondary tumours (Qian et al., 2011). Furthermore, the literature has suggested that the formation of fibrin micro-clots, and platelet activation within the pre-metastatic niche might drive innate immune cell recruitment to cancer cells, which subsequently mediate cancer cell survival and metastasis (Labelle et al., 2014; Gil-Bernabé et al., 2012). Here, I aim to probe this relationship further and establish roles for platelets and the coagulation cascade in mediating innate immune cell behaviours within the pre-metastatic niche.

4.2 Results

4.2.1 The innate immune response to laser-induced clotting

Zebrafish larvae have been used as a model for thrombosis using multiple methods to generate thrombosis (Gregory et al., 2002). Here, an ablation laser was used to cause sufficient damage to the vessel to induce clotting, without generating a lesion in the vessel such that a cell could move through without undergoing classical extravasation.

A laser-triggered thrombocyte plug is visible both by using the brightfield or by imaging the fluorescence of GFP labelled thrombocytes (**Figure 4.1**). Time to occlusion is very rapid, taking less than a minute to block the vessel completely. Once a vessel is occluded, clot size is generally stable as the loss of flow prevents new cells from entering the plug. As previously described, there is heterogeneity in the brightness of *itga2b*:GFP positive cells, with dimmer cells and brighter cells both contributing the plug (Thattaliyath et al., 2005). There also appear to be completely unlabelled cells trapped within the plug, which may be erythrocytes that have been captured in the blockage (**Figure 4.1**).

Resolution of the thrombus generally occurs about 5-6 hours after its formation. During this period, innate immune cells are recruited to the region of the clot, and interact with the clot directly (**Figure 4.2**). Neutrophil numbers within the tails of larvae with laser-induced thrombi, or with mock wounds in the stroma (that do not cause clotting) were quantified over time. The total neutrophil numbers in the field of view peaked shortly after the resolution of the thrombocyte plug and restoration of blood flow into the vessels beyond the injury (**Figure 4.2**). This delayed peak in neutrophil response may suggest an ischemia reperfusion injury response, whereby a large number of immune cells may be recruited to a site of an ischemic injury soon after normoxia has been restored (Zhang et al., 1994; King et al., 2000).

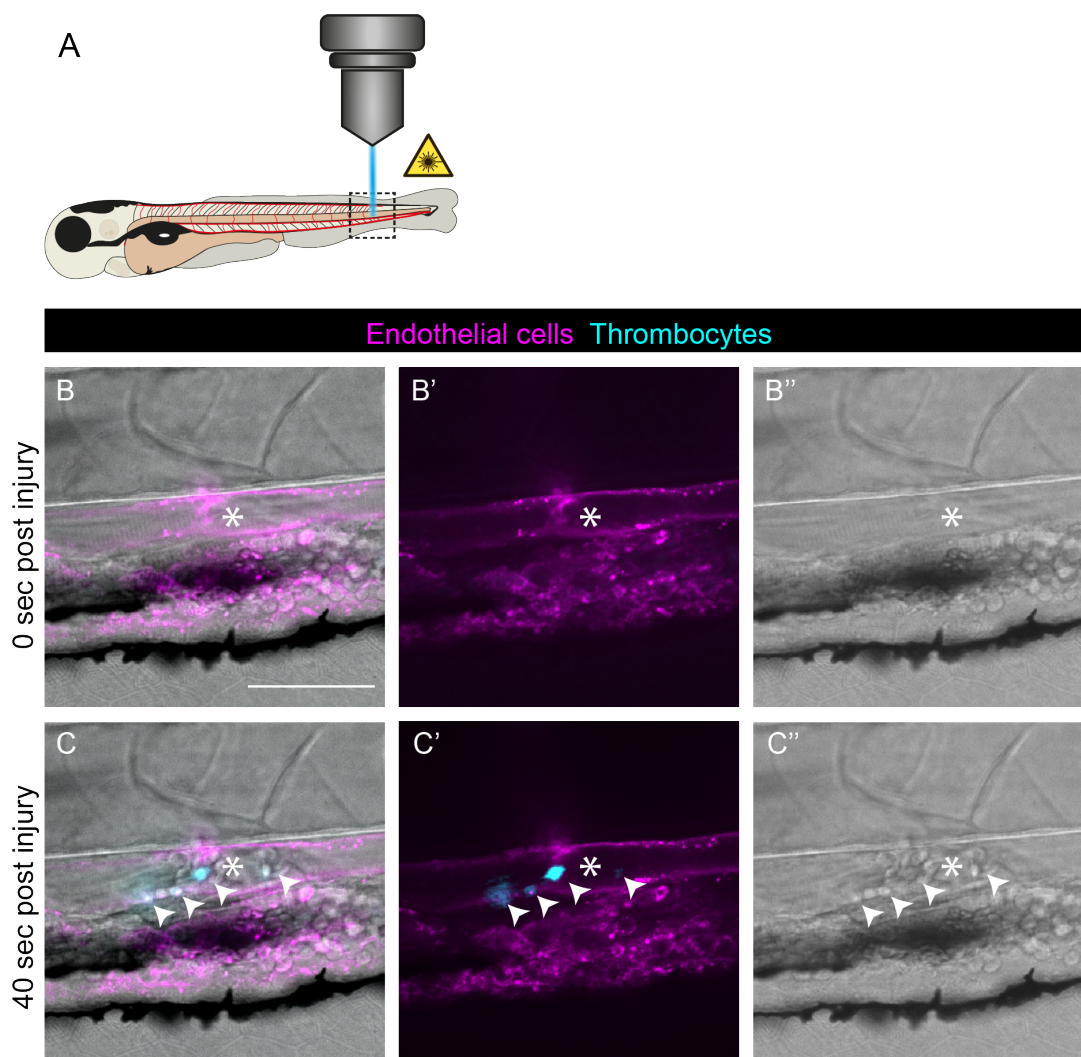


FIGURE 4.1. Visualising the Formation of a Thrombotic Plug in Zebrafish Larvae Following Laser Insult. **A** Schematic to show the location of laser injury and subsequent imaging. **B-B''** Shows combined fluorescence and brightfield views of the dorsal aorta (magenta) immediately following laser-injury. Asterisk shows the location of the laser-wound. **C-C''** Combined fluorescent and brightfield views of the generated thrombotic plug at peak size. Activated thrombocytes (cyan, arrow heads) and other, unlabelled, cells make up the plug. Scale bar = 50 μ m.

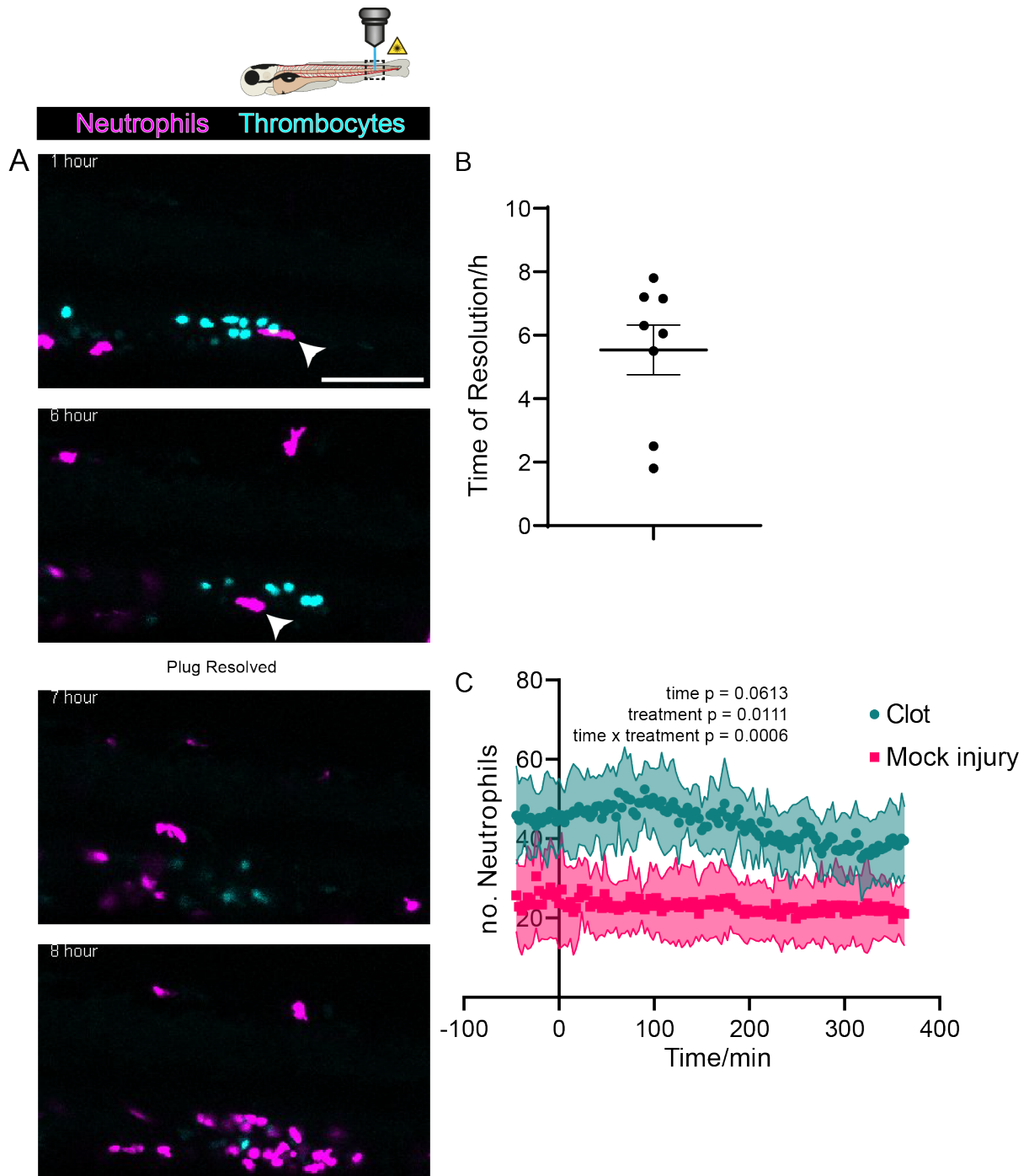


FIGURE 4.2. Describing the Resolution of a Clot in Zebrafish Larvae.

A Still images from timelapse microscopy of a laser-induced thrombus in the dorsal aorta of a 3 dpf larva. Thrombocytes (cyan) make up a plug within the vessel. Neutrophils (magenta) interact with the plug (arrows). Shortly after resolution of the plug, neutrophil numbers in the tissue dramatically peak. **B** Shows quantification of the mean time to resolve a thrombotic plug. **(C)** Quantification of neutrophils detected in the region of the plug, analysed by two-way ANOVA. Scale bar = 50 μ m.

4.2.2 The Role of the Thrombocytic Plug in Innate Immune Recruitment

Following these data suggesting the importance of macrophages and neutrophils for metastasis, innate immune cell recruitment to cancer cells arrested in the blood vessels was then investigated. To study how a thrombocytic plug might affect innate immune cell recruitment, 3 dpf larvae were laser wounded within the dorsal aorta prior to cancer cell injection. Cancer cells were injected distally to the site of the wound and some of these were subsequently observed to be in the vicinity of the thrombocytic plug.

First, macrophage recruitment was studied. An increase in macrophage interactions with cancer cells in larvae with a thrombocytic plug was observed, from around 1.3 macrophage:tumour cell interactions per cell in each timepoint in larvae without thrombosis, up to a mean of about 2.4 interactions per cell in those with thrombosis (**Figure 4.3**).

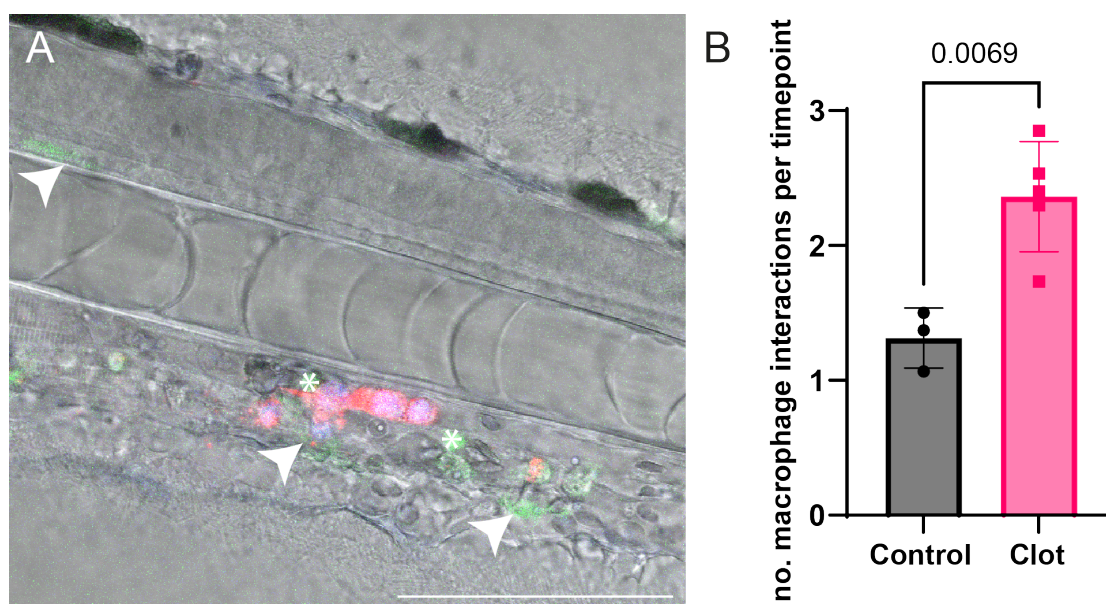


FIGURE 4.3. Thrombocytic Plugs Lead to Recruitment of Macrophages to Cancer Cells. **A** shows ZMEL cancer cells (magenta, blue nuclei) within the flank of a 3 dpf larva with a laser-induced thrombocytic plug. Thrombocytes (green, asterisks) and macrophages (dim green, arrow heads) can be seen closely associating with cancer cells. **B** shows quantification of local macrophage interactions with cancer cells in larvae with a clot. Analysed using Student's t-test.

Perhaps surprisingly, the presence of a thrombotic plug in the region of the cancer cells did not appear to change the number of neutrophils interacting with cancer cells at each time point. However, as previously discussed, following the resolution of a thrombotic plug and reperfusion of the blood vessel, there is a rapid increase in neutrophils recruited to the vicinity of the clot with many more neutrophils found within the blood vessels and within the tissue around the wound. This increase in neutrophils after reperfusion was retained in the presence of cancer cells, and led to tumour cells in the region subsequently experiencing a more than 2-fold increase in interactions with neutrophils, peaking around 3 hours after reperfusion of the vessel and returning to baseline levels another 3 hours after that. (**Figure 4.4**).

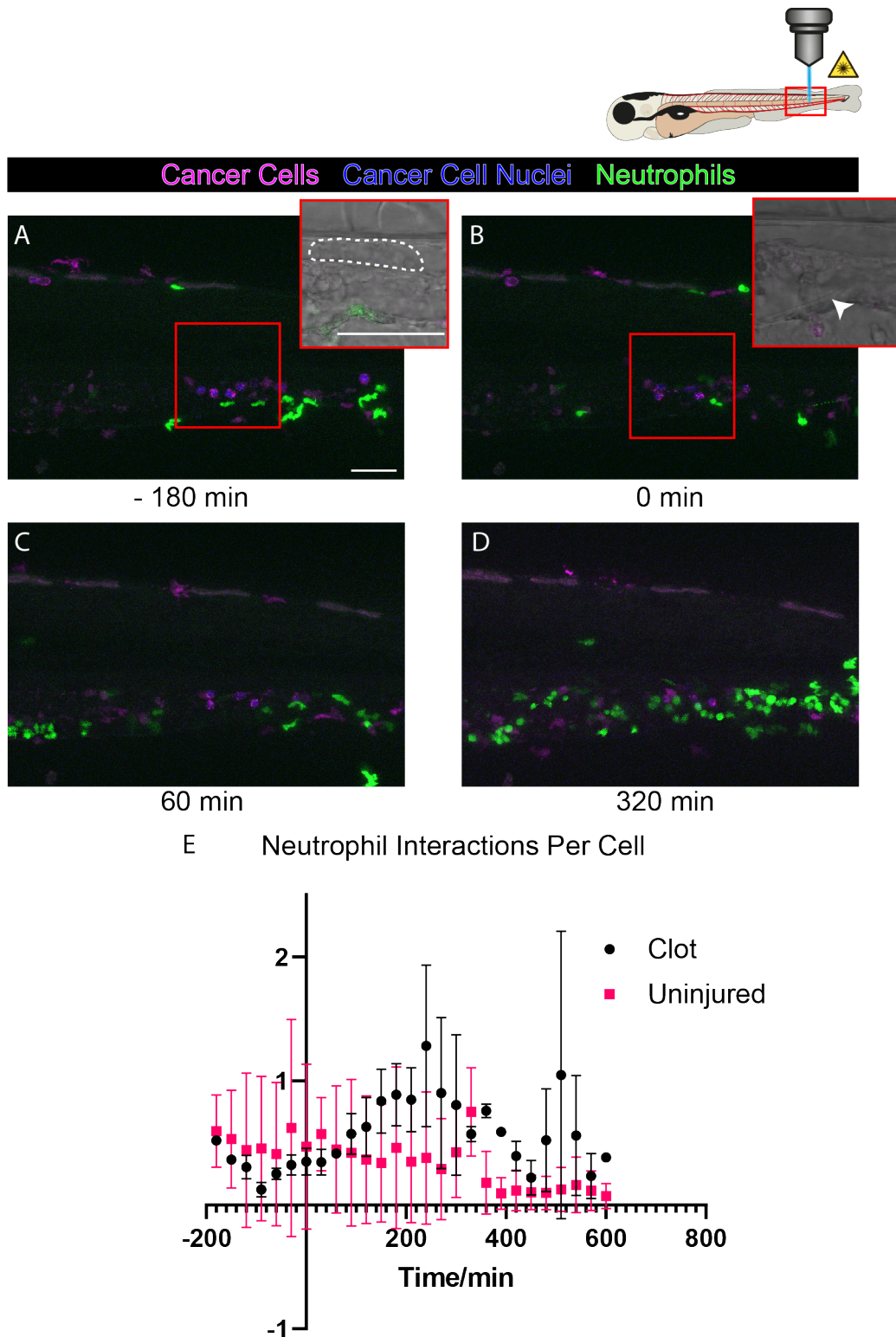



FIGURE 4.4. **Reperfusion Leads to Increased Neutrophil Interactions with Cancer Cells.** (Legend continues on next page.)

Figure 4.4: (Continued) **A-D** Show a timecourse of neutrophils (green) and ZMEL cancer cells (magenta, blue nuclei) in the flank of a 3 dpf larval zebrafish, injected 2 hours prior. Time shown is relative to the resolution of the clot. **A** Shows the presence of the clot at early timepoints before the clot is resolved (dashed outline). Red box indicates the area of the inset. **B** Shows the timepoint of resolution. A blood cell can be seen passing through caudal vein (arrowhead), showing perfusion past the location of the clot. **C-D** Show later timepoints as neutrophils accumulate. **E** Quantification of the number of neutrophil interactions with each cancer cells observed within the flank of the fish in each timepoint. Scale bars = 50 μm .



4.2.3 Fibrin is a Member of the Pre-Metastatic Niche in Zebrafish Larvae

Previous studies in mice have demonstrated that circulating tumour cells are frequently able to induce the conversion of fibrinogen into fibrin, due to expression of tissue factor (Gil-Bernabé et al., 2012). To test whether grafted cancer cells might also be capable of inducing this conversion in zebrafish, human FITC-labelled fibrinogen was co-injected with ZMEL cancer cells into 2 dpf larvae. In the absence of cancer cells, FITC fluorescence is rapidly diminished as fibrinogen is turned over. However, co-injection of cancer cells with FITC-fibrinogen led to the formation of bright, cancer cell associated fibre like structures that closely resemble those seen when fibrinogen is injected during laser injury, suggesting that fibrin formation is triggered by the addition of cancer cells. These fibrin microclots were visible up to 14 hours post-injection and remained strongly associated with cancer cells within the vessels. Interestingly, blood flow did not appear to be disrupted by this fibrin formation, perhaps due to the absence of thrombocytes at 2 dpf, which might otherwise become activated and boost fibrin production (**Figure 4.5**).

Further, the formation of fibrin clots was assessed when larvae were treated with drugs that alter coagulation (**Figure 4.6**). Previous research in zebrafish larvae has shown that warfarin administration effectively blocks coagulation at a range of concentrations (Gregory et al., 2002). Co-injection of fibrinogen and cancer cells in larvae pre-treated with 50 $\mu\text{g}/\text{mL}$ warfarin for 24 hours appeared to lead to fewer fibrin clots forming than in DMSO treated larvae (**Figure 4.6**). Additionally, there appeared to be a higher intensity of fluorescence in the vessels of these by comparison to control, DMSO-treatment, potentially indicating a reduction in processing of

fibrinogen to fibrin.

A range of drugs have previously been used in zebrafish larvae to induce thrombosis, including phenylhydrazine, ferric chloride and ponatinib (Jiang et al., 2020; Gregory et al., 2002). Ponatinib was originally approved for clinical use as a tyrosine kinase inhibitor, targeting mutated BCR-ABL in leukemia (Cortes et al., 2012). However, the drug was removed from the market due to high risk of vascular thrombosis (Prasad and Mailankody, 2014), which has later been attributed to a combination of vascular endothelial growth factor receptor (VEGFR) inhibition, vWF-mediated platelet activation, and TxA₂ generation (Zhu et al., 2020; Latifi et al., 2019; Ai et al., 2018). Interestingly, here, 3 µg/mL ponatinib treatment led to fewer clots observed within the vessels of the tail than in DMSO treated larvae (**Figure 4.6 C'**). However, there was also seen to be a reduction in FITC fluorescence within the vessels. Upon imaging the injection site at the Duct of Cuvier and the heart of the larvae, there was observed a large deposit of green fluorescence here by comparison to control or warfarin-treated larvae (**Figure 4.6 C**).

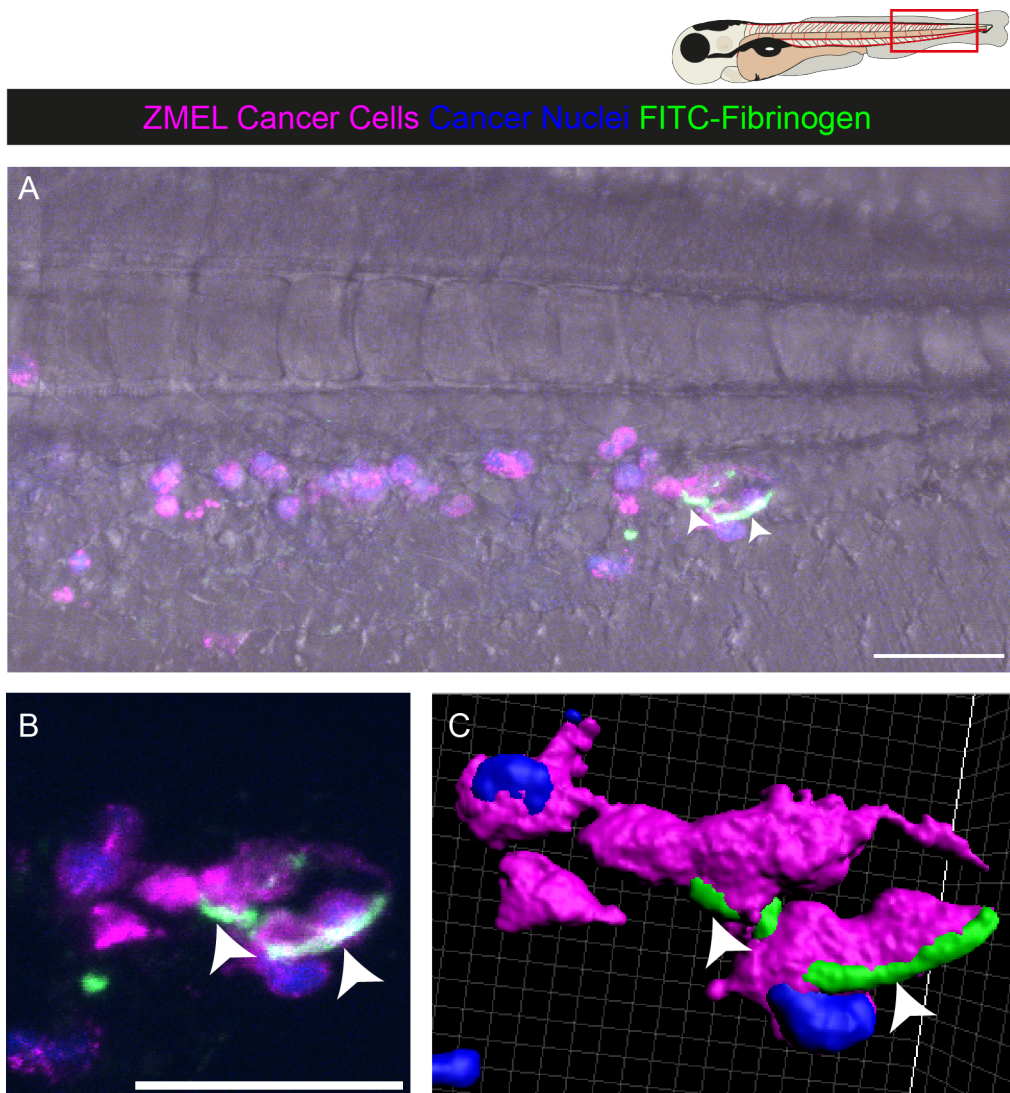


FIGURE 4.5. Grafted Cancer Cells Induce the Conversion of Human Fibrinogen to Fibrin. **A** shows a low magnification view of the flank of a 2 dpf zebrafish larva in which ZMEL cancer cells (magenta, blue nuclei) and FITC-hFibrinogen (green) were injected 2 hours previously. **B** Higher magnification view of the same fish. Arrows show fibrin fibres. **C** 3D rendering of ZMEL cancer cells associating closely with FITC-hFibrinogen. Scale bars = 50 μm .

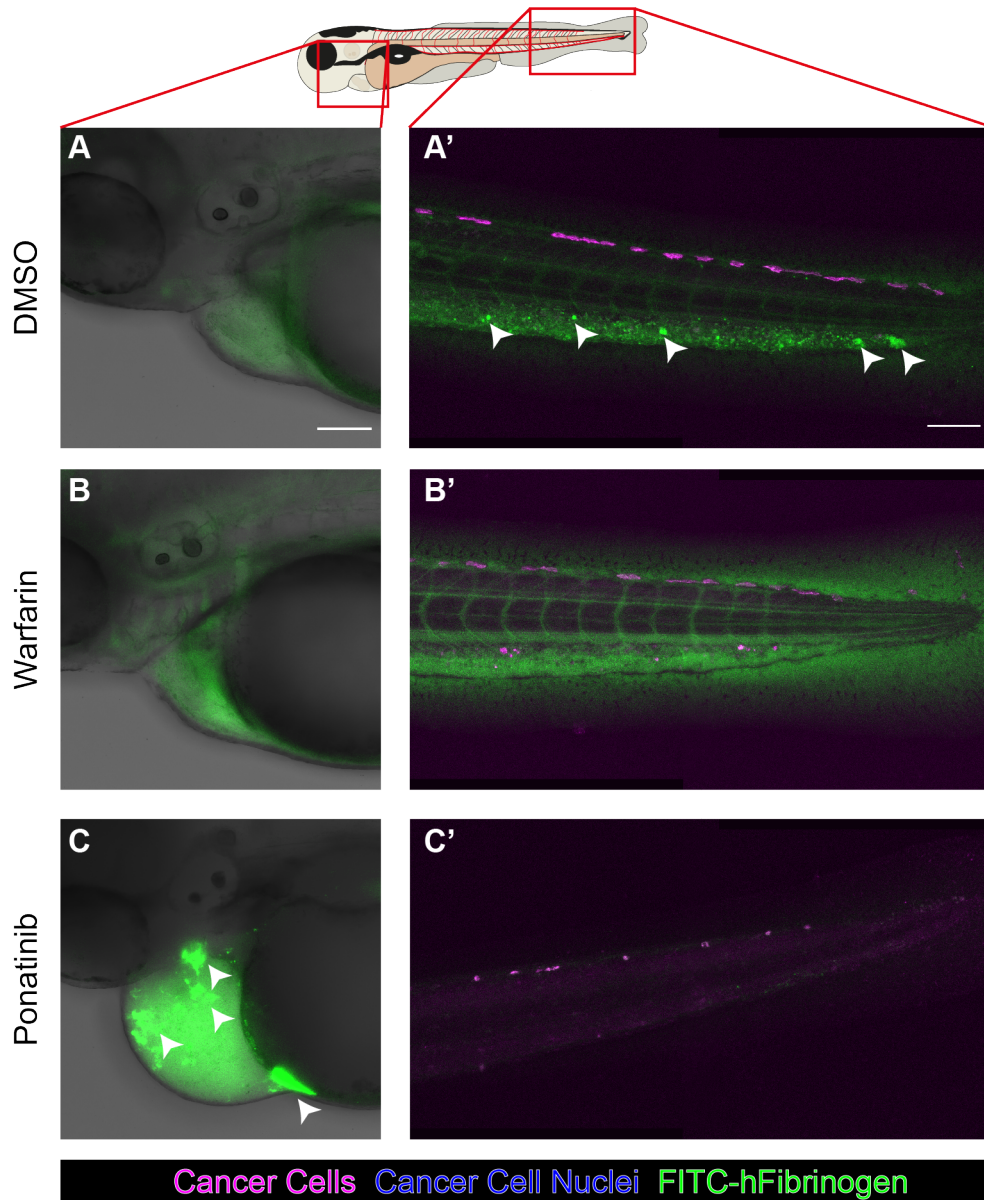


FIGURE 4.6. Drug Treatments Allow Modulation of Clotting. Representative projections of FITC-hFibrinogen (green) and ZMEL cancer cell-injected larvae 16 hpi, arrow heads show punctate material. **A-C** Show 3 dpf larval hearts and the injection site of FITC-hFibrinogen and ZMEL cancer cells over the yolk sac. **A'-C'** The same larvae viewed at the tail end, showing differing levels of FITC-hFibrinogen within the vessels. Scale bars = 50 μm.

4.2.4 Fibrin is Necessary for Cancer Cell Extravasation

To assess the effect of fibrin within the pre-metastatic niche, cancer and innate immune cell behaviour was studied whilst modulating fibrin formation. Associated with its inhibition of clotting, warfarin treatment almost completely eliminated extravasation in 2dpf zebrafish larvae (**Figure 4.7**). Extravasation levels dropped from close to 40% of total injected cells extravasating within 16 hours, to only 2% cells in warfarin-treated fish. Percentages were adjusted to weighted means to account for differences in cell numbers between samples.

Previous murine studies have shown the importance of fibrin for the recruitment of macrophages to cancer cells in the pre-metastatic niche (Gil-Bernabé et al., 2012). To assess whether the observed association of fibrin with cancer cells in zebrafish larvae might be a pre-requisite for innate immune cell recruitment to cancer cells, warfarin treatment was used to block coagulation. The effect of this warfarin treatment on innate immune cell behaviour was assessed by live imaging. Macrophage and cancer cell positions were tracked using TrackMate, generating coordinate positions for all cells. These positions were then compared to find the number of macrophages within 30 μm of cancer cells, indicating close interactions.

Warfarin treatment prior to ZMEL cancer cell injection led to a dramatic reduction in macrophage interactions with cancer cells. With roughly half as many macrophage:cancer cell interactions per timepoint seen when compared to DMSO-treated larvae (**Figure 4.8**). A reduction of observed interactions could be caused by a loss of macrophages within the tissue. To validate that the observed loss of interactions was due to changes in macrophage behaviour, rather than just a reduced macrophage number, the number of macrophages present within the field of view was counted and no significant difference in number was observed between warfarin- and DMSO-treated larvae.

Interestingly, there appeared to be no change in macrophage speed within the trunk of warfarin-treated larvae (**Figure 4.8**). But mean directionality of macrophage movement was significantly decreased after warfarin treatment, Which perhaps suggests a reduction in recruit-

ment signals of macrophages to cancer cells.

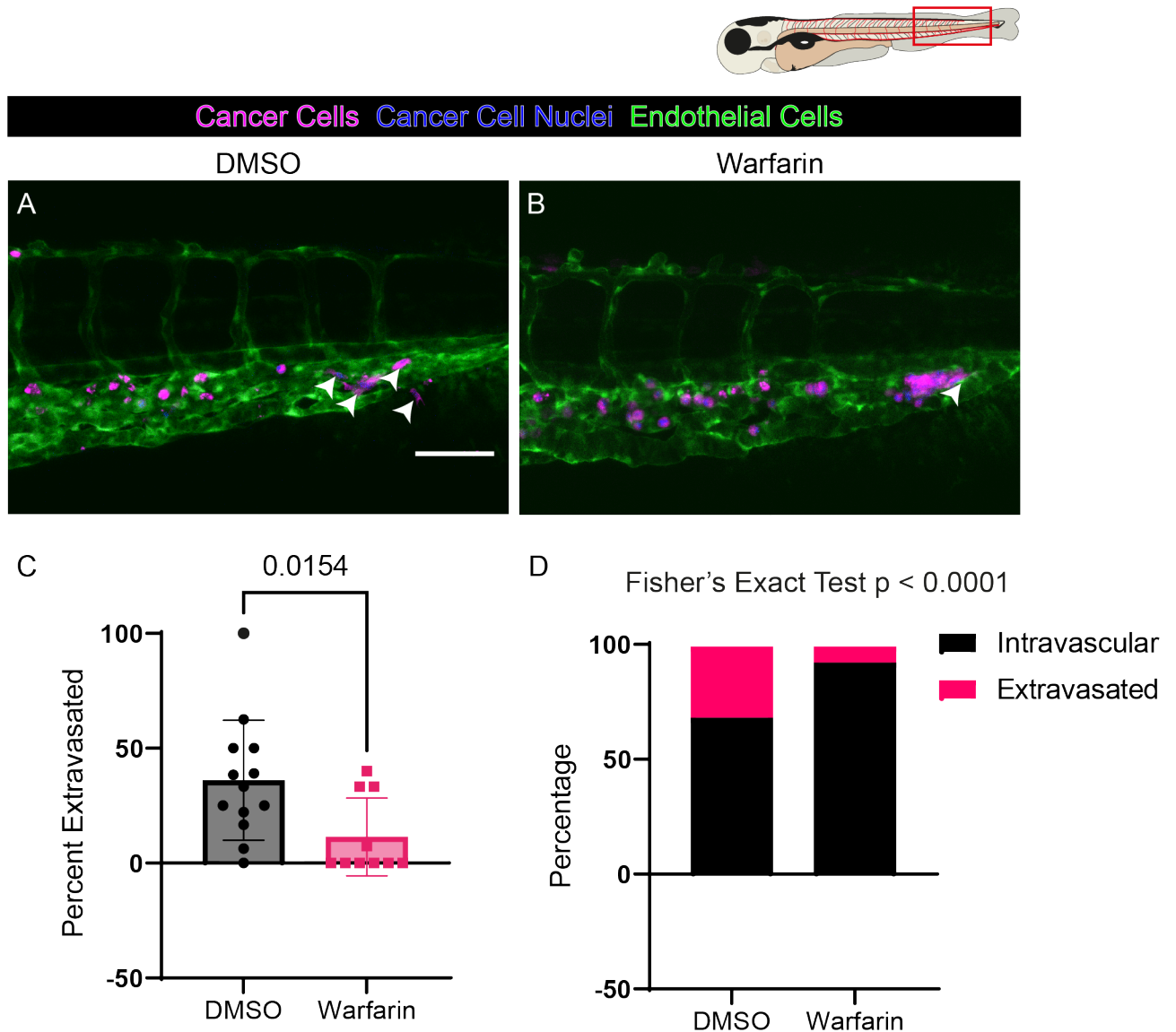


FIGURE 4.7. Warfarin Inhibits Cancer Cell Extravasation. **A-B** Shows representative images of the flank of 72 hpf larvae after warfarin or DMSO treatment and 16 hours post injection of ZMEL cancer cells. Arrows show extravasated cancer cells. **B** Quantification of the percentage of cancer cells in the tail of warfarin-treated larvae that have extravasated, analysed using a Mann-Whitney U test. **D** Shows a proportional graph of extravasated cancer cells, analysed using a Fisher's Exact test. Scale bar = 50 μm .

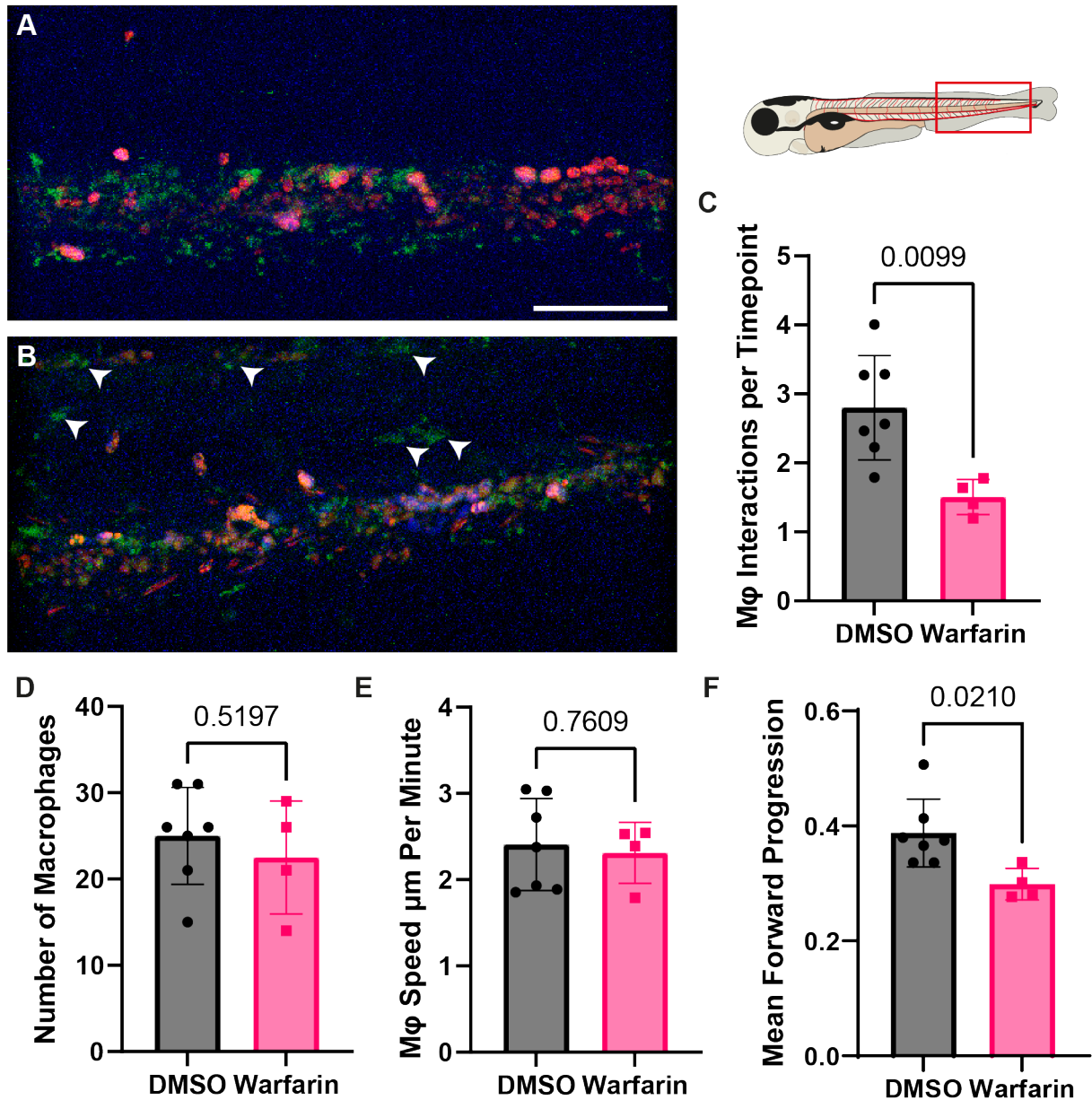


FIGURE 4.8. Warfarin Reduces Macrophage Recruitment. **A-B** shows projections of drug-treated 3 dpf larval tails with ZMEL cancer cells (magenta, blue nuclei) injected 2 hours prior to timelapse imaging. 20 equally spaced frames were captured and superimposed. Arrowheads show macrophage nuclei (green) found distant from the location of cancer cells. **C** shows quantification of the average number of macrophage interactions each cancer cell experiences per timepoint. **D** shows quantification of the total number of macrophages detected within the first frame of imaging. **E** shows quantification of average macrophage speed. **F** Shows quantification of mean directionality of macrophages. **C-F** Student's t tests. Scale bar = 50 μm .

These data appear to indicate that warfarin treatment is effective at reducing extravasation events, perhaps suggesting a role for fibrin in the pre-metastatic niche in recruiting innate immune cells, which may drive metastasis. To investigate whether an increase in fibrin formation was rate limiting for increasing metastatic events, chemical induction of fibrin formation was used. Previous research has shown ponatinib can cause occlusion and leads to the conversion of fibrinogen to fibrin in larval zebrafish (Jiang et al., 2020). Interestingly, an increase in the percentage of extravasated cancer cells was observed when 3 $\mu\text{g}/\text{mL}$ ponatinib treatment was used to stimulate clotting for 24 hours prior to cancer cell injection, when compared to control DMSO-treated fish (**Figure 4.9**). This further suggests the importance of fibrin in the pre-metastatic niche for cancer metastasis.

As a change in innate immune cell behaviour was observed during warfarin treatment, recruitment of innate immune cells was also quantified in ponatinib-treated larvae (**Figure 4.9**). Neutrophil interactions with cancer cells were tracked throughout a 14 hour live-imaging timecourse, with close interactions classified as those where cells were seen within 30 μm of one another. There appeared to be an increase in the average number of neutrophils interacting with each cancer cell per timepoint in ponatinib-treated larvae. In DMSO treated larvae, roughly 1.5 neutrophils interact with each cancer cell at each timepoint. In ponatinib-treated larvae, this appears to increase to just over 2 neutrophil interactions per timepoint. To further study this drug treatment, macrophage interactions should also be quantified.

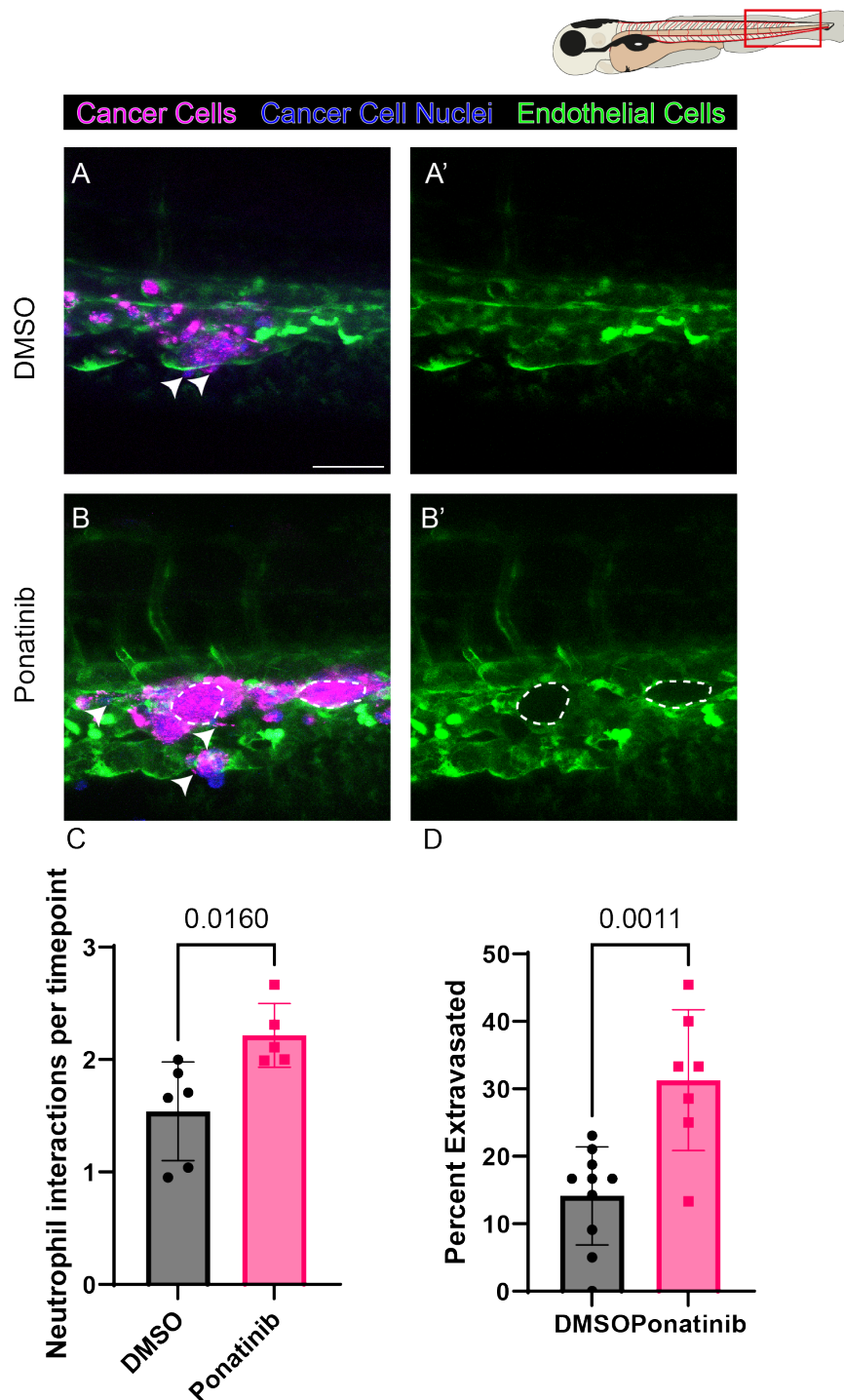


FIGURE 4.9. Ponatinib treatment increases cancer cell extravasation. **A-B'** Show ZMEL cancer cells in the tails of ponatinib-treated and DMSO control treated 3 dpf larvae 16 hours after cancer cell injection. Arrowheads show extravasated cancer cells and dashed lines show potential endothelial remodelling. **C** Quantification of neutrophil interactions with cancer cells averaged across timepoints, analysed by Student's t test. **D** Shows quantification of cancer cell extravasation in ponatinib-treated larvae, analysed by Student's t test. Scale bar = 50 μ m.

4.2.5 Loss of Fibrin Drives a Pro-Inflammatory Response to Cancer Cells

To further characterise these observed changes in innate immune cell behaviour, expression of *tnfa* in immune cells was assessed. Here, a fluorescent reporter line under the control of the *tnfa* promoter was used. As previously discussed, an increase in *tnfa* reporter expression may indicate a shift towards more pro-inflammatory macrophage phenotypes, which may in turn lead to an anti-metastatic response (Nguyen-Chi et al., 2015; Park et al., 2020).

Warfarin treatment appeared to increase the number of *tnfa* positive innate immune cells within the tail of the fish, observed by live imaging. Interestingly, *tnfa* positive cells do not appear to accumulate until after cancer cells have been injected, suggesting that warfarin alone is not sufficient to cause an increase in *tnfa* expression. As there is a smaller, but still present, increase in *tnfa* expression in larvae treated with DMSO it seems possible that cancer cells and warfarin together have a synergetic effect on increasing *tnfa* expression. These data could implicate fibrin in the mediation of macrophage phenotypes within the pre-metastatic niche, but, important to consider, warfarin may induce off-target effects that were not anticipated.

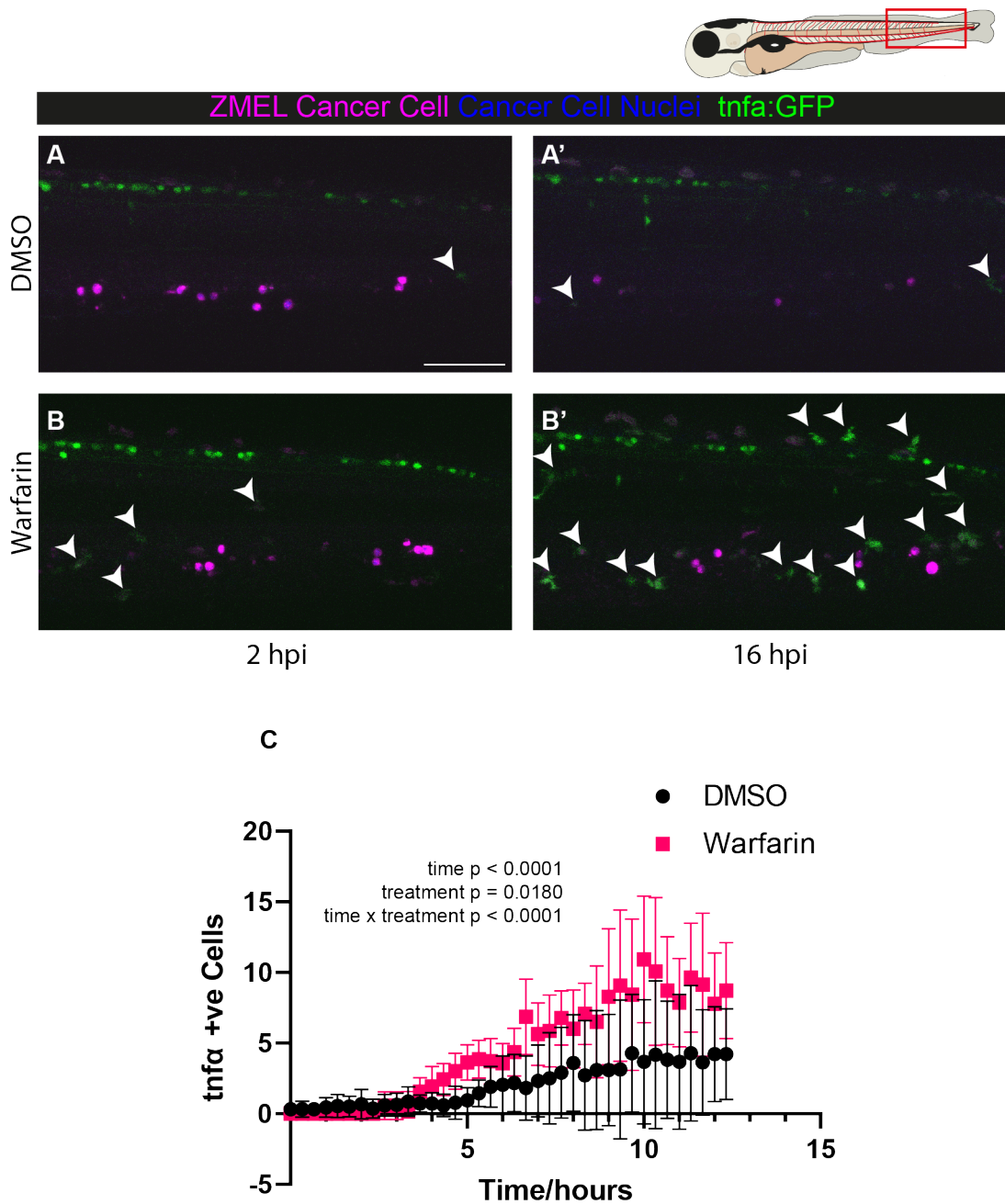


FIGURE 4.10. **Warfarin Induces a Shift to a More Pro-inflammatory Phenotype.**

A-B' Representative stills from timelapse imaging of the tails of 3 dpf larvae. ZMEL cancer cells (magenta, blue nuclei), injected 2 hours prior to imaging, are seen within the vessels of 3 dpf larvae. *tnfa* positive immune cells (green, white arrow heads) increase within the region over time from the beginning of imaging. **C** Shows quantification of the number of *tnfa* positive innate immune cells within the tissue over time, analysed by two-way ANOVA. Scale bar = 100 μm .

Next, in order to more specifically determine whether the effects seen in these pharmacological treatments were due to altered production of fibrin, knockdowns of fibrinogen subunit alpha (*fga*) were performed. Prior studies using knockdown of the *fga* subunit have shown a loss of thrombosis and, rarely, haemorrhaging in morphant zebrafish larvae (Vo et al., 2013). Here, morpholino knockdown of *fga* resulted in a reduction in *fga* mRNA measured by qPCR of 3 dpf larvae, compared to a 5 nt mismatch control morpholino (**Figure 4.11**). This loss of fibrin was sufficient to prevent occlusion of the vessel by thrombus during vascular injury in 3dpf larvae (data not shown).

To determine whether this more specific loss of fibrin from the pre-metastatic niche was sufficient to recapitulate the effects of warfarin, ZMEL cancer cells were injected into 2 dpf morphant larve. A significant reduction in percentage cancer cell extravasation was observed at 16 hpi, compared to control morphants. This was seen as a roughly 6-fold lower percentage of observed cells having extravasated in *fga* morphants compared to mismatch controls (**Figure 4.11**).

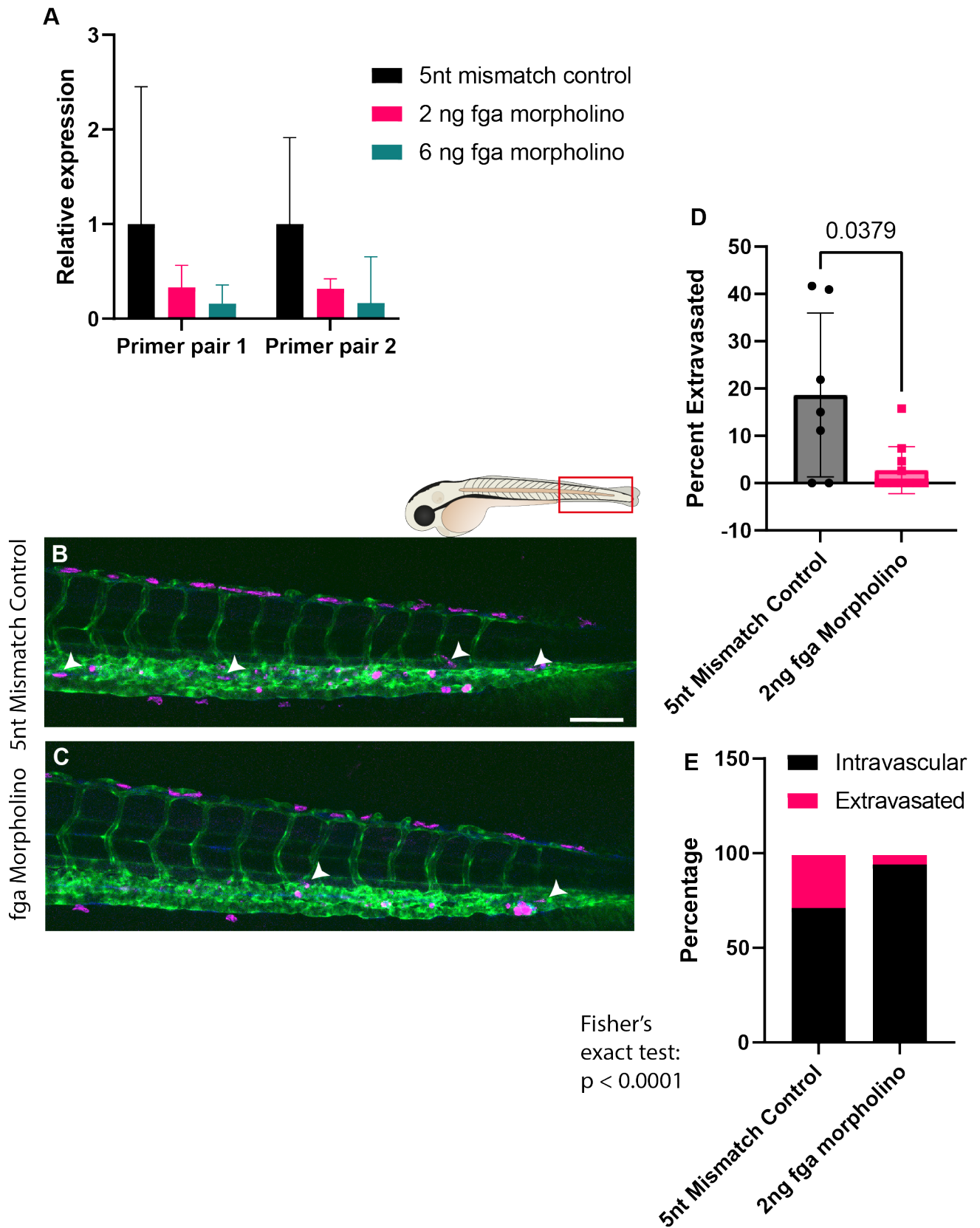


FIGURE 4.11. Morpholino Knockdown of *fga* Causes Significant Reduction of Cancer Cell Extravasation. (Legend continues on next page.)

Figure 4.11: (Continued) **A** qPCR results showing knockdown of *fga* expression using two different primer pairs against *fga*, relative to expression when using a 5nt mismatch control. **B-C** Representative tilescans of the trunks of control and active morpholino-treated fish. Cancer cells (magenta) may be seen outside of vessels (green). Extravasated cancer cells are shown with arrow heads. **D** Quantification of percentage extravasated cells, analysed using Student's t-test. **E** Quantification of percentage extravasated cells using Fisher's exact test to account for differences in number of arrested cells within the tail. Scale bar = 50 μm .

To further investigate the observed pro-inflammatory effect during warfarin treatment, *tnfa* expression in innate immune cells was measured in morpholino-treated larvae by live imaging (**Figure 4.12**). *tnfa* -expressing innate immune cells remained largely absent in control morpholino-treated larvae. Conversely, knockdown of *fga* led to a dramatic, significant, increase in *tnfa* positive cells detected throughout the timecourse of imaging, providing further evidence that fibrin may alter innate immune cell phenotypes within the pre-metastatic niche.

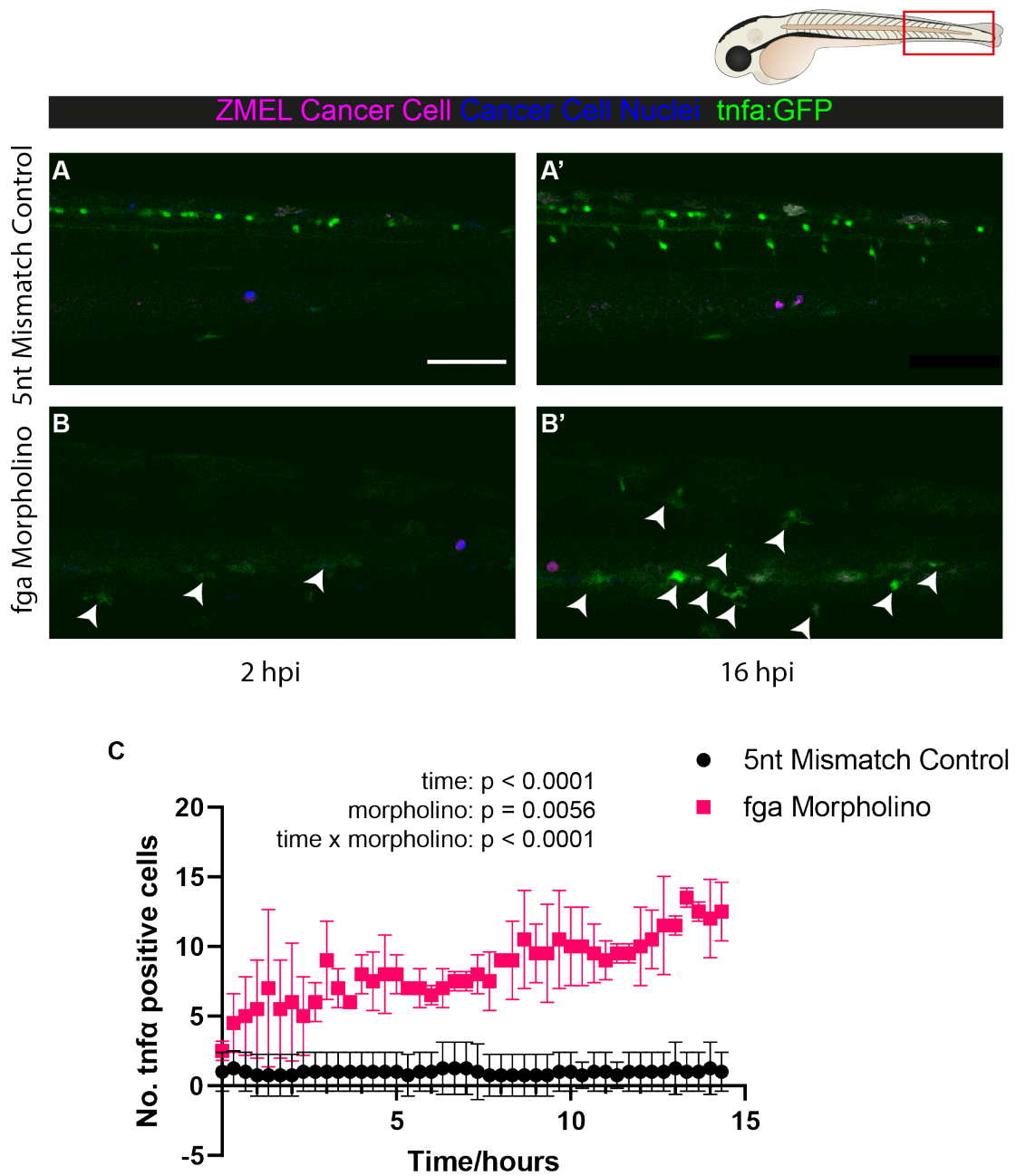


FIGURE 4.12. Morpholino Knockdown of *fga* Causes Increased *tnfa* Expression.

A-B' Representative stills from timelapse confocal imaging of morpholino treated larvae. *tnfa* positive immune cells are denoted with arrow heads. **C** Quantification of *tnfa* positive cells in the tail of larvae. Analysed using a two-way ANOVA. Scale bar = 50 μ m.

4.2.6 Induction of a Pro-Inflammatory Phenotype Using a TLR7/8 Agonist Reduces Extravasation

To determine whether the observed inflammatory phenotype was contributing to the reduction in cancer cell extravasation, a pro-inflammatory phenotype was induced in macrophages independently from changes to fibrin. Previous research has shown how resiquimod (R848) drives anti-tumoural activity in macrophages by activating toll-like receptor (TLR) 7/8, leading to an increase in M1-like behaviours and markers (Sallam et al., 2021; Anfray et al., 2021). A previous student in our lab, Paco Lopez-Cuevas, optimised R848 treatment in larval zebrafish, reporting that a single intravascular injection between 0.5 mM and 10 mM was sufficient to cause significantly increased numbers of *tnfa* positive macrophages up to 48 hours after injection (López-Cuevas, 2022).

Here, 10 mM R848 injection 24 hours prior to cancer cell grafting caused a significant increase in *tnfa* expression, measured by the sum of green fluorescence within the tail 16 hours after cancer cell injections (**Figure 4.13**). An almost two-fold change in fluorescent intensity was observed in drug-injected larvae compared to DMSO-injected larvae, measured by the sum of green pixel intensities. Increased GFP expression, indicating expression of *tnfa*, could be seen in both innate immune cells and stromal cells. Associated with this increase in *tnfa* positive cells, cancer cell extravasation was reduced in the tail of R848 treated larvae compared to DMSO injected larvae. R848 injection reduced the extravasated percentage of cancer cells observed within the tail of larvae from around 40% to around 20% (**Figure 4.13**). This potentially indicates the importance of macrophage phenotype within the pre-metastatic niche.

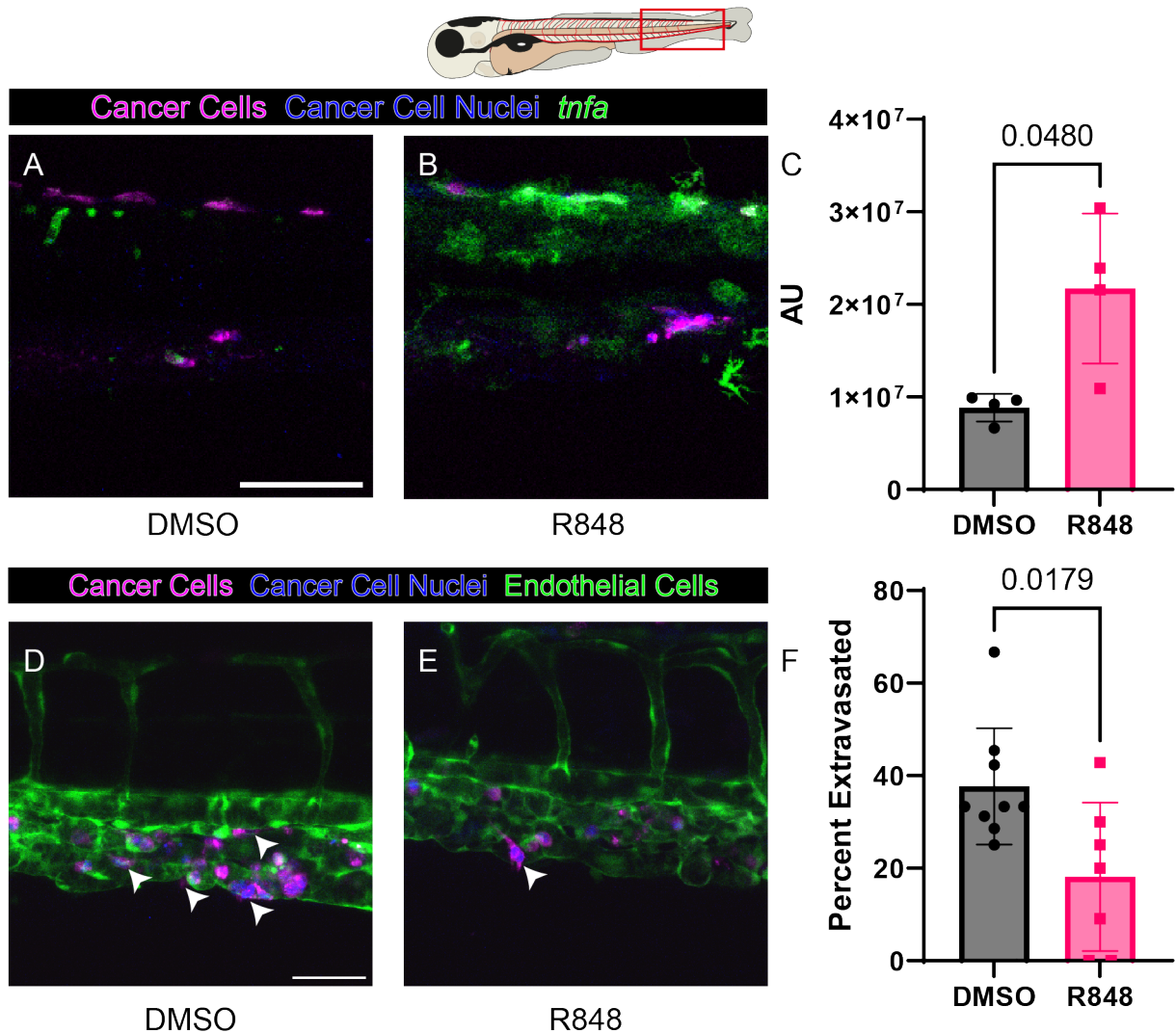


FIGURE 4.13. Resiquimod Causes an Inflammatory Phenotype and Reduces Number of Extravasation Events. **A-B** Shows the flank of 3 dpf R848-treated larvae showing *tnfa* expression (green). **C** Quantification of *tnfa* expression by fluorescent intensity, analysed using Student's t-test. **D-E** Shows the tail vessels of 3 dpf larvae injected with ZMEL cancer cells (magenta, blue nuclei). Arrowheads show extravasated cancer cells. **F** Quantification of cancer cell extravasation in R848-treated larvae, analysed using Mann-Whitney U test. Scale bars; **A & B** = 100 μm , **C & D** = 50 μm

4.3 Discussion

4.3.1 The Innate Immune Response to a Laser-Induced Thrombus

Zebrafish larvae make an ideal model for observing haemostasis *in vivo*. Their translucency allows detailed live imaging while the position of their dorsal aorta, the major artery for the tail of the fish, close the skin allows precise laser injuries to be made within the vessel while causing minimal excess damage. With careful attenuation of an ablation laser, I can trigger thrombosis within the dorsal aorta without visibly damaging the vessel wall. This is particularly important for the future investigation of cancer cell extravasation, as creating additional damage, serving as an alternative escape route through the vessel wall would likely nullify this study.

As previously observed, there is heterogeneity among the thrombocytes within the plug, with not all cells being GFP positive (Thattaliyath et al., 2005). This has been posited to be due to the presence of immature thrombocytes that are not expressing CD41 highly (Thattaliyath et al., 2005). It is also expected that some of non-fluorescent material visible in the brightfield is the fibrin that forms the clot (Rost et al., 2016). Due to the heterogeneity of fluorescence within the clot, it is difficult to assess the time point at which a clot is resolved. I have arbitrarily used the time point at which normal blood flow is seen to be restored to the vessel beyond the clot as the time of clot resolution.

As the peak of neutrophil recruitment correlates with a timepoint just after the thrombocyte plug has been resolved, I speculated that this could be due to the rapid return of blood flow to the vessels in the region, inducing a reperfusion injury-like effect. When a vessel becomes blocked, the tissues in that region become hypoxic, causing damage and, eventually, necrosis. In the clinic, resolving this blockage is essential to limit any permanent damage to the patient (Maroko et al., 1972). Paradoxically, clinical interventions to reperfuse the blocked vessel may induce damage additional to that of the initial ischemia, this has been studied in the contexts of myocardial infarction, stroke, and organ transplantation (Braunwald and Kloner, 1985; King et al., 2000; Zhang et al., 1994).

Because Labelle et al. (2014) had previously suggested that platelet activation and presence within the pre-metastatic niche was required for neutrophil recruitment to cancer cells, I investigated the role of activated thrombocytes through laser injury of the dorsal aorta prior to cancer cell injection. After induction of a thrombocytic plug, I saw no significant change in neutrophil recruitment to cancer cells up to 5 hours post injection. As neutrophils are generally the first immune cells to arrive at a site of inflammation, and are thought to resolve or die when macrophage recruitment commences, this experiment may miss the key time window when early elevated levels of neutrophils interact with cancer cells. This is because live imaging did not begin until 2 hpi, to allow cancer cells sufficient time to move into the vasculature of the larvae, and subsequently allow screening of larvae positive for cancer cells within the vessels.

However, neutrophil interactions with cancer cells begin to increase at about 5 hpi. This coincides remarkably well with the resolution of the thrombocyte plug and reperfusion of the vessels beyond the clot. Neutrophil numbers in the tissue increase during this time and some of these cells are seen to interact with cancer cells. As the diameter of the larval dorsal aorta mimicks the size of human capillaries, at roughly 10 μm across, it is possible that tumour cell activation of platelets in humans might lead to similar micro-blockages, and that later reperfusion of these regions could similarly trigger neutrophil recruitment to cancer cells, supporting metastasis at these sites.

Pre-clinical studies have shown an association between ischemia-reperfusion and tumour growth and metastasis (Lim et al., 2013; Tashiro et al., 2020). Clinical treatment of liver cancers frequently requires resection of part of the liver, or full liver removal followed by transplantation (Agrawal and Belghiti, 2011). These procedures include clamping of vessels in the liver to prevent bleeding during the operation, leading to the potential for ischemia-reperfusion injury (Bahde and Spiegel, 2010). Some clinical studies have reported an increased recurrence of cancer in patients with higher markers of ischemia-reperfusion injury (Grat et al., 2018). The zebrafish data represented here shows live-imaging evidence for this "reperfusion injury" associated inflammatory response, which might have clinical relevance, not just in surgery scenarios, but also after dissolution of microclots and other thrombotic lesions in cancer patients.

4.3.2 Fibrin is Required for the Recruitment of Pro-Metastatic Innate Immune Cells to the Pre-Metastatic Niche

Many cancer cells overexpress factors that may directly or indirectly cause drive the production of fibrin (Razak et al., 2018). Direct induction of coagulation includes expression of tissue factor and thrombin (Khorana et al., 2007; Wojtukiewicz et al., 2000), while activation of neutrophils to produce neutrophil Extracellular Traps (NETs) may provide an indirect route to platelet activation and coagulation (Mauracher et al., 2018). It has previously been demonstrated that the association of fibrin with cancer cells may drive pro-metastatic innate immune cell interactions with cancer cells (Gil-Bernabé et al., 2012). Here, I have developed a model to show that cancer cells grafted into zebrafish larvae are able to drive the production of fibrin, and have used a range of different methods to modulate this fibrin production and study the consequences of this on the dynamics of immune cell mediated cancer metastasis.

Gregory *et al.* showed that FITC-labelled human fibrinogen (FITC-hFibrinogen), injected intravascularly in unwounded larvae, results in a diffuse signal throughout the entirety of the vessels soon after injection, before being rapidly turned over (Gregory et al., 2002). On the generation of a clot by laser injury, the human fibrinogen is converted into fibrin and forms bright, local fluorescence where the FITC-labelled protein has been incorporated into the newly-formed clot (Gregory et al., 2002). This clot-associated fluorescence is retained for much longer than the systemically observed fibrinogen, likely because fibrin in the clot must undergo fibrinolysis, which is suppressed while the wound is healing (Gregory et al., 2002).

I was able to adapt the above techniques to observe fibrin within the pre-metastatic niche by co-injecting FITC-hFibrinogen with cancer cells. I found that fibrin appears to associate with grafted cancer cells. This is likely due to cancer cells driving the conversion of the injected fibrinogen to fibrin, either directly or indirectly, causing its formation close to these cells and its adherence to them. However, as this is an injection of exogenous human fibrinogen, this proxy,

observable fluorescent fibrin might not entirely reflect how endogenous fibrin might interact with cancer cells. A transgenic zebrafish line expressing an *fgb*-EGFP fusion protein has been produced and might better report the formation of fibrin, although it too might suffer from artifacts of overexpression (Vo et al., 2013). Alternatively, polyclonal antibodies against zebrafish orthologues of fibrin have been used in previous studies, and could be used to overcome potential artifacts caused by this exogenous application of fibrinogen (Fish et al., 2014).

The use of warfarin has previously been characterised in zebrafish larvae, showing anti-coagulant activity mediated by inhibition of vitamin K dependent γ carboxylase activity (Hanumanthaiah et al., 2001). Additionally, the developmental effects of the loss of functional vitamin K in zebrafish embryos have been compared to those seen in human warfarin embryopathy (Granadeiro et al., 2019), and the LC₅₀ and EC₅₀ concentrations have been determined (Weigt et al., 2012). This made it an appealing initial choice to study the effects of fibrin in the pre-metastatic niche. I showed that warfarin treatment indeed led to a strong loss of extravasation events. As ablation of innate immune cells within the larvae had previously led to a reduction of metastases forming (**Section 3.2.3**), I speculated that a reduction of immune cell interactions with cancer cells during anti-coagulant treatment could contribute to the loss of extravasation.

Additionally, these data reveal a potential role for fibrin in pushing innate immune cells towards pro-metastatic interactions with circulating tumour cells and preventing anti-tumoural activity. As previously discussed, *tnfa* reporter expression may be used as a proxy for pro-inflammatory macrophage phenotypes (Nguyen-Chi et al., 2015). Warfarin treatment appeared to increase the number of *tnfa* positive macrophages in the tail of the fish, local to cancer cells. Next, it would be useful to characterise this macrophage phenotype further. Other fluorescent reporters including *il1 β* could be used to show multiple markers of classical macrophage inflammation, or more detailed characterisation could be performed by RNA-seq.

It has been shown that *in vitro* macrophages interacting with fibrin were driven towards M2 phenotypes, while macrophages incubated in media containing soluble fibrinogen were driven

towards M1, pro-inflammatory phenotypes (Hsieh et al., 2017; Tanaka et al., 2019). Moreover, injectable platelet rich fibrin reduced the pro-inflammatory response to local *Staphylococcus aureus* in rats, with reduced in expression of *tnfa* and IL-6 (Zhang et al., 2020). I speculate that this might explain my observation of increased *tnfa* when coagulation is inhibited by warfarin treatment. With normal coagulation levels, macrophages interacting with cancer cells may also be interacting with fibrin associated with cancer cells, dampening other inflammatory signals that they would otherwise receive, and preventing switching to an M1 phenotype (Hsieh et al., 2017; Tanaka et al., 2019; Zhang et al., 2020).

However, as warfarin is a vitamin K inhibitor, it has effects beyond the loss of fibrin production alone (Bell et al., 1972). Thus, I wanted to explore whether a more specific deletion of fibrin expression on its own might be enough to cause an increase of *tnfa* expression in macrophages local to cancer cells. To this end, I used morpholino knockdown of the fibrinogen subunit *fga*. Previous studies have characterised the action of this morpholino, showing a loss of up to 90% of fibrinogen mRNA and a significant loss of protein shown by western blot (Vo et al., 2013). A strong loss of coagulation was also observed in this study, with up to 5% of larvae experiencing haemorrhaging either in the brain or intramuscularly, and a complete loss of occlusion when subjected to laser injury to the vessel (Vo et al., 2013). Here, I was able to induce a significant reduction of *fga* transcript detected by qPCR and saw a dramatic loss of occlusion after laser wounding of the vessel.

As hypothesised, fibrinogen knockdown led to a reduction of cancer cell extravasation events and an increase in pro-inflammatory macrophages in the trunk of larvae. Interestingly, Hsieh et al. (2017) indicated that the presence of fibrinogen could contribute to driving pro-inflammatory phenotypes in macrophages. Here, I have knocked down fibrinogen to reduce the formation of fibrin within the pre-metastatic niche but, in doing so, I may also be removing a potential signal to drive more inflammation and increase the anti-metastatic effects seen here. One method to distinguish the effects of fibrinogen from the effects of fibrin is the use of mutant fibrinogen that cannot be cleaved by thrombin. In mice, mutations in the fibrinogen α -chain have been

found that lead to normal circulating levels of fibrinogen, which cannot be processed into fibrin fibres (Prasad et al., 2015). This mutant could be replicated in zebrafish using CRISPR/Cas9 and homology-directed repair or, alternatively, a recombinant mutant protein could be produced and injected into a morphant or knockout fish.

As a further approach, ponatinib was used to induce the production of fibrin. Ponatinib has been previously shown to induce caudal vein thrombosis in zebrafish larvae (Jiang et al., 2020). With ponatinib treatment, I saw an increase of extravasation events, providing additional evidence, supporting the importance of coagulation and fibrin in cancer metastasis. Although this study suffered from a low sample size, it did suggest trend towards an increase of neutrophil interactions with cancer cells. Further repeats of this experiment are needed to gather more details of innate immune cell behaviour in the context of this drug, including its effects on macrophages in the pre-metastatic cancer niche. One drawback to the use of ponatinib as a means to induce coagulation, is that it also acts as an inhibitor of VEGF signalling, leading to visible changes to the structure of the blood vessels of treated larvae. Clearly, these changes could potentially influence metastasis.

Other means of producing clots in zebrafish larvae have been shown to be effective and could be used to further this model. For example, ferric chloride is frequently used in mammalian models of thrombosis and drives coagulation through positively-charged iron binding to negatively charged blood components (Ciciliano et al., 2015). Ferric chloride treatment in zebrafish larvae causes thrombosis predominantly in vessels of the tail, as it fails to penetrate deep enough to affect the vessels of other tissues (Gregory et al., 2002).

Using multiple methods to modulate coagulation, I was able to show the importance of coagulation, and potentially fibrin, in innate immune cell recruitment to the pre-metastatic niche and subsequent cancer cell extravasation. Thus, these data support previous studies where fibrin associated with cancer cells led to increased macrophage interactions with cancer cells and subsequent metastasis (Gil-Bernabé et al., 2012). Building on this, I hypothesise that fibrin plays

a further role in dampening inflammation within the pre-metastatic niche, further aiding cancer cells in their extravasation and metastasis.

To test whether the phenotypic switching was responsible for loss of extravasation, I used a drug that stimulates the production of *tnfa* in zebrafish larvae. Previous student in the lab, Dr Paco Lopez Cuevas, showed that R848, a TLR 7/8 agonist, increased the percentage of *tnfa* positive macrophages in larvae without significant adverse effects to the zebrafish. This followed on from murine studies that have shown how R848 can be effective at switching macrophages to anti-tumoural activities (Anfray et al., 2021; Sallam et al., 2021). Additionally, R848 appears to reduce the metastatic potential of intravascularly injected melanoma cells in mice (Zhou et al., 2022).

Using this drug, I showed a systemic increase of *tnfa* expression and a reduction of extravasated cancer cells. This suggests that the drive towards an inflammatory phenotype caused by a loss of fibrin could be responsible, at least in part, for the loss of cancer cell extravasation. To further investigate the role of *tnfa* expression on cancer extravasation, I could target *tnfa* using drugs. Inhibitors of the production, or release, of *tnfa* have been tested in zebrafish larvae, showing the potential to reduce the inflammatory phenotypes seen in this model (Xie et al., 2020). Additionally, there is a CRISPR knockout of *tnfa* in zebrafish that could allow further investigation into its function in the pre-metastatic niche (Kan et al., 2020). One interesting experiment would be to combine the *tnfa* knockout with warfarin treatment to determine whether this might rescue the extravasation levels seen in untreated fish. However, as this study is using *tnfa* expression in part as a proxy for inflammatory phenotypes in innate immune cells, it is possible that targeting *tnfa* in these ways would not significantly alter these inflammatory phenotypes and thus not rescue normal cancer cell behaviour.

Together, these data suggest the potential for druggable targets that could be used for anti-metastatic therapies. Anti-coagulants have been associated with a reduction in the incidence of metastatic cancers (Haaland et al., 2017), but their long-term use is associated with negative

consequences such as bleeding (Ageno and Donadini, 2018). Instead, it could be possible to intervene in fibrin signalling to macrophages to induce a pro-inflammatory phenotype that may inhibit cancer metastasis. This could cause a similar reduction in metastases as anti-coagulant therapies, while avoiding some of the side effects associated with these drugs.

Chapter 5

CRISPR-Cas9 Targeted Knockout of Thrombocyte-Driven Immune Cell Recruitment

5.1 Introduction

Having established a possible role for thrombocyte activation and the coagulation cascade in immune recruitment and modulation which, in turn, may drive metastasis, I then utilised genetic manipulation to further investigate how thrombocyte signalling might contribute to this process.

Activated mammalian platelets interface with the innate immune system through a range of inflammatory mediators, released from granules or displayed on their surface (Page and Pretorius, 2020). This process is important for recruiting immune cells to a developing thrombus to protect against pathogens and drive resolution of the wound (Eisinger et al., 2018). These signals may also direct immune cell recruitment to the pre-metastatic niche, which appears important for extravasation and formation of metastases. Release of granule contents from platelets is dependent on the soluble N-ethylmaleimide-sensitive factor attachment protein receptor (SNARE) complex for their capture and fusion to the plasma membrane (Savage et al., 2013; Ren et al., 2007; Williams et al., 2018), and knockout data in mice has shown SNAP23 as a critical factor for

platelet degranulation (Williams et al., 2018).

Selectin proteins are adhesion molecules, primarily involved in the recruitment of circulating immune cells to sites of inflammation (McEver, 2015). P-selectin on the surface of activated platelets is important for adhesion of macrophages and neutrophils to a thrombus, and may cause platelet:immune cell signalling (Weyrich et al., 1996; Evangelista et al., 1999).

Here, I targeted two genes that have previously been implicated in platelet signalling, *snap23* and P-selectin (*selp*), for conditional knockout in larval zebrafish thrombocytes, using CRISPR/Cas9. Tissue-specific expression of the Cas9 protein can be used to restrict a gene knockout to a cell of interest, potentially reducing off-target effects, particularly when a gene of interest is widely expressed and/or indispensable for the survival of an organism (Zhuo et al., 2021).

5.2 Methods and Results

5.2.1 Towards a Tissue-Specific CRISPR Knockout in Thrombocytes

Platelets are known to communicate with innate immune cells both during their normal activities and when associated with cancer cells (Kral et al., 2016). These communication events may recruit innate immune cells to cancer cells and drive metastatic events. To disrupt this process, CRISPR/Cas9 knockouts were designed to target candidate genes that might be involved in this platelet:immune cell communication in zebrafish.

Members of the soluble N-ethylmaleimide-sensitive factor attachment protein (SNAP) family form part of the SNARE complex, required for the binding of vesicles to the plasma membrane, and triggering their release outside of the cell (Chen et al., 2000). Transcriptome analysis of human and mouse platelets revealed SNAP23 and SNAP29 as highly expressed members of the SNARE complex (Rowley et al., 2011). Data from murine experiments, where SNAP23 was deleted specifically in platelets, has shown it as essential for their proper activity and degranula-

tion (Williams et al., 2018). Thus, *snap23.1* and *snap23.2* were chosen as targets for knockout by CRISPR-Cas9 in this zebrafish model.

Further, P-selectin is a platelet surface receptor that mediates direct interactions with innate immune cells through P-selectin glycoprotein ligand-1 (PSGL-1). In a wound healing context, P-selectin facilitates the binding of circulating immune cells to platelets to at the site of damage to drive resolution (Evangelista et al., 1999). P-selectin has also been linked to metastasis, making it an ideal candidate for knockout as part of the investigation of platelet:immune cell communication in the pre-metastatic niche (Kim et al., 1998)

Both of the above targets have expression patterns that are not restricted to thrombocytes in zebrafish. *In situ* hybridisation data has previously shown *snap23.1* is expressed ubiquitously in zebrafish larvae from the one cell stage through to 60 hpf (Thisse and Thisse, 2004). P-selectin is also expressed by endothelial cells and is pivotal to allow the rolling of immune cells on their surface (Gotsch et al., 1994). To avoid off-target effects in these studies, conditional knockout was designed in order to restrict effects to the thrombocytes.

First, sgRNA spacer sequences were designed using open access softwares, Benchling and CRISPOR, to predict cutting efficiencies and off-target scores (Concordet and Haeussler, 2018). CRISPOR provides a range of different scores to assess the quality of a guide RNA sequence. Here, an average of scores was taken and guide sequences were ranked based on this average. InDelphi is a machine-learning-based model designed to predict the expected frequencies of insertions and deletions caused by non-homologous end joining, and microhomology-mediated end joining, after Cas9-directed double strand breaks are introduced. This allowed the prediction of frameshift frequencies, to increase the chances of functional knockouts (**Figure 5.1**) (Shen et al., 2018).

CRISPR guides were validated prior to cloning, to ensure adequate activity. Heteroduplex mobility assays have been shown to be a valuable tool for screening CRISPR-edited zebrafish

(Foster et al., 2019). This assay allows screening by PCR of mixed, mutant and wildtype genomic DNA without the need for additional enzymes, such as T7EI mismatch endonucleases. Mobility assays were performed on gDNA isolated from CRISPR-injected larvae to find mutants. Guide efficiency was estimated by percentage of screened larvae with observed mutations. All guides were deemed to have adequate efficiencies as around 60-80% of screened larval DNA formed heteroduplexes (**Figure 5.1**).

Targeting a single gene at multiple loci may increase the efficiency of knockout, further, due to genome duplication events, *snap23* has two paralogues in zebrafish, likely making the expression of multiple CRISPR guides essential for a full functional knockout. To enable ubiquitous expression of multiple sgRNAs, a Golden Gate restriction method was used to enable the assembly of up to 5 different sgRNAs in a single expression vector (Yin et al., 2015). Spacer sequences for CRISPR editing were obtained as primers with overhangs to allow the use of type II restriction cloning to insert specific guide sequences into plasmids containing different U6 promoter sequences, optimised to avoid recombination of repeated sequences (Yin et al., 2015). Once these vectors had been assembled, they were combined into a single expression vector by a second type II restriction reaction (**Figure 5.2**).

CHAPTER 5. CRISPR-CAS9 TARGETED KNOCKOUT OF THROMBOCYTE-DRIVEN IMMUNE CELL RECRUITMENT

A



snap23.1 Exon 1: Danio rerio (ensDanRer), [17:33626197-33626238](#), forward genomic strand

Your input sequence is 42 bp long. It contains 2 possible guide sequences.

Shown below are their PAM sites and the expected cleavage position located -3bp 5' of the PAM site.

Click on a match for the PAM NGG below to show its 20 bp-long guide sequence. (Need help? Look at the [CRISPOR manual](#))

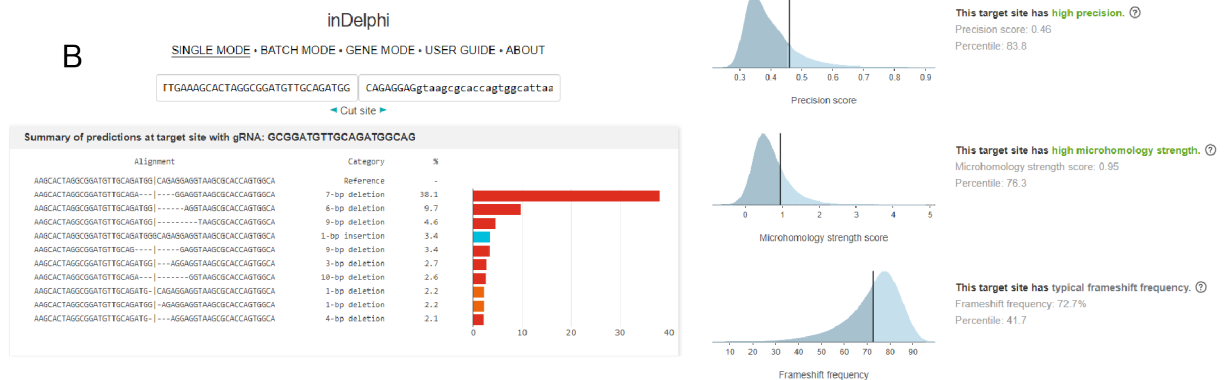
Colors **green**, **yellow** and **red** indicate high, medium and low specificity of the PAM's guide sequence in the genome.

```

Position 0      10     20     30     40     46
Sequence TCAC TTGAAGCACTAGGCGGATGTTGCAGATGGCAGAGGAG
          ---TGG
          ---AGG
    
```

Position/ Strand	Guide Sequence + PAM + Restriction Enzymes <input type="checkbox"/> Only G- <input type="checkbox"/> Only GG- <input type="checkbox"/> Only A-	MIT Specificity Score	CFD Spec. score	Predicted Efficiency <small>Show all scores</small> Doench 116 Mor-Mateos		Outcome Out-of-Frame Indel	Off-targets for 0-1-2-3-4 mismatches + next to PAM
32 / fw	CACTAGGCGGATGTTGCAGA TGG Enzymes: <i>HpyCH4V</i> Cloning / PCR primers	95	98	53	54	76 77	0-0-0-0-2-19 0-0-0-0-1-1 21 off-targets
38 / fw	GCGGATGTTGCAGATGGCAG AGG Cloning / PCR primers	90	97	56	77	64 79	0-0-1-5-25 0-0-0-1-1 31 off-targets

B



C

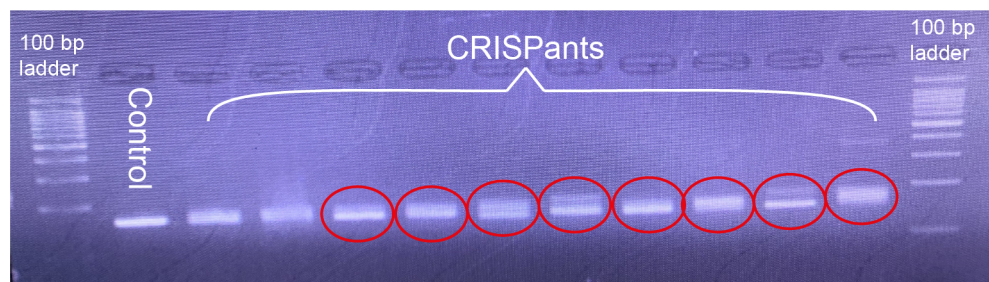


FIGURE 5.1. Workflow for CRISPR Validation. A Shows CRISPOR output for *snap23.1* exon 2 B Shows InDelphi output for a guide sequence. Most common indels are shown on the left and analysis for precision and frameshift rate are shown on the right C Shows a heteroduplex mobility assay on a 4% agarose gel. Bands with altered mobility, or double bands, were deemed mutants (red circles).

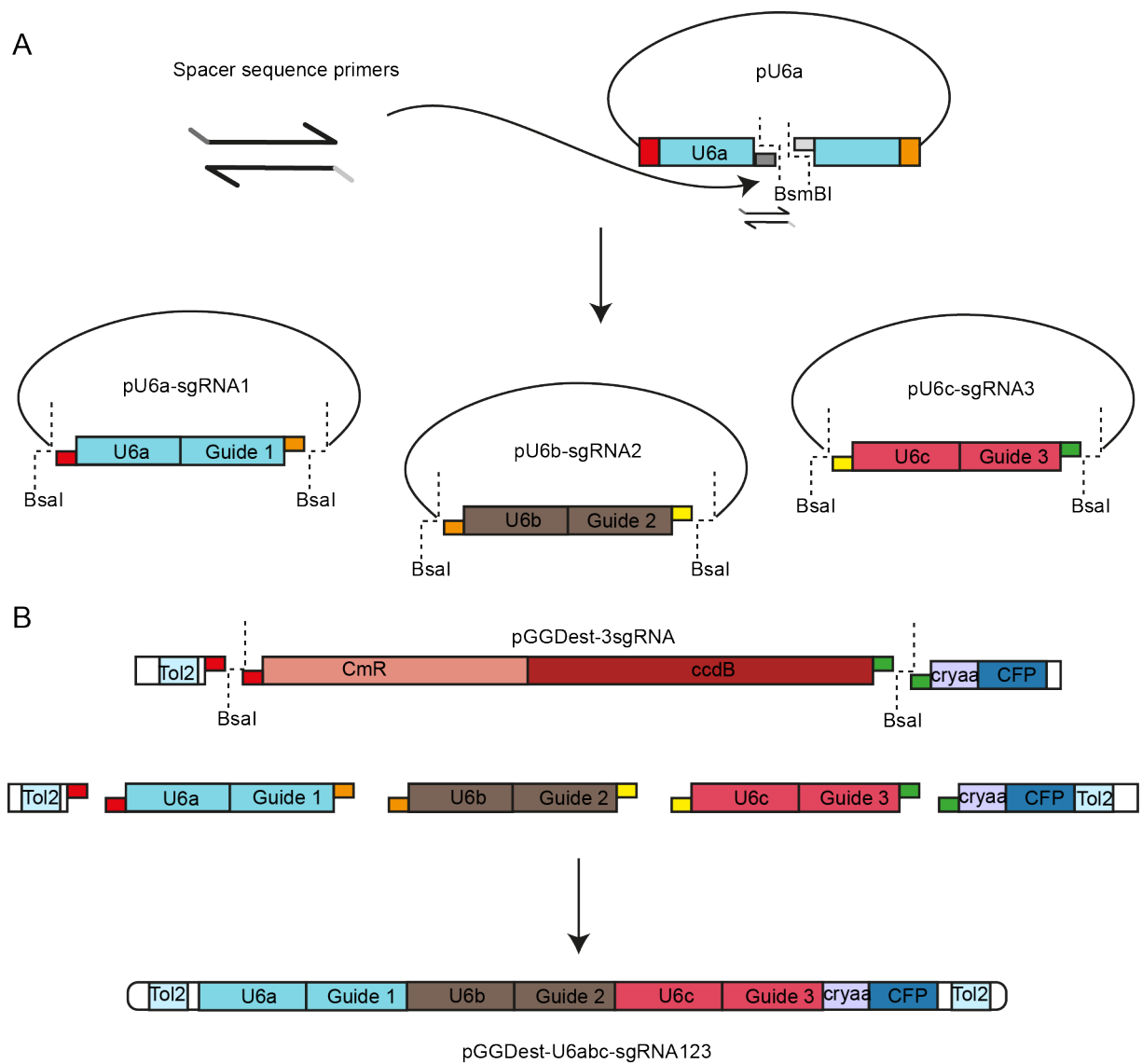


FIGURE 5.2. Assembly of a Vector for Ubiquitous Expression of Multiple sgRNAs. **A** Primers were designed with sense and antisense sequences of the gRNA spacers, with 4 bp overhangs compatible to BsmBI cut sites within U6 plasmids. U6 plasmids were cut with BsmBI and annealed primers were ligated by their overhangs. **B** U6x-sgRNAx plasmids, and a corresponding destination vector, were cut using BsaI to produce compatible overhanging ends. Ligation of these compatible fragments allows the assembly of an expression vector with Tol2 transposon elements.

To allow tissue-specific knockout, constructs were designed to allow the expression of Cas9 protein specifically in thrombocytes. Ablain et al. (2015) created a "middle-entry" vector containing Cas9 protein, codon-optimised for zebrafish, with a cleavable linker to GFP. This "middle-entry" vector is optimised to allow recombination with other plasmids designed within the Tol2kit framework (Kwan et al., 2007). Gateway recombination was used to allow the assembly of multiple fragments, placing Cas9 under the control of a repeated UAS element within tol2 transposons (**Figure 5.3**) (Kwan et al., 2007; Cheo et al., 2004).

During cloning reactions to produce a 5' entry vector containing a thrombocyte-specific promoter, recombination events causing the excision of the promoter insert were observed (**Figure 5.3**). This has been reported previously when using this combination of attB1R and attP4, particularly when incorporating longer inserts (Merritt et al., 2010). To overcome this issue here, Stbl3 competent *E. coli* were used due to their optimisation for use with unstable repeated sequences (Al-Allaf et al., 2012). Further, lowering the temperature of incubation from 37°C to 33°C appeared to reduce undesired recombination events. It has been previously seen that temperature reductions may cause reduced flexibility in DNA molecules (Driessen et al., 2014), so this off-target recombination may be prevented when the DNA is less able to bend sufficiently to allow the recombination sites close contact with one another.

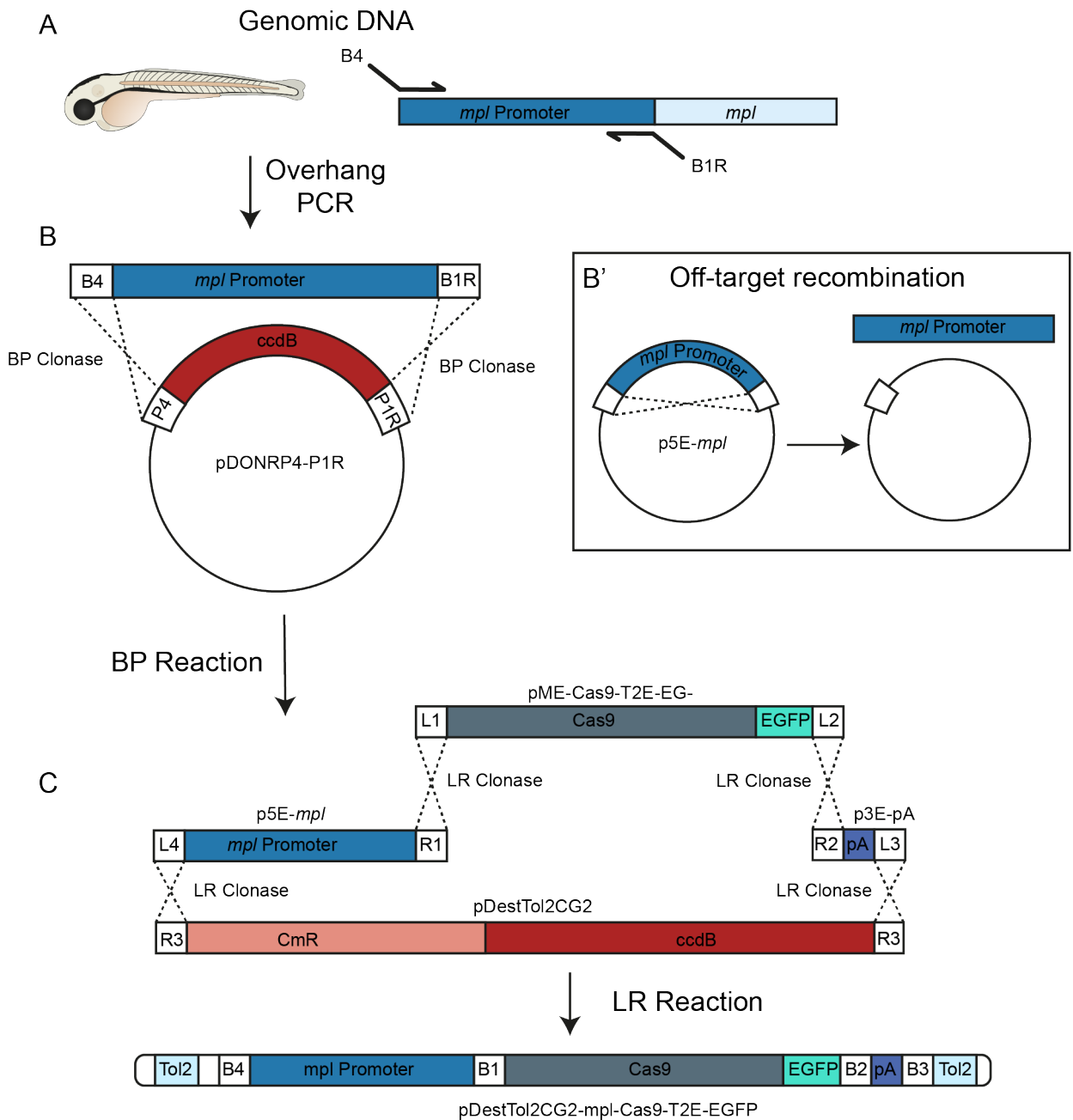


FIGURE 5.3. Assembly of a Thrombocyte-Specific Cas9 Expression Vector.

A Genomic DNA extracted from wildtype larval zebrafish was used for PCR of the *mpl* promoter sequence using primers with *attB* site overhangs. **B** A BP recombination reaction was used to incorporate the promoter sequence into a 5'-entry vector. **B'** Off-target recombination could sometimes cause the excision of the promoter region from the 5'-entry vector. **C** LR clonease was used to combine 5'-, middle- and 3'-entry vectors into a destination vector containing Tol2 transposon elements.

The *mpl* promoter was chosen over *itga2b* to drive expression of Cas9 in order to avoid changes in cell types outside of thrombocytes, as the latter has been seen to be expressed in a population of HSCs (Ma et al., 2011). An *mpl* reporter line expressing GFP appears to show more specific expression within thrombocytes (Lin et al., 2017). Initial f0 founders were established by screening for expression of the *crya:EGFP* reporter, giving a strong signal in the eye of larvae positive for the construct. Once these fish reached sexual maturity, roughly 20 adult fish, for both the *mpl* and *itga2b* promoters, were individually outcrossed and their f1 offspring were screened for expression of GFP within their thrombocytes. However, neither *mpl*- nor *itga2b*-driven expression of Cas9-T2E-EGFP led to sufficient fluorescence in thrombocytes.

To boost expression, *mpl* was used to drive Gal4 expression, and Cas9 protein was placed under a repeated UAS sequence. Injection of these constructs led to the expression of GFP in thrombocytes, confirming the expression and localisation of the Cas9 protein (**Figure 5.4**). This strategy enables further experiments to characterise this expression, such as RNAseq of FAC-sorted thrombocytes. Conditional knockout of genes predicted to be important in platelet-driven immune recruitment to cancer cells is now possible through combination of the Cas9 transgene and the sgRNA transgenes through breeding.

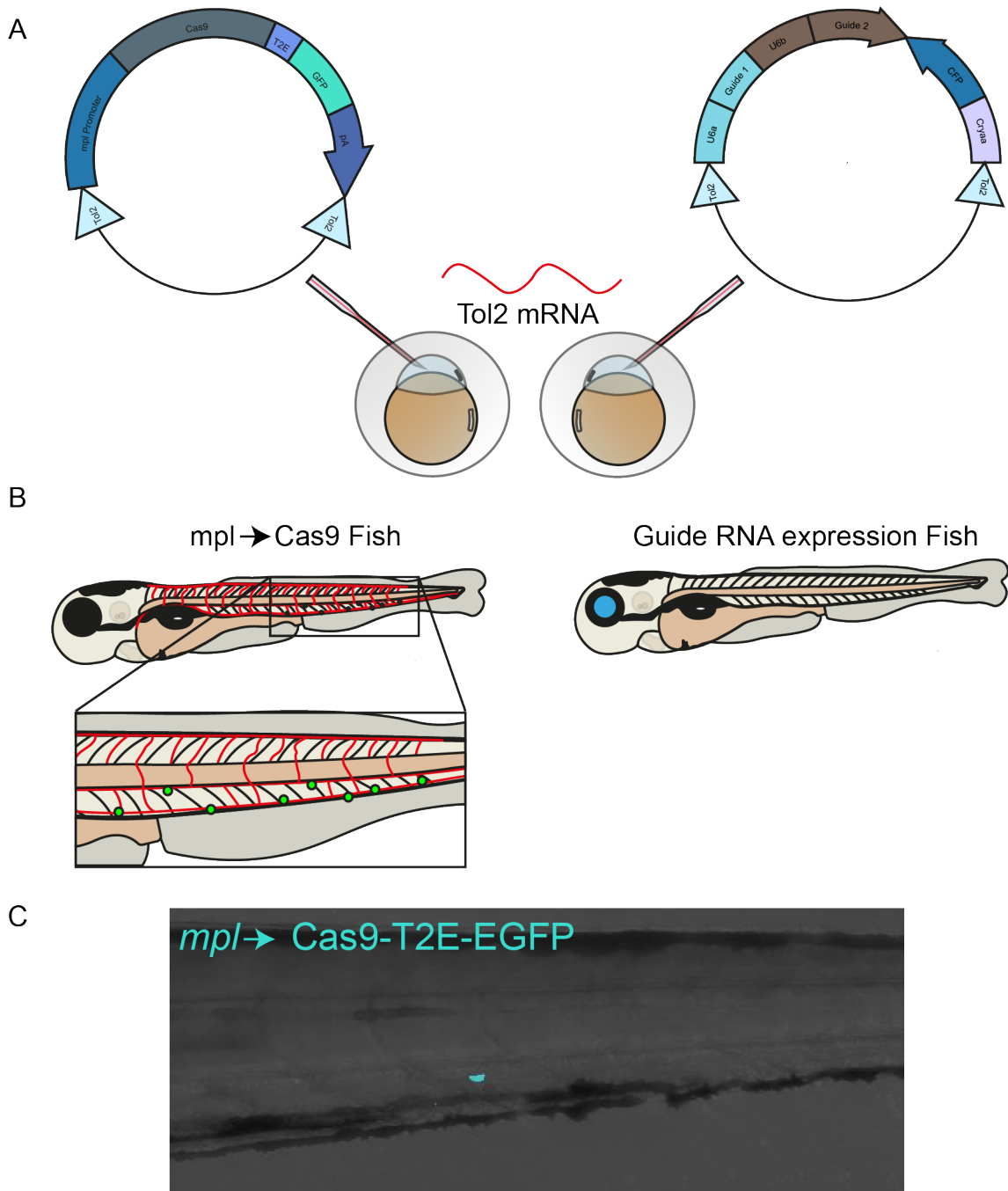


FIGURE 5.4. Injection of Constructs Leads to GFP Reporting of Cas9 Expression. **A** Plasmids were co-injected with Tol2 mRNA into the single cell of zebrafish eggs. **B** Schematic to show fluorescent markers for positive screening. **C** Shows a 3 dpf larva injected with the Cas9 vector, the tail contains a small number of GFP fluorescent cells within the haematopoietic tissue (arrows), likely indicating developing thrombocytes.

5.3 Discussion

Having observed that platelet activation could recruit innate immune cells to cancer cells and potentially drive metastasis, I then wanted to more closely investigate and disrupt this process to potentially find mechanistic insights into this process. Tissue-specific CRISPR may allow the knockout of genes of interest that may be essential for the survival and development of the organism, allowing important processes to be studied within different contexts. Further, a conditional knockout may allow a reduction of off-target effects by eliminating expression outside of a particular cell-type or tissue.

Platelet activation leads to release of granules, containing a variety of signalling factors that may be important for signalling to innate immune cells and recruiting them to cancer cells in the pre-metastatic niche. It has previously been observed that depletion of platelets or inhibition of CXCR2 can prevent neutrophil recruitment to cancer cells. This finding strongly implicates platelet-derived chemokines in innate immune cell recruitment to the pre-metastatic niche (Labelle et al., 2014).

Extensive research has been performed to identify essential factors in platelet granule release. Several members of the SNARE complex have been shown to be important to allow degranulation by mediating the binding of vesicles to the plasma membrane (Savage et al., 2013; Ren et al., 2007; Williams et al., 2018). SNAP23 knockout in murine platelets was shown to completely preclude secretion of granule and lysosome contents which, in turn, led to a loss of thrombosis (Williams et al., 2018). Generation of a thrombocyte-specific *snap23* knockout in zebrafish larvae could allow the ablation of thrombocyte signalling to innate immune cells, potentially allowing finer details to be revealed about this communication.

P-selectin is a member of the selectin family of glycoproteins containing P-selectin, L-selectin and E-selectin (McEver, 2015). These are long, transmembrane lectins that allow interactions between platelets (P-selectin), leukocytes (L-selectin) and endothelial cells (E-selectin) (McEver,

2015). P-selectin has previously been shown to allow signalling to innate immune cells (Weyrich et al., 1996). It also might drive reperfusion injury through binding to neutrophils (Yadav et al., 1999), and may be essential for cancer metastasis (Kim et al., 1998). These interactions implicate P-selectin in platelet:immune cell interactions, making it an appealing target for knockout within this model.

Unfortunately, assembly of the vectors required for tissue-specific CRISPR took longer than anticipated. Gateway recombination is based on lambda phage integration events with bacteria, whereby specific attP (phage) sequences recombine with attB (bacteria) sequences, leaving behind attL or attR sites. Because the att sites used in Tol2kit plasmids are designed to be specific, in theory there should be few off-target recombination events. However, it has previously been observed that the resulting att sites after the BP reaction are somewhat prone to recombination and excision of the desired insertion, particularly if that insertion is relatively long. Here I found this was a frequent occurrence with my sequences for both the *mpl* and *itga2b* promoters, leading to excision of the inserted promoter sequence.

Further, before turning to a Gal4-UAS expression system to boost expression of the Cas9 protein, I had generated a direct Tg(*mpl*:Cas9-T2E-GFP) line in which I did not see adequate expression of Cas9. As Gal4-UAS had to be used to boost expression, this led to an additional delay because of the maturation period needed to generate adult fish for breeding with guide RNA-expressing fish to allow the expression of RNP complexes and gene editing. Unfortunately, these delays led to a thrombocyte-specific Cas9 line not being available during the time of this project.

Future experiments using conditional CRISPR knockout in thrombocytes may allow more targeted studies into the communication between thrombocytes and innate immune cells. This offers the potential to find critical factors within these processes and reveal potentially useful drug targets which could improve survival in patients with metastatic cancer.

Chapter 6

Final Conclusions

Cancer and clotting have been known to be linked for more than a century and a half. In 1865, Parisian doctor Armand Trousseau observed an increase in thrombosis among cancer patients, eventually recognising thrombophlebitis as a symptom of his own, fatal, cancer (Metharom et al., 2019; Trousseau, 1865). As our knowledge of cancer has grown, the bidirectional nature of this cancer:clotting association has become evident; not only do certain tumours drive coagulation, but platelets and clots may also accelerate the progression of the disease (Li et al., 2021). Population health studies have revealed single nucleotide polymorphisms (SNPs) driving hypercoagulation may also lead to a more rapid disease progression in cancer, increasing the incidence of metastases (Li et al., 2021).

Warfarin is a common anti-coagulant, on the WHO list of essential medicines. In the clinic, warfarin and other anti-coagulant medicines have been seen to reduce cancer incidence, though the specific mechanisms of this remain unclear (Haaland et al., 2017; Hejna et al., 1999). However, anticoagulant therapies come with the risk of bleeding, which can be dangerous and prohibitive, especially when many cancer patients also require surgery. This makes the interplay between the haemostatic pathways and cancer metastasis an important area of research, as a deeper understanding could allow for more specific interventions that avoid such severe risks in the future.

Another foundational observation of metastasis is that cancers of different origins are not equally likely to form secondary tumours in any one organ of the body (Paget, 1889). Instead, each primary tumour location appears to favour metastasis to a few, particular tissues. One theory to explain this phenomenon is termed “seed and soil”, whereby cancer cells (“seeds”) metastasise to organs that specifically favour their growth (“soil”) (Paget, 1889; Akhtar et al., 2019). Alternatively, this skewed metastasis could be explained by purely mechanical phenomena; the “favoured” organs could simply be the first opportunity for arrest, in the reduced lumen size of a capillary bed immediately downstream of a cell’s entrance to the vasculature (Ewing, 1928; Coman et al., 1951). As is often the case, the truth appears to lie in a combination of the two mechanisms (Proctor, 1976; Azevedo et al., 2015). Interestingly, platelets and clotting appear to straddle the two, initially disparate, arms of research.

Initially, the field recognised the mechanical advantages afforded to circulating tumour cells (CTCs) by these platelets and microclots. Activated platelets and fibrin were seen to adhere to CTCs, slowing their velocity and facilitating binding to the endothelium (Gasic, 1984). Additionally, it was posited that a coating of fibrin and platelets could protect cancer cells from natural killer cells (NKs) (Gorelik et al., 1984). These early results cemented platelets and microclots as key players in the process of metastasis.

As the “seed and soil” hypothesis has grown in popularity, more focus has been placed on what makes one organ more hospitable to a cancer cell than another. One hypothesis for this is that some tissues favour the development of a specialised pre-metastatic niche, primed by cancer cells to allow their efficient colonisation (Psaila and Lyden, 2009). Research has shown that microclots may play a role in the development of the pre-metastatic niche by recruiting innate immune cells, which may support cancer cells and drive metastasis (Gil-Bernabé et al., 2012; Labelle et al., 2014).

Here, I have developed an *in vivo* model to study this pre-metastatic niche phenomenon in zebrafish larvae, allowing high spacial and temporal resolution imaging of cancer cells, throm-

bocytes and innate immune cells within the pre-metastatic niche. The use of high-resolution live imaging in zebrafish can reveal important behaviours and activities of cells that may not be observable in an opaque model, like the mouse. Indeed, I confirmed that the presence of a thrombocytic plug or a fibrin clot appeared necessary for the recruitment of innate immune cells to the pre-metastatic niche.

Further to this, I also showed that the resolution of a microclot could bring in a secondary wave of neutrophils, which appears similar to an ischemia-reperfusion injury. Such an observation would have been difficult to make in a murine model. This model could be developed further to investigate immune cell behaviour during reperfusion injury, which is an important factor in patient recovery from strokes, myocardial infarction, and organ transplantation (King et al., 2000; Zhang et al., 1994; Braunwald and Kloner, 1985). Moreover, some studies have indicated that reperfusion injury after surgery may increase the risk of cancer resurgence later in life (Lim et al., 2013; Tashiro et al., 2020). The ease of live imaging in larval zebrafish could make this model an invaluable tool to gain mechanistic insights into the process of ischemia-reperfusion.

As in other models, I found that innate immune cells drive increased cancer cell extravasation (Gil-Bernabé et al., 2012; Qian et al., 2011), and ablation of either neutrophils or macrophages caused a significant reduction in cancer cells found outside of the vasculature. However, immune cells are not homogenous in their behaviours, and the activation status of an innate immune cell can drastically alter its response towards circulating tumour cells (Zhou et al., 2022; Park et al., 2020). More M1-like, pro-inflammatory macrophages may instead inhibit metastasis.

Immune cell-mediated cancer therapies have been a particular focus of cancer research in recent years due, in part, to the success of immune checkpoint blockade in the clinic. Monoclonal antibodies targeting PD-1 and cytotoxic T-lymphocyte-associated protein 4 (CTLA4) have been shown to be effective in treating a range of cancers (Ott et al., 2013), and the discoverers of these checkpoint molecules were awarded the Nobel Prize in 2018. Recent work from our own lab has targeted macrophages with inactivated bacteria (López-Cuevas et al., 2021), and synthetic

protocells containing micro RNAs (López-Cuevas et al., 2022) to tune them towards anti-tumour behaviours and limit cancer growth.

In this work, I find that an inflammatory reprogramming strategy could also be effective at limiting the formation of secondary tumours. Pharmacological induction of a pro-inflammatory phenotype by stimulating TLR 7/8 was sufficient to reduce metastasis. Additionally, I discovered a pronounced increase in macrophages expressing *tnfa* when tumour-grafted larvae were treated with warfarin, suggesting a switch towards a more pro-inflammatory phenotype when fibrin is not present in the pre-metastatic niche. One possible explanation for this phenomenon is found in *in vitro* data from Hsieh et al. (2017). They found that macrophages grown on insoluble fibrin were more resistant to becoming pro-inflammatory upon stimulation with lipopolysaccharide (LPS) and interferon gamma ($\text{IFN}\gamma$) than those grown without fibrin or fibrinogen (Hsieh et al., 2017).

Thus, I propose a model in which cancer cells may drive the production of fibrin in the pre-metastatic niche, the presence of which drives the recruitment of innate immune cells to circulating tumour cells. I further speculate that macrophages recruited to tumour cells may have a dampened polarisation response, preventing them from mounting an anti-tumour defence and, instead, driving metastasis. Hence, when fibrin is lost from the pre-metastatic niche, *tnfa* positive macrophages accumulate, and extravasation is diminished. Further research is needed to characterise these *tnfa* positive macrophages and understand how fibrin loss drives these phenotypes, which may identify therapeutic targets for the future.

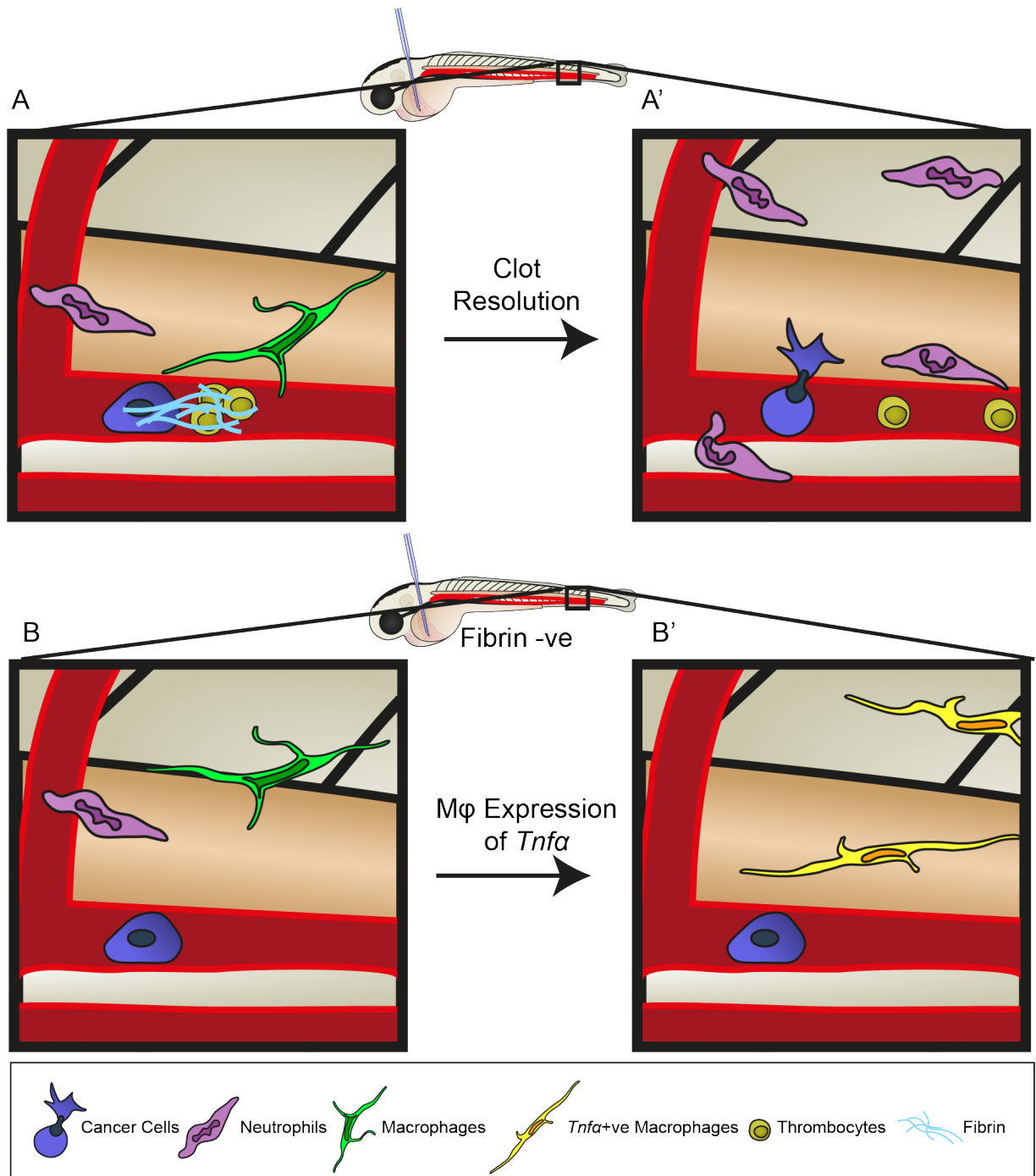


FIGURE 6.1. Proposed Model. **A-A'** Schematic representation of the pre-metastatic niche in the presence of fibrin and a thrombotic plug. Pro-metastatic macrophages and neutrophils are recruited to circulating tumour cells. A large influx of neutrophils occurs immediately following the resolution of the clot, which may drive cancer cell extravasation. **B-B'** Shows schematic representation of the pre-metastatic niche in the absence of fibrin. A reduction in innate immune cell recruitment is seen and over time anti-metastatic, *tnfa* positive macrophages accumulate, reducing cancer cell extravasation.

Bibliography

- Ablain, J., Durand, E. M., Yang, S., Zhou, Y. and Zon, L. I. (2015). A CRISPR/Cas9 vector system for tissue-specific gene disruption in zebrafish. *Developmental cell* 32, 756–764.
- Ageno, W. and Donadini, M. (2018). Breadth of complications of long-term oral anticoagulant care. *Hematology: the American Society of Hematology Education Program* 2018, 432.
- Agrawal, S. and Belghiti, J. (2011). Oncologic resection for malignant tumors of the liver. *Annals of Surgery* 253, 656–665.
- Ai, N., Chong, C.-M., Chen, W., Hu, Z., Su, H., Chen, G., Lei Wong, Q. W. and Ge, W. (2018). Ponatinib exerts anti-angiogenic effects in the zebrafish and human umbilical vein endothelial cells via blocking VEGFR signaling pathway. *Oncotarget* 9, 31958–31970.
- Akashi, K., Traver, D., Miyamoto, T. and Weissman, I. L. (2000). A clonogenic common myeloid progenitor that gives rise to all myeloid lineages. *Nature* 2000 404:6774 404, 193–197.
- Akhtar, M., Haider, A., Rashid, S. and Al-Nabet, A. D. M. (2019). Paget’s “Seed and Soil” Theory of Cancer Metastasis: An Idea Whose Time has Come. *Advances in Anatomic Pathology* 26, 69–74.
- Al-Allaf, F. A., Tolmachov, O. E., Zambetti, L. P., Tchetchelnitski, V. and Mehmet, H. (2012). Remarkable stability of an instability-prone lentiviral vector plasmid in *Escherichia coli* Stbl3. *3 Biotech* 3, 61–70.

- Al-Hajj, M., Wicha, M. S., Benito-Hernandez, A., Morrison, S. J. and Clarke, M. F. (2003). Prospective identification of tumorigenic breast cancer cells. *Proceedings of the National Academy of Sciences* *100*, 3983–3988.
- Albregues, J., Shields, M. A., Ng, D., Park, C. G., Ambrico, A., Poindexter, M. E., Upadhyay, P., Uyeminami, D. L., Pommier, A., Küttner, V., Bružas, E., Maiorino, L., Bautista, C., Carmona, E. M., Gimotty, P. A., Fearon, D. T., Chang, K., Lyons, S. K., Pinkerton, K. E., Trotman, L. C., Goldberg, M. S., Yeh, J. T. and Egeblad, M. (2018). Neutrophil extracellular traps produced during inflammation awaken dormant cancer cells in mice. *Science* *361*.
- Alshetaiwi, H., Pervolarakis, N., McIntyre, L. L., Ma, D., Nguyen, Q., Rath, J. A., Nee, K., Hernandez, G., Evans, K., Torosian, L., Silva, A., Walsh, C. and Kessenbrock, K. (2020). Defining the emergence of myeloid-derived suppressor cells in breast cancer using single-cell transcriptomics. *Science Immunology* *5*.
- Amatruda, J. F. and Zon, L. I. (1999). Dissecting Hematopoiesis and Disease Using the Zebrafish. *Developmental Biology* *216*, 1–15.
- Ambler, R., Edmunds, G. L., Tan, S. L., Cirillo, S., Pernes, J. I., Ruan, X., Huete-Carrasco, J., Wong, C. C., Lu, J., Ward, J. et al. (2020). PD-1 suppresses the maintenance of cell couples between cytotoxic T cells and target tumor cells within the tumor. *Science signaling* *13*, eaau4518.
- Anfray, C., Mainini, F., Digifico, E., Maeda, A., Sironi, M., Erreni, M., Anselmo, A., Ummarino, A., Gandoy, S., Expósito, F., Redrado, M., Serrano, D., Calvo, A., Martens, M., Bravo, S., Mantovani, A., Allavena, P. and Andón, F. T. (2021). Intratumoral combination therapy with poly(I:C) and resiquimod synergistically triggers tumor-associated macrophages for effective systemic antitumoral immunity. *Journal for ImmunoTherapy of Cancer* *9*, e002408.
- Annese, T., Tamma, R., Ruggieri, S. and Ribatti, D. (2019). Angiogenesis in Pancreatic Cancer: Pre-Clinical and Clinical Studies. *Cancers* 2019, Vol. 11, Page 381 *11*, 381.
- Antonio, N., Bonnelykke-Behrndtz, M. L., Ward, L. C., Collin, J., Christensen, I. J., Steiniche, T., Schmidt, H., Feng, Y. and Martin, P. (2015). The wound inflammatory response exacerbates growth of pre-neoplastic cells and progression to cancer. *The EMBO Journal* *34*, 2219–2236.

- Anvari, S., Osei, E. and Maftoon, N. (2021). Interactions of platelets with circulating tumor cells contribute to cancer metastasis. *Scientific Reports* *11*, 1–16.
- Asgari, A., Lesyk, G., Poitras, E., Govindasamy, N., Terry, K., To, R., Back, V., Rudzinski, J. K., Lewis, J. D. and Jurasz, P. (2021). Platelets stimulate programmed death-ligand 1 expression by cancer cells: Inhibition by anti-platelet drugs. *Journal of Thrombosis and Haemostasis* *19*, 2862–2872.
- Azevedo, A. S., Follain, G., Patthabhiraman, S., Harlepp, S. and Goetz, J. G. (2015). Metastasis of circulating tumor cells: Favorable soil or suitable biomechanics, or both? *Cell Adhesion & Migration* *9*, 345–356.
- Bahde, R. and Spiegel, H. U. (2010). Hepatic ischaemia–reperfusion injury from bench to bedside. *British Journal of Surgery* *97*, 1461–1475.
- Baixauli, F., Martín-Cófreces, N. B., Morlino, G., Carrasco, Y. R., Calabia-Linares, C., Veiga, E., Serrador, J. M. and Sánchez-Madrid, F. (2011). The mitochondrial fission factor dynamin-related protein 1 modulates T-cell receptor signalling at the immune synapse. *The EMBO Journal* *30*, 1238–1250.
- Barclay, A. N. and Van Den Berg, T. K. (2014). The Interaction Between Signal Regulatory Protein Alpha (SIRP α) and CD47: Structure, Function, and Therapeutic Target. <https://doi.org/10.1146/annurev-immunol-032713-120142> *32*, 25–50.
- Barrett, T. J., Cornwell, M., Myndzar, K., Rolling, C. C., Xia, Y., Drenkova, K., Biebuyck, A., Fields, A. T., Tawil, M., Luttrell-Williams, E., Yuriditsky, E., Smith, G., Cotzia, P., Neal, M. D., Kornblith, L. Z., Pittaluga, S., Rapkiewicz, A. V., Burgess, H. M., Mohr, I., Stapleford, K. A., Voora, D., Ruggles, K., Hochman, J. and Berger, J. S. (2021). Platelets amplify endotheliopathy in COVID-19. *Science Advances* *7*.
- Baumgarth, N. (2021). The Shaping of a B Cell Pool Maximally Responsive to Infections. <https://doi.org/10.1146/annurev-immunol-042718-041238> *39*, 103–129.

- Beatty, G. L., Chiorean, E. G., Fishman, M. P., Saboury, B., Teitelbaum, U. R., Sun, W., Huhn, R. D., Song, W., Li, D., Sharp, L. L., Torigian, D. A., O'Dwyer, P. J. and Vonderheide, R. H. (2011). CD40 agonists alter tumor stroma and show efficacy against pancreatic carcinoma in mice and humans. *Science* 331, 1612–1616.
- Behnke, O. (1967). Electron microscopic observations on the membrane systems of the rat blood platelet. *The Anatomical Record* 158, 121–137.
- Bell, R. G., Sadowski, J. A. and Matschiner, J. T. (1972). Mechanism of Action of Warfarin. Warfarin and Metabolism of Vitamin. *Biochemistry* 11, 1959–1961.
- Bergers, G. and Fendt, S. M. (2021). The metabolism of cancer cells during metastasis. *Nature Reviews Cancer* 2021 21:3 21, 162–180.
- Bertero, T., Oldham, W. M., Grasset, E. M., Bourget, I., Boulter, E., Pisano, S., Hofman, P., Bellvert, F., Meneguzzi, G., Bulavin, D. V. et al. (2019). Tumor-stroma mechanics coordinate amino acid availability to sustain tumor growth and malignancy. *Cell metabolism* 29, 124–140.
- Bertrand, J. Y., Kim, A. D., Teng, S. and Traver, D. (2008). CD41+ cmyb+ precursors colonize the zebrafish pronephros by a novel migration route to initiate adult hematopoiesis. *Development* 135, 1853–1862.
- Bertrand, J. Y., Kim, A. D., Violette, E. P., Stachura, D. L., Cisson, J. L. and Traver, D. (2007). Definitive hematopoiesis initiates through a committed erythromyeloid progenitor in the zebrafish embryo. *Development (Cambridge, England)* 134, 4147–4156.
- Best, M. G., Sol, N., In 't Veld, S. G., Vancura, A., Muller, M., Niemeijer, A. L. N., Fejes, A. V., Tjon Kon Fat, L. A., Huis In 't Veld, A. E., Leurs, C., Le Large, T. Y., Meijer, L. L., Kooi, I. E., Rustenburg, F., Schellen, P., Verschueren, H., Post, E., Wedekind, L. E., Bracht, J., Esenkbrink, M., Wils, L., Favaro, F., Schoonhoven, J. D., Tannous, J., Meijers-Heijboer, H., Kazemier, G., Giovannetti, E., Reijneveld, J. C., Idema, S., Killestein, J., Heger, M., de Jager, S. C., Urbanus, R. T., Hoefler, I. E., Pasterkamp, G., Mannhalter, C., Gomez-Arroyo, J., Bogaard, H. J., Noske, D. P., Vandertop, W. P., van den Broek, D., Ylstra, B., Nilsson, R. J. A., Wesseling, P., Karachaliou,

- N., Rosell, R., Lee-Lewandrowski, E., Lewandrowski, K. B., Tannous, B. A., de Langen, A. J., Smit, E. F., van den Heuvel, M. M. and Wurdinger, T. (2017). Swarm Intelligence-Enhanced Detection of Non-Small-Cell Lung Cancer Using Tumor-Educated Platelets. *Cancer cell* 32, 238–252.
- Bijker, M. S., van den Eeden, S. J. F., Franken, K. L., Melief, C. J. M., Offringa, R. and van der Burg, S. H. (2007). CD8+ CTL priming by exact peptide epitopes in incomplete Freund's adjuvant induces a vanishing CTL response, whereas long peptides induce sustained CTL reactivity. *Journal of immunology* (Baltimore, Md. : 1950) 179, 5033–5040.
- Boutillier, A. J., Elsawa, S. F., Kzhyshkowska, J. and Supuran, C. T. (2021). Macrophage Polarization States in the Tumor Microenvironment. *International Journal of Molecular Sciences* 2021, Vol. 22, Page 6995 22, 6995.
- Braunwald, E. and Kloner, R. A. (1985). Myocardial Reperfusion: A Double-edged Sword? *The Journal of clinical investigation* 76, 1713–1719.
- Brownlie, D., Doughty-Shenton, D., Yh Soong, D., Nixon, C., O Carragher, N., M Carlin, L. and Kitamura, T. (2021). Metastasis-associated macrophages constrain antitumor capability of natural killer cells in the metastatic site at least partially by membrane bound transforming growth factor β . *Journal for ImmunoTherapy of Cancer* 9, e001740.
- Calde, P. C. (2020). Eicosanoids. *Essays in Biochemistry* 64, 423–441.
- Campbell, K., Rossi, F., Adams, J., Pitsidianaki, I., Barriga, F. M., Garcia-Gerique, L., Batlle, E., Casanova, J. and Casali, A. (2019). Collective cell migration and metastases induced by an epithelial-to-mesenchymal transition in *Drosophila* intestinal tumors. *Nature Communications* 10, 2311.
- Cao, Z., Bao, M., Miele, L., Sarkar, F. H., Wang, Z. and Zhou, Q. (2013). Tumour vasculogenic mimicry is associated with poor prognosis of human cancer patients: a systemic review and meta-analysis. *European journal of cancer* 49, 3914–3923.

- Casbon, A. J., Reynau, D., Park, C., Khu, E., Gan, D. D., Schepers, K., Passegué, E. and Werb, Z. (2015). Invasive breast cancer reprograms early myeloid differentiation in the bone marrow to generate immunosuppressive neutrophils. *Proceedings of the National Academy of Sciences of the United States of America* *112*, E566–E575.
- Cassetta, L. and Kitamura, T. (2018). Macrophage targeting: opening new possibilities for cancer immunotherapy. *Immunology* *155*, 285–293.
- Chen, D., Lemons, P. P., Schraw, T. and Whiteheart, S. W. (2000). Molecular mechanisms of platelet exocytosis: role of SNAP-23 and syntaxin 2 and 4 in lysosome release. *Blood* *96*, 1782–1788.
- Chen, X., Feng, J., Chen, W., Shao, S., Chen, L. and Wan, H. (2022). Small extracellular vesicles: from promoting pre-metastatic niche formation to therapeutic strategies in breast cancer. *Cell Communication and Signaling* *20*, 141.
- Cheo, D. L., Titus, S. A., Byrd, D. R., Hartley, J. L., Temple, G. F. and Brasch, M. A. (2004). Concerted Assembly and Cloning of Multiple DNA Segments Using In Vitro Site-Specific Recombination: Functional Analysis of Multi-Segment Expression Clones. *Genome Research* *14*, 2111.
- Ciciliano, J. C., Sakurai, Y., Myers, D. R., Fay, M. E., Hechler, B., Meeks, S., Li, R., Dixon, J. B., Lyon, L. A., Gachet, C. and Lam, W. A. (2015). Resolving the multifaceted mechanisms of the ferric chloride thrombosis model using an interdisciplinary microfluidic approach. *Blood* *126*, 817–824.
- Claffey, K. P., Brown, L. F., Del Aguila, L. F., Tognazzi, K., Yeo, K. T., Manseau, E. J. and Dvorak, H. F. (1996). Expression of vascular permeability factor/vascular endothelial growth factor by melanoma cells increases tumor growth, angiogenesis, and experimental metastasis. *Cancer Research* *56*, 172–181.
- Coffelt, S. B., Kersten, K., Doornebal, C. W., Weiden, J., Vrijland, K., Hau, C. S., Verstegen, N. J., Ciampricotti, M., Hawinkels, L. J., Jonkers, J. and De Visser, K. E. (2015). IL-17-producing $\gamma\delta$

- T cells and neutrophils conspire to promote breast cancer metastasis. *Nature* 2015 522:7556 522, 345–348.
- Coman, D. R., de, L. R. and Mcc, U. M. (1951). Studies on the mechanisms of metastasis; the distribution of tumors in various organs in relation to the distribution of arterial emboli. *Cancer Res* 11, 648–51.
- Concordet, J. P. and Haeussler, M. (2018). CRISPOR: intuitive guide selection for CRISPR/Cas9 genome editing experiments and screens. *Nucleic Acids Research* 46, W242–W245.
- Cortes, J. E., Kantarjian, H., Shah, N. P., Bixby, D., Mauro, M. J., Flinn, I., O'Hare, T., Hu, S., Narasimhan, N. I., Rivera, V. M., Clackson, T., Turner, C. D., Haluska, F. G., Druker, B. J., Deininger, M. W. N. and Talpaz, M. (2012). Ponatinib in refractory Philadelphia chromosome-positive leukemias. *New England Journal of Medicine* 367, 2075 – 2088.
- Cuenca-Zamora, E. J., Ferrer-Marín, F., Rivera, J. and Teruel-Montoya, R. (2019). Tubulin in Platelets: When the Shape Matters. *International Journal of Molecular Sciences* 20.
- CURTIS, A. S. G. and SEEHAR, G. M. (1978). The control of cell division by tension or diffusion. *Nature* 274, 52–53.
- Dancey, J. T., Deubelbeiss, K. A. and Harker and Finch, L. A. (1976). Neutrophil kinetics in man. *The Journal of Clinical Investigation* 58, 705–715.
- Davie, E. W. and Ratnoff, O. D. (1964). Waterfall Sequence for Intrinsic Blood Clotting. *Science* 145, 1310–1312.
- Davison, J. M., Akitake, C. M., Goll, M. G., Rhee, J. M., Gosse, N., Baier, H., Halpern, M. E., Leach, S. D. and Parsons, M. J. (2007). Transactivation from Gal4-VP16 transgenic insertions for tissue-specific cell labeling and ablation in zebrafish. *Developmental Biology* 304, 811–824.
- De Oliveira, S., Rosowski, E. E. and Huttenlocher, A. (2016). Neutrophil migration in infection and wound repair: going forward in reverse. *Nature Reviews Immunology* 2016 16:6 16, 378–391.

- Dee, C. T., Nagaraju, R. T., Athanasiadis, E. I., Gray, C., Fernandez del Ama, L., Johnston, S. A., Secombes, C. J., Cvejic, A. and Hurlstone, A. F. L. (2016). CD4-Transgenic Zebrafish Reveal Tissue-Resident Th2- and Regulatory T Cell-like Populations and Diverse Mononuclear Phagocytes. *The Journal of Immunology* *197*, 3520–3530.
- Denkert, C., von Minckwitz, G., Darb-Esfahani, S., Lederer, B., Heppner, B. I., Weber, K. E., Budczies, J., Huober, J., Klauschen, F., Furlanetto, J. et al. (2018). Tumour-infiltrating lymphocytes and prognosis in different subtypes of breast cancer: a pooled analysis of 3771 patients treated with neoadjuvant therapy. *The lancet oncology* *19*, 40–50.
- Detrich, H. W., Kieran, M. W., Chan, F. Y., Barone, L. M., Yee, K., Rundstadler, J. A., Pratt, S., Ransom, D. and Zon, L. I. (1995). Intraembryonic hematopoietic cell migration during vertebrate development. *Proceedings of the National Academy of Sciences* *92*, 10713–10717.
- Diskin, B., Adam, S., Cassini, M. F., Sanchez, G., Liria, M., Aykut, B., Buttar, C., Li, E., Sundberg, B., Salas, R. D. et al. (2020). PD-L1 engagement on T cells promotes self-tolerance and suppression of neighboring macrophages and effector T cells in cancer. *Nature immunology* *21*, 442–454.
- Dooley, K. and Zon, L. I. (2000). Zebrafish: a model system for the study of human disease. *Current Opinion in Genetics & Development* *10*, 252–256.
- Downes, K., Zhao, X., Gleadall, N. S., McKinney, H., Kempster, C., Batista, J., Thomas, P. L., Cooper, M., Michael, J. V., Kreuzhuber, R., Wedderburn, K., Waller, K., Varney, B., Verdier, H., Kriek, N., Ashford, S. E., Stirrups, K. E., Dunster, J. L., McKenzie, S. E., Ouwehand, W. H., Gibbins, J. M., Yang, J., Astle, W. J. and Ma, P. (2022). G protein-coupled receptor kinase 5 regulates thrombin signaling in platelets via PAR-1. *Blood Advances* *6*, 2319–2330.
- Driessen, R. P., Sitters, G., Laurens, N., Moolenaar, G. F., Wuite, G. J., Goosen, N. and Dame, R. T. (2014). Effect of temperature on the intrinsic flexibility of DNA and its interaction with architectural proteins. *Biochemistry* *53*, 6430–6438.

- Du, J., Cao, J., Zhou, C., Pan, D., Geng, F. and Wang, Y. (2022). Insight into the mechanism of myosin-fibrin gelation induced by non-disulfide covalent cross-linking. *Food Research International* 156, 111168.
- Egan, K., Cooke, N. and Kenny, D. (2014). Living in shear: platelets protect cancer cells from shear induced damage. *Clinical & Experimental Metastasis* 31, 697–704.
- Eisinger, F., Patzelt, J. and Langer, H. F. (2018). The platelet response to tissue injury. *Frontiers in Medicine* 5, 317.
- Ellett, F., Pase, L., Hayman, J. W., Andrianopoulos, A. and Lieschke, G. J. (2011). mpeg1 promoter transgenes direct macrophage-lineage expression in zebrafish. *Blood* 117.
- Entenberg, D., Oktay, M. H., D'Alfonso, T., Ginter, P. S., Robinson, B. D., Xue, X., Rohan, T. E., Sparano, J. A., Jones, J. G. and Condeelis, J. S. (2020). Validation of an Automated Quantitative Digital Pathology Approach for Scoring TMEM: A Prognostic Biomarker for Metastasis. *Cancers (Basel)* 12.
- Evangelista, V., Manarini, S., Sideri, R., Rotondo, S., Martelli, N., Piccoli, A., Totani, L., Piccardoni, P., Vestweber, D., de Gaetano, G. and Cerletti, C. (1999). Platelet/Polymorphonuclear Leukocyte Interaction: P-Selectin Triggers Protein-Tyrosine Phosphorylation–Dependent CD11b/CD18 Adhesion: Role of PSGL-1 as a Signaling Molecule. *Blood* 93, 876–885.
- Ewing, J. (1928). Neoplastic Diseases: A Treatise on Tumours. *British Journal of Surgery* 16, 174–175.
- Fallatah, W., De, R., Burks, D., Azad, R. K. and Jagadeeswaran, P. (2022). Analysis of transcribed sequences from young and mature zebrafish thrombocytes. *PLOS ONE* 17, e0264776.
- Feng, Y. (2012). Live imaging of tumor initiation in zebrafish larvae reveals a trophic role for leukocyte-derived PGE. *Curr. Biol.* 22.
- Feng, Y. and Martin, P. (2015). Imaging innate immune responses at tumour initiation: new insights from fish and flies. *Nature Reviews Cancer* 15, 556–562.

- Feng, Y., Renshaw, S. and Martin, P. (2012). Live imaging of tumor initiation in zebrafish larvae reveals a trophic role for leukocyte-derived PGE₂. *Current Biology* 22, 1253–1259.
- Feng, Y., Santoriello, C., Mione, M., Hurlstone, A. and Martin, P. (2010). Live Imaging of Innate Immune Cell Sensing of Transformed Cells in Zebrafish Larvae: Parallels between Tumor Initiation and Wound Inflammation. *PLoS Biology* 8, e1000562.
- Fish, R. J., Di Sanza, C. and Neerman-Arbez, M. (2014). Targeted mutation of zebrafish fga models human congenital afibrinogenemia. *Blood* 123, 2278–2281.
- Folkman, J. (1971). Tumor angiogenesis: therapeutic implications. *New england journal of medicine* 285, 1182–1186.
- Follain, G., Osmani, N., Azevedo, A. S., Allio, G., Mercier, L., Karreman, M. A., Solecki, G., Garcia Leòn, M. J., Lefebvre, O., Fekonja, N., Hille, C., Chabannes, V., Dollé, G., Metivet, T., Hovsepian, F. D., Prudhomme, C., Pichot, A., Paul, N., Carapito, R., Bahram, S., Ruthensteiner, B., Kemmling, A., Siemonsen, S., Schneider, T., Fiehler, J., Glatzel, M., Winkler, F., Schwab, Y., Pantel, K., Harlepp, S. and Goetz, J. G. (2018). Hemodynamic Forces Tune the Arrest, Adhesion, and Extravasation of Circulating Tumor Cells. *Developmental Cell* 45, 33–52.
- Foster, S. D., Glover, S. R., Turner, A. N., Chatti, K. and Challa, A. K. (2019). A mixing heteroduplex mobility assay (mHMA) to genotype homozygous mutants with small indels generated by CRISPR-Cas9 nucleases. *MethodsX* 6, 1.
- Frese, K. K. and Tuveson, D. A. (2007). Maximizing mouse cancer models. *Nature Reviews Cancer* 7, 645–658.
- Fu, Y., Liu, S., Yin, S., Niu, W., Xiong, W., Tan, M., Li, G. and Zhou, M. (2017). The reverse Warburg effect is likely to be an Achilles' heel of cancer that can be exploited for cancer therapy. *Oncotarget* 8, 57813.
- Funes, S. C., Rios, M., Escobar-Vera, J. and Kalergis, A. M. (2018). Implications of macrophage polarization in autoimmunity. *Immunology* 154, 186–195.

- Gachet, C. and Hechler, B. (2020). Platelet Purinergic Receptors in Thrombosis and Inflammation. *Hamostaseologie* 40, 145–152.
- Gale, A. J. (2011). Current Understanding of Hemostasis. *Toxicologic pathology* 39, 273.
- Gasic, G. J. (1984). Role of plasma, platelets, and endothelial cells in tumor metastasis. *Cancer Metastasis Rev* 3, 99–114.
- Gil-Bernabé, A. M., Ferjančič, Š., Tlalka, M., Zhao, L., Allen, P. D., Im, J. H., Watson, K., Hill, S. A., Amirkhosravi, A., Francis, J. L., Pollard, J. W., Ruf, W., Muschel, R. J. and Gil-Bernabe, A. M. (2012). Recruitment of monocytes/macrophages by tissue factor-mediated coagulation is essential for metastatic cell survival and premetastatic niche establishment in mice. *Blood* 119, 3164–3175.
- Gordon, S. (2003). Alternative activation of macrophages. *Nature Reviews Immunology* 2003 3:1 3, 23–35.
- Gorelik, E., Bere, W. W. and Herberman, R. B. (1984). Role of NK cells in the antimetastatic effect of anticoagulant drugs. *Int J Cancer* 33, 87–94.
- Goto, S., Ikeda, Y., Saldívar, E. and Ruggeri, Z. M. (1998). Distinct mechanisms of platelet aggregation as a consequence of different shearing flow conditions. *The Journal of clinical investigation* 101, 479–486.
- Gotsch, U., Jäger, U., Dominis, M. and Vestweber, D. (1994). Expression of P-selectin on Endothelial Cells is Upregulated by LPS and TNF- α in Vivo. *Cell Adhesion and Communication* 2, 7–14.
- Gralnick, H. R., Williams, S. B. and Collier, B. S. (1985). Asialo von Willebrand factor interactions with platelets. Interdependence of glycoproteins Ib and IIb/IIIa for binding and aggregation. *Journal of Clinical Investigation* 75, 19.
- Granadeiro, L., Dirks, R. P., Ortiz-Delgado, J. B., Gavaia, P. J., Sarasquete, C., Laizé, V., Canela, M. L. and Fernández, I. (2019). Warfarin-exposed zebrafish embryos resembles human

- warfarin embryopathy in a dose and developmental-time dependent manner - From molecular mechanisms to environmental concerns. *Ecotoxicology and environmental safety* 181, 559–571.
- Grat, M., Krawczyk, M., Wronka, K. M., Stypułkowski, J., Lewandowski, Z., Wasilewicz, M., Krawczyk, P., Grat, K., Patkowski, W. and Zieniewicz, K. (2018). Ischemia-reperfusion injury and the risk of hepatocellular carcinoma recurrence after deceased donor liver transplantation. *Scientific Reports* 2018 8:1 8, 1–13.
- Gray, C., Loynes, C. A., Whyte, M. K., Crossman, D. C., Renshaw, S. A. and Chico, T. J. (2011). Simultaneous intravital imaging of macrophage and neutrophil behaviour during inflammation using a novel transgenic zebrafish. *Thrombosis and Haemostasis* 105, 811–819.
- Gregory, M., Hanumanthaiah, R. and Jagadeeswaran, P. (2002). Genetic Analysis of Hemostasis and Thrombosis Using Vascular Occlusion. *Blood Cells, Molecules, and Diseases* 29, 286–295.
- Grover, S. P. and Mackman, N. (2019). Intrinsic Pathway of Coagulation and Thrombosis. *Arteriosclerosis, Thrombosis, and Vascular Biology* 39, 331–338.
- Güç, E. and Pollard, J. W. (2021). Redefining macrophage and neutrophil biology in the metastatic cascade. *Immunity* 54, 885–902.
- Gudbrandsdottir, S., Hasselbalch, H. C. and Nielsen, C. H. (2013). Activated Platelets Enhance IL-10 Secretion and Reduce TNF- α Secretion by Monocytes. *The Journal of Immunology* 191, 4059–4067.
- Gurevich, D. B., Severn, C. E., Twomey, C., Greenhough, A., Cash, J., Toyne, A. M., Mellor, H. and Martin, P. (2018). Live imaging of wound angiogenesis reveals macrophage orchestrated vessel sprouting and regression. *The EMBO Journal* 37, e97786.
- Haaland, G. S., Falk, R. S., Straume, O. and Lorens, J. B. (2017). Association of Warfarin Use With Lower Overall Cancer Incidence Among Patients Older Than 50 Years. *JAMA Internal Medicine* 177, 1774.

- Hall, C., Flores, M., Storm, T., Crosier, K. and Crosier, P. (2007). The zebrafish lysozyme C promoter drives myeloid-specific expression in transgenic fish. *BMC Developmental Biology* 7, 42.
- Hanumanthaiah, R., Day, K. and Jagadeeswaran, P. (2002). Comprehensive analysis of blood coagulation pathways in teleostei: Evolution of coagulation factor genes and identification of Zebrafish factor VIIi. *Blood Cells, Molecules, and Diseases* 29, 57–68.
- Hanumanthaiah, R., Thankavel, B., Day, K., Gregory, M. and Jagadeeswaran, P. (2001). Developmental expression of vitamin K-dependent gamma-carboxylase activity in zebrafish embryos: effect of warfarin. *Blood cells, molecules & diseases* 27, 992–999.
- Heilmann, S., Ratnakumar, K., Langdon, E., Kansler, E., Kim, I., Campbell, N. R., Perry, E., McMahan, A., Kaufman, C., Rooijen, E. v., Lee, W., Iacobuzio-Donahue, C., Hynes, R., Zon, L., Xavier, J. and White, R. (2015). A quantitative system for studying metastasis using transparentzebrafish. *Cancer research* 75, 4272.
- Hejna, M., Raderer, M. and Zielinski, C. C. (1999). Inhibition of Metastases by Anticoagulants. *JNCI: Journal of the National Cancer Institute* 91, 22–36.
- Hendrix, M. J., Seftor, E. A., Meltzer, P. S., Gardner, L. M., Hess, A. R., Kirschmann, D. A., Schatteman, G. C. and Seftor, R. E. (2001). Expression and functional significance of VE-cadherin in aggressive human melanoma cells: role in vasculogenic mimicry. *Proceedings of the National Academy of Sciences* 98, 8018–8023.
- Hess, I. and Boehm, T. (2012). Intravital imaging of thymopoiesis reveals dynamic lympho-epithelial interactions. *Immunity* 36, 298–309.
- Hirayama, D., Iida, T. and Nakase, H. (2017). The Phagocytic Function of Macrophage-Enforcing Innate Immunity and Tissue Homeostasis. *International Journal of Molecular Sciences* 2018, Vol. 19, Page 92 19, 92.
- Hisada, Y. and Mackman, N. (2021). Tissue Factor and Extracellular Vesicles: Activation of Coagulation and Impact on Survival in Cancer. *Cancers* 13.

- Hortle, E., Johnson, K. E., Johansen, M. D., Nguyen, T., Shavit, J. A., Britton, W. J., Tobin, D. M. and Oehlers, S. H. (2019). Thrombocyte Inhibition Restores Protective Immunity to Mycobacterial Infection in Zebrafish. *Journal of Infectious Diseases* 220, 524–534.
- Hsieh, J. Y., Smith, T. D., Meli, V. S., Tran, T. N., Botvinick, E. L. and Liu, W. F. (2017). Differential regulation of macrophage inflammatory activation by fibrin and fibrinogen. *Acta Biomaterialia* 47, 14–24.
- Hu, H., Wu, J., Cao, C. and Ma, L. (2020). Exosomes derived from regulatory T cells ameliorate acute myocardial infarction by promoting macrophage M2 polarization. *IUBMB life* 72, 2409–2419.
- Hua, X., Wu, X., Xu, K., Zhan, P., Liu, H., Zhang, F., Lv, T. and Song, Y. (2022). Zebrafish patient-derived xenografts accurately and quickly reproduce treatment outcomes in non-small cell lung cancer patients. *Experimental biology and medicine (Maywood, N.J.)* 0, 15353702221142612.
- Isles, H. M., Loynes, C. A., Alasmari, S., Kon, F. C., Henry, K. M., Kadochnikova, A., Hales, J., Muir, C. F., Keightley, M. C., Kadirkamanathan, V., Hamilton, N., Lieschke, G. J., Renshaw, S. A. and Elks, P. M. (2021). Pioneer neutrophils release chromatin within in vivo swarms. *eLife* 10.
- Ivanovs, A., Rybtsov, S., Ng, E. S., Stanley, E. G., Elefanty, A. G. and Medvinsky, A. (2017). Human haematopoietic stem cell development: from the embryo to the dish. *Development* 144, 2323–2337.
- Iyer, N., Al Qaryoute, A., Kacham, M. and Jagadeeswaran, P. (2021). Identification of zebrafish ortholog for human coagulation factor IX and its age-dependent expression. *Journal of Thrombosis and Haemostasis* 19, 2137–2150.
- Jaberi, N., Soleimani, A., Pashirzad, M., Abdeahad, H., Mohammadi, F., Khoshakhlagh, M., Khazaei, M., Ferns, G. A., Avan, A. and Hassanian, S. M. (2019). Role of thrombin in the pathogenesis of atherosclerosis. *Journal of Cellular Biochemistry* 120, 4757–4765.

- Jagadeeswaran, P. and Sheehan, J. P. (1999). Analysis of blood coagulation in the zebrafish. *Blood Cells, Molecules, and Diseases* 25, 239–249.
- Jagadeeswaran, P., Sheehan, J. P., Craig, F. E. and Troyer, D. (1999). Identification and characterization of zebrafish thrombocytes. *British Journal of Haematology* 107, 731–738.
- Jia, X., Shen, G., Jia, J., Zhang, Y., Zhang, D., Li, W., Zhang, J., Huang, X. and Tian, J. (2022). Lineage Tracing and Molecular Real-Time Imaging of Cancer Stem Cells. *Biosensors* 12, 703.
- Jiang, Y., Rong, Y., Wu, R., Wen, Y. and Hu, L. (2020). A Zebrafish Thrombosis Model for Assessing Antiplatelet Drugs. *International Journal of Pharma Medicine and Biological Sciences* 9, 38–42.
- Kan, Y., Meng, L., Xie, L., Liu, L., Dong, W., Feng, J., Yan, Y., Zhao, C., Peng, G., Wang, D., Lu, M., Yang, C. and Niu, C. (2020). Temporal modulation of host aerobic glycolysis determines the outcome of *Mycobacterium marinum* infection. *Fish & Shellfish Immunology* 96, 78–85.
- Kanth Manne, B., Denorme, F., Middleton, E. A., Portier, I., Rowley, J. W., Stubben, C., Petrey, A. C., Tolley, N. D., Guo, L., Cody, M., Weyrich, A. S., Yost, C. C., Rondina, M. T. and Campbell, R. A. (2020). Platelet gene expression and function in patients with COVID-19. *Blood* 136, 1317–1329.
- Kaplan, R. N., Riba, R. D., Zacharoulis, S., Bramley, A. H., Vincent, L., Costa, C., MacDonald, D. D., Jin, D. K., Shido, K., Kerns, S. A., Zhu, Z., Hicklin, D., Wu, Y., Port, J. L., Altorki, N., Port, E. R., Ruggero, D., Shmelkov, S. V., Jensen, K. K., Rafii, S. and Lyden, D. (2005). VEGFR1-positive haematopoietic bone marrow progenitors initiate the pre-metastatic niche. *Nature* 2005 438:7069 438, 820–827.
- Kasprowicz, R., Rand, E., O’Toole, P. J. and Signoret, N. (2018). A correlative and quantitative imaging approach enabling characterization of primary cell-cell communication: Case of human CD4+ T cell-macrophage immunological synapses. *Scientific Reports* 2018 8:1 8, 1–17.

- Kennedy, M., D'Souza, S. L., Lynch-Kattman, M., Schwantz, S. and Keller, G. (2007). Development of the hemangioblast defines the onset of hematopoiesis in human ES cell differentiation cultures. *Blood* *109*, 2679–2687.
- Khorana, A. A., Ahrendt, S. A., Ryan, C. K., Francis, C. W., Hruban, R. H., Ying, C. H., Hostetter, G., Harvey, J. and Taubman, M. B. (2007). Tissue factor expression, angiogenesis, and thrombosis in pancreatic cancer. *Clinical cancer research : an official journal of the American Association for Cancer Research* *13*, 2870–2875.
- Kim, H., Chung, H., Kim, J., Choi, D.-h. D.-H., Shin, Y., Guk Kang, Y., Kim, B.-m. B.-M., Seo, S.-U., Chung, S., Hyeok Seok, S., Kim, H., Kim, J., Choi, D.-h. D.-H., Chung, S., Chung, H., Seok, S. H., Shin, Y., Kang, Y. G. and Kim, B.-m. B.-M. (2019a). Macrophages-Triggered Sequential Remodeling of Endothelium-Interstitial Matrix to Form Pre-Metastatic Niche in Microfluidic Tumor Microenvironment. *Advanced Science* *6*, 1900195.
- Kim, H., Young Wang, S., Kwak, G., Yang, Y., Chan Kwon, I., Hwa Kim, S., Kim, H., Wang, S. Y., Kwak, G., Kwon, I. C., Yang, Y. and Kim, S. H. (2019b). Exosome-Guided Phenotypic Switch of M1 to M2 Macrophages for Cutaneous Wound Healing. *Advanced Science* *6*, 1900513.
- Kim, S. Y. and Nair, M. G. (2019). Macrophages in wound healing: activation and plasticity. *Immunology and Cell Biology* *97*, 258–267.
- Kim, Y. J., Borsig, L., Varki, N. M. and Varki, A. (1998). P-selectin deficiency attenuates tumor growth and metastasis. *Proceedings of the National Academy of Sciences* *95*, 9325–9330.
- King, R. C., Binns, O. A., Rodriguez, F., Kanithanon, R. C., Daniel, T. M., Spotnitz, W. D., Tribble, C. G. and Kron, I. L. (2000). Reperfusion injury significantly impacts clinical outcome after pulmonary transplantation. *The Annals of Thoracic Surgery* *69*, 1681–1685.
- Kissa, K., Murayama, E., Zapata, A., Cortés, A., Perret, E., Machu, C. and Herbomel, P. (2008). Live imaging of emerging hematopoietic stem cells and early thymus colonization. *Blood* *111*, 1147–1156.

- Koch, M. K., Jaeschke, A., Murekatete, B., Ravichandran, A., Tsurkan, M., Werner, C., Soon, P., Hutmacher, D. W., Haupt, L. M. and Bray, L. J. (2020). Stromal fibroblasts regulate microvascular-like network architecture in a bioengineered breast tumour angiogenesis model. *Acta Biomaterialia* 114, 256–269.
- Kondo, M., Weissman, I. L. and Akashi, K. (1997). Identification of Clonogenic Common Lymphoid Progenitors in Mouse Bone Marrow. *Cell* 91, 661–672.
- Kral, J. B., Schrottmaier, W. C., Salzmann, M. and Assinger, A. (2016). Platelet Interaction with Innate Immune Cells.
- Kuczek, D. E., Larsen, A. M. H., Thorseth, M.-L., Carretta, M., Kalvisa, A., Siersbæk, M. S., Simões, A. M. C., Roslind, A., Engelholm, L. H., Noessner, E. et al. (2019). Collagen density regulates the activity of tumor-infiltrating T cells. *Journal for immunotherapy of cancer* 7, 1–15.
- Kwan, K. M., Fujimoto, E., Grabher, C., Mangum, B. D., Hardy, M. E., Campbell, D. S., Parant, J. M., Yost, H. J., Kanki, J. P. and Chien, C. B. (2007). The Tol2kit: A multisite gateway-based construction Kit for Tol2 transposon transgenesis constructs. *Developmental Dynamics* 236, 3088–3099.
- Labelle, M., Begum, S. and Hynes, R. O. (2014). Platelets guide the formation of early metastatic niches. *Proceedings of the National Academy of Sciences of the United States of America* 111, E3053–E3061.
- Laklai, H., Miroshnikova, Y. A., Pickup, M. W., Collisson, E. A., Kim, G. E., Barrett, A. S., Hill, R. C., Lakins, J. N., Schlaepfer, D. D., Mouw, J. K., LeBleu, V. S., Roy, N., Novitskiy, S. V., Johansen, J. S., Poli, V., Kalluri, R., Iacobuzio-Donahue, C. A., Wood, L. D., Hebrok, M., Hansen, K., Moses, H. L. and Weaver, V. M. (2016). Genotype tunes pancreatic ductal adenocarcinoma tissue tension to induce matricellular fibrosis and tumor progression. *Nature Medicine* 22, 497–505.
- Langenau, D. M., Ferrando, A. A., Traver, D., Kutok, J. L., Hezel, J. P. D., Kanki, J. P., Zon, L. I., Thomas Look, A. and Trede, N. S. (2004). In vivo tracking of T cell development, ablation, and

- engraftment in transgenic zebrafish. *Proceedings of the National Academy of Sciences of the United States of America* *101*, 7369–7374.
- Latifi, Y., Moccetti, F., Wu, M., Xie, A., Packwood, W., Qi, Y., Ozawa, K., Shentu, W., Brown, E., Shirai, T., McCarty, O. J., Ruggeri, Z., Moslehi, J., Chen, J., Druker, B. J., López, J. A. and Lindner, J. R. (2019). Thrombotic microangiopathy as a cause of cardiovascular toxicity from the BCR-ABL1 tyrosine kinase inhibitor ponatinib. *Blood* *133*, 1597–1606.
- Lawson, K. A., Sousa, C. M., Zhang, X., Kim, E., Akthar, R., Caumanns, J. J., Yao, Y., Mikolajewicz, N., Ross, C., Brown, K. R. et al. (2020). Functional genomic landscape of cancer-intrinsic evasion of killing by T cells. *Nature* *586*, 120–126.
- Lawson, N. D. and Weinstein, B. M. (2002). In vivo imaging of embryonic vascular development using transgenic zebrafish. *Developmental Biology* *248*, 307–318.
- Lechertier, T., Reynolds, L. E., Kim, H., Pedrosa, A. R., Gómez-Escudero, J., Muñoz-Félix, J. M., Batista, S., Dukinfield, M., Demircioglu, F., Wong, P. P. et al. (2020). Pericyte FAK negatively regulates Gas6/Axl signalling to suppress tumour angiogenesis and tumour growth. *Nature communications* *11*, 1–14.
- Lévesque, M., Feng, Y., Jones, R. A. and Martin, P. (2013). Inflammation drives wound hyperpigmentation in zebrafish by recruiting pigment cells to sites of tissue damage. *DMM Disease Models and Mechanisms* *6*, 508–515.
- Li, J., Du, J., Wang, Y. and Jia, H. (2021). A Coagulation-Related Gene-Based Prognostic Model for Invasive Ductal Carcinoma. *Front Genet* *12*, 722992.
- Li, T., Kang, G., Wang, T. and Huang, H. (2018). Tumor angiogenesis and anti-angiogenic gene therapy for cancer. *Oncology letters* *16*, 687–702.
- Li, W., Guo, R., Song, Y. and Jiang, Z. (2021). Erythroblastic Island Macrophages Shape Normal Erythropoiesis and Drive Associated Disorders in Erythroid Hematopoietic Diseases.
- Lieschke, G. J., Oates, A. C., Paw, B. H., Thompson, M. A., Hall, N. E., Ward, A. C., Ho, R. K., Zon, L. I. and Layton, J. E. (2002). Zebrafish SPI-1 (PU.1) Marks a Site of Myeloid Development

- Independent of Primitive Erythropoiesis: Implications for Axial Patterning. *Developmental Biology* 246, 274–295.
- Liew, P. X. and Kubes, P. (2019). The Neutrophil's role during health and disease. *Physiological Reviews* 99, 1223–1248.
- Lim, C., Broqueres-You, D., Brouland, J. P., Merkulova-Rainon, T., Faussat, A. M., Hilal, R., Rouquie, D., Eveno, C., Audollent, R., Levy, B. I. and Pocard, M. (2013). Hepatic ischemia-reperfusion increases circulating bone marrow-derived progenitor cells and tumor growth in a mouse model of colorectal liver metastases. *Journal of Surgical Research* 184, 888–897.
- Lin, E. Y., Li, J. f., Bricard, G., Wang, W., Deng, Y., Sellers, R., Porcelli, S. A. and Pollard, J. W. (2007). Vascular endothelial growth factor restores delayed tumor progression in tumors depleted of macrophages. *Molecular Oncology* 1, 288–302.
- Lin, E. Y., Nguyen, A. V., Russell, R. G. and Pollard, J. W. (2001). Colony-Stimulating Factor 1 Promotes Progression of Mammary Tumors to Malignancy. *Journal of Experimental Medicine* 193, 727–740.
- Lin, H. F., Traver, D., Zhu, H., Dooley, K., Paw, B. H., Zon, L. I. and Handin, R. I. (2005). Analysis of thrombocyte development in CD41-GFP transgenic zebrafish. *Blood* 106, 3803–3810.
- Lin, Q., Zhang, Y., Zhou, R., Zheng, Y., Zhao, L., Huang, M., Zhang, X., Leung, A. Y. and Zhang, W. (2017). Establishment of a congenital amegakaryocytic thrombocytopenia model and a thrombocyte-specific reporter line in zebrafish. *Leukemia* 31, 1206–1216.
- Linke, B., Schreiber, Y., Picard-Willems, B., Slattery, P., Nüsing, R. M., Harder, S., Geisslinger, G. and Scholich, K. (2017). Activated Platelets Induce an Anti-Inflammatory Response of Monocytes/Macrophages through Cross-Regulation of PGE2 and Cytokines. *Mediators of Inflammation* 2017.
- Linnemann, C., Van Buuren, M. M., Bies, L., Verdegaal, E. M., Schotte, R., Calis, J. J., Behjati, S., Velds, A., Hilkmann, H., Atmioui, D. E., Visser, M., Stratton, M. R., Haanen, J. B., Spits, H., Van Der Burg, S. H. and Schumacher, T. N. (2015). High-throughput epitope discovery reveals

- frequent recognition of neo-antigens by CD4+ T cells in human melanoma. *Nature Medicine* *21*, 81–85.
- Liongue, C., Hall, C. J., O'Connell, B. A., Crosier, P. and Ward, A. C. (2009). Zebrafish granulocyte colony-stimulating factor receptor signaling promotes myelopoiesis and myeloid cell migration. *Blood* *113*, 2535–2546.
- Liu, Y., Kretz, C. A., Maeder, M. L., Richter, C. E., Tsao, P., Vo, A. H., Huarng, M. C., Rode, T., Hu, Z., Mehra, R., Olson, S. T., Joung, J. K. and Shavit, J. A. (2014). Targeted mutagenesis of zebrafish antithrombin III triggers disseminated intravascular coagulation and thrombosis, revealing insight into function. *Blood* *124*, 142–150.
- Loeffler, D. and Schroeder, T. (2021). Symmetric and asymmetric activation of hematopoietic stem cells. *Current Opinion in Hematology* *28*, 262–268.
- López-Cuevas, P. (2022). Reprogramming the host inflammatory response to wound healing and cancer through infection and protocell treatment – a study in zebrafish. PhD thesis, School of Biochemistry, University of Bristol, UK.
- López-Cuevas, P., Cross, S. J. and Martin, P. (2021). Modulating the Inflammatory Response to Wounds and Cancer Through Infection. *Frontiers in Cell and Developmental Biology* *9*.
- López-Cuevas, P., Xu, C., Severn, C. E., Oates, T. C., Cross, S. J., Toyne, A. M., Mann, S. and Martin, P. (2022). Macrophage Reprogramming with Anti-miR223-Loaded Artificial Protocells Enhances In Vivo Cancer Therapeutic Potential. *Advanced Science* *n/a*, 2202717.
- Loynes, C. A., Lee, J. A., Robertson, A. L., Steel, M. J., Ellett, F., Feng, Y., Levy, B. D., Whyte, M. K. and Renshaw, S. A. (2018). PGE2 production at sites of tissue injury promotes an anti-inflammatory neutrophil phenotype and determines the outcome of inflammation resolution in vivo. *Science Advances* *4*.
- Lu, H., Clauser, K. R., Tam, W. L., Fröse, J., Ye, X., Eaton, E. N., Reinhardt, F., Donnenberg, V. S., Bhargava, R., Carr, S. A. and Weinberg, R. A. (2014). A breast cancer stem cell niche supported by juxtacrine signalling from monocytes and macrophages. *Nature Cell Biology* *16*, 1105–1117.

- Lucotti, S., Cerutti, C., Soyer, M., Gil-Bernabé, A. M., Gomes, A. L., Allen, P. D., Smart, S., Markelc, B., Watson, K., Armstrong, P. C., Mitchell, J. A., Warner, T. D., Ridley, A. J. and Muschel, R. J. (2019). Aspirin blocks formation of metastatic intravascular niches by inhibiting platelet-derived COX-1/thromboxane A2. *The Journal of Clinical Investigation* *129*, 1845–1862.
- Ma, D., Zhang, J., Lin, H. F., Italiano, J. and Handin, R. I. (2011). The identification and characterization of zebrafish hematopoietic stem cells. *Blood* *118*, 289.
- MacCarthy-Morrogh, L. and Martin, P. (2020). The hallmarks of cancer are also the hallmarks of wound healing. *Science Signaling* *13*, 8690.
- Macfarlane, R. G. (1964). An enzyme cascade in the blood clotting mechanism, and its function as a biochemical amplifier [23]. *Nature* *202*, 498–499.
- Mackman, N., Tilley, R. E. and Key, N. S. (2007). Role of the Extrinsic Pathway of Blood Coagulation in Hemostasis and Thrombosis. *Arteriosclerosis, Thrombosis, and Vascular Biology* *27*, 1687–1693.
- Maeda, S., Murakami, K., Inoue, A., Yonezawa, T. and Matsuki, N. (2019). CCR4 Blockade Depletes Regulatory T Cells and Prolongs Survival in a Canine Model of Bladder Cancer Anti-Treg Immunotherapy for Canine Bladder Cancer. *Cancer immunology research* *7*, 1175–1187.
- Maniotis, A. J., Folberg, R., Hess, A., Seftor, E. A., Gardner, L. M., Pe'er, J., Trent, J. M., Meltzer, P. S. and Hendrix, M. J. (1999). Vascular channel formation by human melanoma cells in vivo and in vitro: vasculogenic mimicry. *The American journal of pathology* *155*, 739–752.
- Maroko, P. R., Libby, P., Ginks, W. R., Bloor, C. M., Shell, W. E., Sobel, B. E. and Ross, J. (1972). Coronary artery reperfusion. I. Early effects on local myocardial function and the extent of myocardial necrosis. *The Journal of clinical investigation* *51*, 2710–2716.
- Maruno, T., Fukuda, A., Goto, N., Tsuda, M., Ikuta, K., Hiramatsu, Y., Ogawa, S., Nakanishi, Y., Yamaga, Y., Yoshioka, T. et al. (2021). Visualization of stem cell activity in pancreatic cancer expansion by direct lineage tracing with live imaging. *Elife* *10*, e55117.

- Marwick, J. A., Mills, R., Kay, O., Michail, K., Stephen, J., Rossi, A. G., Dransfield, I. and Hirani, N. (2018). Neutrophils induce macrophage anti-inflammatory reprogramming by suppressing NF- κ B activation. *Cell Death and Disease* 9, 1–13.
- Mathias, J. R., Perrin, B. J., Liu, T.-X., Kanki, J., Look, A. T. and Huttenlocher, A. (2006). Resolution of inflammation by retrograde chemotaxis of neutrophils in transgenic zebrafish. *Journal of Leukocyte Biology* 80, 1281–1288.
- Matsushita, H., Vesely, M. D., Koboldt, D. C., Rickert, C. G., Uppaluri, R., Magrini, V. J., Arthur, C. D., White, J. M., Chen, Y. S., Shea, L. K., Hundal, J., Wendl, M. C., Demeter, R., Wylie, T., Allison, J. P., Smyth, M. J., Old, L. J., Mardis, E. R. and Schreiber, R. D. (2012). Cancer exome analysis reveals a T-cell-dependent mechanism of cancer immunoediting. *Nature* 482, 400–404.
- Maugeri, N., Campana, L., Gavina, M., Covino, C., De Metrio, M., Panciroli, C., Maiuri, L., Maseri, A., D'Angelo, A., Bianchi, M. E., Rovere-Querini, P. and Manfredi, A. A. (2014). Activated platelets present high mobility group box 1 to neutrophils, inducing autophagy and promoting the extrusion of neutrophil extracellular traps. *Journal of Thrombosis and Haemostasis* 12, 2074–2088.
- Mauracher, L. M., Posch, F., Martinod, K., Grilz, E., Däullary, T., Hell, L., Brostjan, C., Zielinski, C., Ay, C., Wagner, D. D., Pabinger, I. and Thaler, J. (2018). Citrullinated histone H3, a biomarker of neutrophil extracellular trap formation, predicts the risk of venous thromboembolism in cancer patients. *Journal of thrombosis and haemostasis : JTH* 16, 508–518.
- Mayya, V., Judokusumo, E., Abu-Shah, E., Neiswanger, W., Sachar, C., Depoil, D., Kam, L. C. and Dustin, M. L. (2019). Cutting edge: synapse propensity of human memory CD8 T cells confers competitive advantage over naive counterparts. *The Journal of Immunology* 203, 601–606.
- McEver, R. P. (2015). Selectins: initiators of leucocyte adhesion and signalling at the vascular wall. *Cardiovascular Research* 107, 331–339.

- McManama, G., Lindon, J. N., Kloczewiak, M., Smith, M. A., Ware, J. A., Hawiger, J., Merrill, E. W. and Salzman, E. W. (1986). Platelet Aggregation by Fibrinogen Polymers Crosslinked Across the E Domain. *Blood* 68, 363–371.
- Mei, Z., Liu, Y., Liu, C., Cui, A., Liang, Z., Wang, G., Peng, H., Cui, L. and Li, C. (2014). Tumour-infiltrating inflammation and prognosis in colorectal cancer: systematic review and meta-analysis. *British journal of cancer* 110, 1595–1605.
- Merritt, C., Gallo, C. M., Rasoloson, D. and Seydoux, G. (2010). Transgenic solutions for the germline. In *WormBook* chapter 7. <https://www.oncotarget.com/article/24110/>.
- Metharom, P., Falasca, M. and Berndt, M. C. (2019). The History of Armand Trousseau and Cancer-Associated Thrombosis. *Cancers (Basel)* 11.
- Migliaccio, G., Migliaccio, A. R., Petti, S., Mavilio, F., Russo, G., Lazzaro, D., Testa, U., Marinucci, M. and Peschle, C. (1986). Human embryonic hemopoiesis. Kinetics of progenitors and precursors underlying the yolk sac—liver transition. *The Journal of Clinical Investigation* 78, 51–60.
- Mitchell, J. A., Shala, F., Elghazouli, Y., Warner, T. D., Gaston-Massuet, C., Crescente, M., Armstrong, P. C., Herschman, H. R. and Kirkby, N. S. (2019). Cell-specific gene deletion reveals the antithrombotic function of COX1 and explains the vascular COX1/prostacyclin paradox. *Circulation Research* 125, 847–854.
- Morris, J. L., Cross, S. J., Lu, Y., Kadler, K. E., Lu, Y., Dallas, S. L. and Martin, P. (2018). Live imaging of collagen deposition during skin development and repair in a collagen I – GFP fusion transgenic zebrafish line. *Developmental biology* 441, 4–11.
- Morrissey, S. M., Zhang, F., Ding, C., Montoya-Durango, D. E., Hu, X., Yang, C., Wang, Z., Yuan, F., Fox, M., Zhang, H. g., Guo, H., Tieri, D., Kong, M., Watson, C. T., Mitchell, R. A., Zhang, X., McMasters, K. M., Huang, J. and Yan, J. (2021). Tumor-derived exosomes drive immunosuppressive macrophages in a pre-metastatic niche through glycolytic dominant metabolic reprogramming. *Cell Metabolism* 33, 2040–2058.

- Murayama, E., Kissa, K., Zapata, A., Mordelet, E., Briolat, V., Lin, H. F., Handin, R. I. and Herbomel, P. (2006). Tracing Hematopoietic Precursor Migration to Successive Hematopoietic Organs during Zebrafish Development. *Immunity* 25, 963–975.
- Muruganandah, V., Sathkumara, H. D., Navarro, S. and Kupz, A. (2018). A systematic review: The role of resident memory T cells in infectious diseases and their relevance for vaccine development. *Frontiers in Immunology* 9, 1574.
- Mutua, V. and Gershwin, L. J. (2020). A Review of Neutrophil Extracellular Traps (NETs) in Disease: Potential Anti-NETs Therapeutics. *Clinical Reviews in Allergy & Immunology* 2020 61:2 61, 194–211.
- Neubauer, K. and Zieger, B. (2022). Endothelial cells and coagulation. *Cell and Tissue Research* 387, 391–398.
- Nguyen-Chi, M., Laplace-Builhe, B., Travnickova, J., Luz-Crawford, P., Tejedor, G., Phan, Q. T., Duroux-Richard, I., Levraud, J. P., Kissa, K., Lutfalla, G., Jorgensen, C. and Djouad, F. (2015). Identification of polarized macrophage subsets in zebrafish. *eLife* 4.
- Nieto, M. A., Huang, R. Y. Y., Jackson, R. A. A. and Thiery, J. P. P. (2016). Emt: 2016. *Cell* 166, 21–45.
- O'Donnell, J. S., O'Sullivan, J. M. and Preston, R. J. (2019). Advances in understanding the molecular mechanisms that maintain normal haemostasis. *British Journal of Haematology* 186, 24–36.
- Olive, K. P., Jacobetz, M. A., Davidson, C. J., Gopinathan, A., McIntyre, D., Honess, D., Madhu, B., Goldgraben, M. A., Caldwell, M. E., Allard, D., Frese, K. K., DeNicola, G., Feig, C., Combs, C., Winter, S. P., Ireland-Zecchini, H., Reichelt, S., Howat, W. J., Chang, A., Dhara, M., Wang, L., Rückert, F., Grützmann, R., Pilarsky, C., Izeradjene, K., Hingorani, S. R., Huang, P., Davies, S. E., Plunkett, W., Egorin, M., Hruban, R. H., Whitebread, N., McGovern, K., Adams, J., Iacobuzio-Donahue, C., Griffiths, J. and Tuveson, D. A. (2009). Inhibition of Hedgehog signaling enhances delivery of chemotherapy in a mouse model of pancreatic cancer. *Science* 324, 1457–1461.

- Ott, P. A., Hodi, F. S. and Robert, C. (2013). CTLA-4 and PD-1/PD-L1 Blockade: New Immunotherapeutic Modalities with Durable Clinical Benefit in Melanoma Patients. *Clinical Cancer Research* *19*, 5300–5309.
- Page, M. J. and Pretorius, E. (2020). A Champion of Host Defense: A Generic Large-Scale Cause for Platelet Dysfunction and Depletion in Infection. *Seminars in Thrombosis and Hemostasis* *46*, 302–319.
- Paget, S. (1889). The Distribution Of Secondary Growths In Cancer Of The Breast. *The Lancet* *133*, 571–573.
- Papanicolaou, M., Parker, A. L., Yam, M., Filipe, E. C., Wu, S. Z., Chitty, J. L., Wyllie, K., Tran, E., Mok, E., Nadalini, A. et al. (2022). Temporal profiling of the breast tumour microenvironment reveals collagen XII as a driver of metastasis. *Nature communications* *13*, 1–21.
- Park, S. M., Do-Thi, V. A., Lee, J. O., Lee, H. and Kim, Y. S. (2020). Interleukin-9 Inhibits Lung Metastasis of Melanoma through Stimulating Anti-Tumor M1 Macrophages. *Mol Cells* *43*, 479–490.
- Patton, E. E., Widlund, H. R., Kutok, J. L., Kopani, K. R., Amatruda, J. F., Murphey, R. D., Berghmans, S., Mayhall, E. A., Traver, D., Fletcher, C. D., Aster, J. C., Granter, S. R., Look, A. T., Lee, C., Fisher, D. E. and Zon, L. I. (2005). BRAF Mutations Are Sufficient to Promote Nevi Formation and Cooperate with p53 in the Genesis of Melanoma. *Current Biology* *15*, 249–254.
- Patton, E. E., Zon, L. I. and Langenau, D. M. (2021). Zebrafish disease models in drug discovery: from preclinical modelling to clinical trials. *Nature Reviews Drug Discovery* *20*, 611–628.
- Pavoni, V., Gianesello, L., Pazzi, M., Stera, C., Meconi, T. and Frigieri, F. C. (2020). Evaluation of coagulation function by rotation thromboelastometry in critically ill patients with severe COVID-19 pneumonia. *Journal of Thrombosis and Thrombolysis* *50*, 281–286.

- Pellin, D., Loperfido, M., Baricordi, C., Wolock, S. L., Montepeloso, A., Weinberg, O. K., Biffi, A., Klein, A. M. and Biasco, L. (2019). A comprehensive single cell transcriptional landscape of human hematopoietic progenitors. *Nature Communications* 2019 10:1 10, 1–15.
- Peranzoni, E., Lemoine, J., Vimeux, L., Feuillet, V., Barrin, S., Kantari-Mimoun, C., Bercovici, N., Guérin, M., Biton, J., Ouakrim, H., Régnier, F., Lupo, A., Alifano, M., Damotte, D. and Donnadieu, E. (2018). Macrophages impede CD8 T cells from reaching tumor cells and limit the efficacy of anti-PD-1 treatment. *Proceedings of the National Academy of Sciences of the United States of America* 115, E4041–E4050.
- Perrella, G., Nagy, M., Watson, S. P. and Heemskerk, J. W. (2021). Platelet GPVI (Glycoprotein VI) and Thrombotic Complications in the Venous System. *Arteriosclerosis, Thrombosis, and Vascular Biology* 41, 2681–2692.
- Petrie, T. A., Strand, N. S., Yang, C.-T., Rabinowitz, J. S. and Moon, R. T. (2015). Macrophages modulate adult zebrafish tail fin regeneration. *Development* 142, 406–406.
- Philippeos, C., Telerman, S. B., Oulès, B., Pisco, A. O., Shaw, T. J., Elgueta, R., Lombardi, G., Driskell, R. R., Soldin, M., Lynch, M. D. et al. (2018). Spatial and single-cell transcriptional profiling identifies functionally distinct human dermal fibroblast subpopulations. *Journal of Investigative Dermatology* 138, 811–825.
- Pidwill, G. R., Gibson, J. F., Cole, J., Renshaw, S. A. and Foster, S. J. (2021). The Role of Macrophages in *Staphylococcus aureus* Infection. *Frontiers in Immunology* 11, 3506.
- Prasad, J. M., Gorkun, O. V., Raghu, H., Thornton, S., Mullins, E. S., Palumbo, J. S., Ko, Y. P., Höök, M., David, T., Coughlin, S. R., Degen, J. L. and Flick, M. J. (2015). Mice expressing a mutant form of fibrinogen that cannot support fibrin formation exhibit compromised antimicrobial host defense. *Blood* 126, 2047–2058.
- Prasad, V. and Mailankody, S. (2014). The Accelerated Approval of Oncologic Drugs: Lessons From Ponatinib. *JAMA* 311, 353–354.

- Proctor, J. W. (1976). Rat sarcoma model supports both "soil seed" and "mechanical" theories of metastatic spread. *Br J Cancer* 34, 651–4.
- Provenzano, P. P., Cuevas, C., Chang, A. E., Goel, V. K., Von Hoff, D. D. and Hingorani, S. R. (2012). Enzymatic targeting of the stroma ablates physical barriers to treatment of pancreatic ductal adenocarcinoma. *Cancer cell* 21, 418–429.
- Psaila, B. and Lyden, D. (2009). The metastatic niche: adapting the foreign soil. *Nature Reviews Cancer* 9, 285–293.
- Qian, B. Z., Li, J., Zhang, H., Kitamura, T., Zhang, J., Campion, L. R., Kaiser, E. A., Snyder, L. A. and Pollard, J. W. (2011). CCL2 recruits inflammatory monocytes to facilitate breast-tumour metastasis. *Nature* 475, 222–225.
- Raskov, H., Orhan, A., Christensen, J. P. and Gögenur, I. (2021). Cytotoxic CD8+ T cells in cancer and cancer immunotherapy. *British journal of cancer* 124, 359–367.
- Razak, N. B. A., Jones, G., Bhandari, M., Berndt, M. C. and Metharom, P. (2018). Cancer-associated thrombosis: An overview of mechanisms, risk factors, and treatment.
- Ren, Q., Barber, H. K., Crawford, G. L., Karim, Z. A., Zhao, C., Choi, W., Wang, C. C., Hong, W. and Whiteheart, S. W. (2007). Endobrevin/VAMP-8 is the primary v-SNARE for the platelet release reaction. *Molecular Biology of the Cell* 18, 24–33.
- Renshaw, S. A., Loynes, C. A., Trushell, D. M., Elworthy, S., Ingham, P. W. and Whyte, M. K. (2006). A transgenic zebrafish model of neutrophilic inflammation. *Blood* 108, 3976–3978.
- Reuden, C., Pinkert, M., Evans, E. and Liu, Y. (2020). pyimagej.
- Ribatti, D., Tamma, R. and Annese, T. (2020). Epithelial-Mesenchymal Transition in Cancer: A Historical Overview. *Translational Oncology* 13, 100773.
- Riva, L., Pandiri, A. R., Li, Y. R., Droop, A., Hewinson, J., Quail, M. A., Iyer, V., Shepherd, R., Herbert, R. A., Campbell, P. J., Sills, R. C., Alexandrov, L. B., Balmain, A. and Adams, D. J. (2020). The mutational signature profile of known and suspected human carcinogens in mice. *Nature Genetics* 52, 1189–1197.

- Robertson, A. L., Holmes, G. R., Bojarczuk, A. N., Burgon, J., Loynes, C. A., Chimen, M., Sawtell, A. K., Hamza, B., Willson, J., Walmsley, S. R., Anderson, S. R., Coles, M. C., Farrow, S. N., Solari, R., Jones, S., Prince, L. R., Irimia, D., Rainger, G. E., Kadirkamanathan, V., Whyte, M. K. B. and Renshaw, S. A. (2014). A Zebrafish Compound Screen Reveals Modulation of Neutrophil Reverse Migration as an Anti-Inflammatory Mechanism. *Science Translational Medicine* 6, 225ra29–225ra29.
- Rodriguez-Martinez, A., Simon-Saez, I., Perales, S., Garrido-Navas, C., Russo, A., de Miguel-Perez, D., Pucho-Sanz, I., Alaminos, C., Ceron, J., Lorente, J. A., Molina, M. P., Gonzalez, C., Cristofanilli, M., Ortigosa-Palomo, A., Real, P. J., Rolfo, C. and Serrano, M. J. (2022). Exchange of cellular components between platelets and tumor cells: impact on tumor cells behavior. *Theranostics* 12, 2150.
- Roh-Johnson, M., Shah, A. N., Stonick, J. A., Poudel, K. R., Kargl, J., Yang, G. H., di Martino, J., Hernandez, R. E., Gast, C. E., Zarour, L. R., Antoku, S., Houghton, A. M. G., Bravo-Cordero, J. J., Wong, M. H., Condeelis, J. and Moens, C. B. (2017). Macrophage-Dependent Cytoplasmic Transfer during Melanoma Invasion In Vivo. *Developmental Cell* 43, 549–562.
- Rost, M., Grzegorski, S. and Shavit, J. (2016). Quantitative methods for studying hemostasis in zebrafish larvae. *Methods in cell biology* 134, 377.
- Rowley, J. W., Oler, A. J., Tolley, N. D., Hunter, B. N., Low, E. N., Nix, D. A., Yost, C. C., Zimmerman, G. A. and Weyrich, A. S. (2011). Genome-wide RNA-seq analysis of human and mouse platelet transcriptomes. *Blood* 118, e101–e111.
- Sahai, E., Astsaturov, I., Cukierman, E., DeNardo, D. G., Egeblad, M., Evans, R. M., Fearon, D., Greten, F. R., Hingorani, S. R., Hunter, T., Hynes, R. O., Jain, R. K., Janowitz, T., Jorgensen, C., Kimmelman, A. C., Kolonin, M. G., Maki, R. G., Powers, R. S., Puré, E., Ramirez, D. C., Scherz-Shouval, R., Sherman, M. H., Stewart, S., Tlsty, T. D., Tuveson, D. A., Watt, F. M., Weaver, V., Weeraratna, A. T. and Werb, Z. (2020a). A framework for advancing our understanding of cancer-associated fibroblasts. *Nature Reviews Cancer* 20:3 20, 174–186.

- Sahai, E., Astsaturov, I., Cukierman, E., DeNardo, D. G., Egeblad, M., Evans, R. M., Fearon, D., Greten, F. R., Hingorani, S. R., Hunter, T. et al. (2020b). A framework for advancing our understanding of cancer-associated fibroblasts. *Nature Reviews Cancer* 20, 174–186.
- Sakaguchi, S., Mikami, N., Wing, J. B., Tanaka, A., Ichiyama, K. and Ohkura, N. (2020). Regulatory T cells and human disease. *Annual review of immunology* 38, 541–566.
- Sallam, M. A., Wyatt Shields IV, C., Prakash, S., Kim, J., Pan, D. C. and Mitragotri, S. (2021). A dual macrophage polarizer conjugate for synergistic melanoma therapy. *Journal of Controlled Release* 335, 333–344.
- Salvesen, H. B. and Akslen, L. A. (1999). Significance of tumour-associated macrophages, vascular endothelial growth factor and thrombospondin-1 expression for tumour angiogenesis and prognosis in endometrial carcinomas. *International journal of cancer* 84, 538–543.
- Savage, J. S., Williams, C. M., Konopatskaya, O., Hers, I., Harper, M. T. and Poole, A. W. (2013). Munc13-4 is critical for thrombosis through regulating release of ADP from platelets. *Journal of Thrombosis and Haemostasis* 11, 771–775.
- Schumacher, T. N., Scheper, W. and Kvistborg, P. (2019). Cancer neoantigens. *Annual review of immunology* 37, 173–200.
- Seifert, J., Rheinlaender, J., Lang, F., Gawaz, M. and Schäffer, T. E. (2017). Thrombin-induced cytoskeleton dynamics in spread human platelets observed with fast scanning ion conductance microscopy. *Scientific Reports* 2017 7:1 7, 1–11.
- Selvadurai, M. V. and Hamilton, J. R. (2018). Structure and function of the open canalicular system – the platelet’s specialized internal membrane network. <https://doi.org/10.1080/09537104.2018.1431388> 29, 319–325.
- Sharma, S. K., Chintala, N. K., Vadrevu, S. K., Patel, J., Karbowiczek, M. and Markiewski, M. M. (2015). Pulmonary Alveolar Macrophages Contribute to the Premetastatic Niche by Suppressing Antitumor T Cell Responses in the Lungs. *The Journal of Immunology* 194, 5529–5538.

- Sharma, V. P., Tang, B., Wang, Y., Duran, C. L., Karagiannis, G. S., Xue, E. A., Entenberg, D., Borriello, L., Coste, A., Eddy, R. J., Kim, G., Ye, X., Jones, J. G., Grunblatt, E., Agi, N., Roy, S., Bandyopadhyaya, G., Adler, E., Surve, C. R., Esposito, D., Goswami, S., Segall, J. E., Guo, W., Condeelis, J. S., Wakefield, L. M. and Oktay, M. H. (2021). Live tumor imaging shows macrophage induction and TMEM-mediated enrichment of cancer stem cells during metastatic dissemination. *Nature Communications* 12, 7300.
- Shaul, M. E. and Fridlender, Z. G. (2019). Tumour-associated neutrophils in patients with cancer. *Nature Reviews Clinical Oncology* 2019 16:10 16, 601–620.
- Shen, M. W., Arbab, M., Hsu, J. Y., Worstell, D., Culbertson, S. J., Krabbe, O., Cassa, C. A., Liu, D. R., Gifford, D. K. and Sherwood, R. I. (2018). Predictable and precise template-free CRISPR editing of pathogenic variants. *Nature* 2018 563:7733 563, 646–651.
- Shimizu, J., Yamazaki, S. and Sakaguchi, S. (1999). Induction of tumor immunity by removing CD25+ CD4+ T cells: a common basis between tumor immunity and autoimmunity. *The Journal of Immunology* 163, 5211–5218.
- Silvestri, V. L., Henriët, E., Linville, R. M., Wong, A. D., Searson, P. C. and Ewald, A. J. (2020). A tissue-engineered 3d microvessel model reveals the dynamics of mosaic vessel formation in breast cancer. *Cancer Research* 80, 4288–4301.
- Simões, F. C., Cahill, T. J., Kenyon, A., Gavriouchkina, D., Vieira, J. M., Sun, X., Pezzolla, D., Ravaut, C., Masmanian, E., Weinberger, M., Mayes, S., Lemieux, M. E., Barnette, D. N., Gunadasa-Rohling, M., Williams, R. M., Greaves, D. R., Trinh, L. A., Fraser, S. E., Dallas, S. L., Choudhury, R. P., Sauka-Spengler, T. and Riley, P. R. (2020). Macrophages directly contribute collagen to scar formation during zebrafish heart regeneration and mouse heart repair. *Nature Communications* 2020 11:1 11, 1–17.
- Sreeramkumar, V., Adrover, J. M., Ballesteros, I., Cuartero, M. I., Rossaint, J., Bilbao, I., Náchér, M., Pitaval, C., Radovanovic, I., Fukui, Y., McEver, R. P., Filippi, M. D., Lizasoain, I., Ruiz-Cabello, J., Zarbock, A., Moro, M. A. and Hidalgo, A. (2014). Neutrophils scan for activated platelets to initiate inflammation. *Science* 346, 1234–1238.

- Stott, S. L., Richard, L., Nagrath, S., Min, Y., Miyamoto, D. T., Ulkus, L., Inserra, E. J., Ulman, M., Springer, S., Nakamura, Z., Moore, A. L., Tsukrov, D., Kempner, M. E., Dahl, D. M., Chin-lee, W., Iafrate, J. A., Smith, M. R., Tompkins, R. G., Sequist, L. V., Toner, M., Haber, D. A. and Maheswaran, S. (2010). Isolation and characterization of circulating tumor cells from patients with localized and metastatic prostate cancer. *Science Translational Medicine* 2, 25ra23.
- Strilic, B. and Offermanns, S. (2017). Intravascular Survival and Extravasation of Tumor Cells. *Cancer cell* 32, 282–293.
- Sun, W., Wei, F. Q., Li, W. J., Wei, J. W., Zhong, H., Wen, Y. H., Lei, W. B., Chen, L., Li, H., Lin, H. Q., Iqbal, M. and Wen, W. P. (2017). A positive-feedback loop between tumour infiltrating activated Treg cells and type 2-skewed macrophages is essential for progression of laryngeal squamous cell carcinoma. *British Journal of Cancer* 2017 117:11 117, 1631–1643.
- Sun, Y., Myers, D. R., Nikolov, S. V., Oshinowo, O., Baek, J., Bowie, S. M., Lambert, T. P., Woods, E., Sakurai, Y., Lam, W. A. and Alexeev, A. (2021). Platelet heterogeneity enhances blood clot volumetric contraction: An example of asynchrono-mechanical amplification. *Biomaterials* 274, 120828.
- Sweeney, P. W., d'Esposito, A., Walker-Samuel, S. and Shipley, R. J. (2019). Modelling the transport of fluid through heterogeneous, whole tumours in silico. *PLOS Computational Biology* 15, e1006751.
- Taibi, A., Albouys, J., Jacques, J., Perrin, M. L., Yardin, C., Fontanier, S. D. and Bardet, S. M. (2019). Comparison of implantation sites for the development of peritoneal metastasis in a colorectal cancer mouse model using non-invasive bioluminescence imaging. *PLOS ONE* 14, e0220360.
- Tamura, R., Tanaka, T., Yamamoto, Y., Akasaki, Y. and Sasaki, H. (2018). Dual role of macrophage in tumor immunity. *Immunotherapy* 10, 899–909.
- Tanaka, R., Saito, Y., Fujiwara, Y., Jo, J. i. and Tabata, Y. (2019). Preparation of fibrin hydrogels to promote the recruitment of anti-inflammatory macrophages. *Acta Biomaterialia* 89, 152–165.

- Tang-Huau, T. ., Gueguen, P., Goudot, C., Durand, M., Bohec, M., Baulande, S., Pasquier, B., Amigorena, S. and Segura, E. (2018). Human in vivo-generated monocyte-derived dendritic cells and macrophages cross-present antigens through a vacuolar pathway. *Nature Communications* *9*.
- Tashiro, Y., Nishino, H., Higuchi, T., Sugisawa, N., Fukuda, Y., Yamamoto, J., Inubushi, S., Aoki, T., Murakami, M., Singh, S. R., Bouvet, M. and Hoffman, R. M. (2020). Ischemia reperfusion-induced metastasis is resistant to PPAR γ agonist pioglitazone in a murine model of colon cancer. *Scientific Reports* *10*, 1–5.
- Tavian, M., Robin, C., Coulombel, L. and Péault, B. (2001). The Human Embryo, but Not Its Yolk Sac, Generates Lympho-Myeloid Stem Cells: Mapping Multipotent Hematopoietic Cell Fate in Intraembryonic Mesoderm. *Immunity* *15*, 487–495.
- Thattaliyath, B., Cykowski, M. and Jagadeeswaran, P. (2005). Young thrombocytes initiate the formation of arterial thrombi in zebrafish. *Blood* *106*, 118–124.
- Thisse, B. and Thisse, C. (2004). Fast Release Clones: A High Throughput Expression Analysis.
- Tinevez, J.-Y., Perry, N., Schindelin, J., Hoopes, G. M., Reynolds, G. D., Laplantine, E., Bednarek, S. Y., Shorte, S. L. and Eliceiri, K. W. (2017). TrackMate: An open and extensible platform for single-particle tracking. *Methods* *115*, 80–90.
- Tokunaga, Y., Shirouzu, M., Sugahara, R., Yoshiura, Y., Kiryu, I., Ototake, M., Nagasawa, T., Somamoto, T. and Nakao, M. (2017). Comprehensive validation of T- and B-cell deficiency in rag1-null zebrafish: Implication for the robust innate defense mechanisms of teleosts. *Scientific Reports* *2017* 7:1 *7*, 1–10.
- Trinh, L. A., Chong-Morrison, V., Gavriouchkina, D., Hochgreb-Hägele, T., Senanayake, U., Fraser, S. E. and Sauka-Spengler, T. (2017). Biotagging of Specific Cell Populations in Zebrafish Reveals Gene Regulatory Logic Encoded in the Nuclear Transcriptome. *Cell Reports* *19*, 425–440.
- Trousseau, A. (1865). Phlegmasia alba dolens. *Clinique medicale de l'Hotel-Dieu de Paris*. *94*.

- Velten, L., Haas, S. F., Raffel, S., Blaszkiewicz, S., Islam, S., Hennig, B. P., Hirche, C., Lutz, C., Buss, E. C., Nowak, D., Boch, T., Hofmann, W. K., Ho, A. D., Huber, W., Trumpp, A., Essers, M. A. and Steinmetz, L. M. (2017). Human haematopoietic stem cell lineage commitment is a continuous process. *Nature Cell Biology* 2017 19:4 19, 271–281.
- Vo, A. H., Swaroop, A., Liu, Y., Norris, Z. G. and Shavit, J. A. (2013). Loss of Fibrinogen in Zebrafish Results in Symptoms Consistent with Human Hypofibrinogenemia. *PLOS ONE* 8, e74682.
- Voll, R. E., Herrmann, M., Roth, E. A., Stach, C., Kalden, J. R. and Girkontaite, I. (1997). Immunosuppressive effects of apoptotic cells. *Nature* 1997 390:6658 390, 350–351.
- Wang, D., Tan, C., Xiao, F., Zou, L., Wang, L., Wei, Y., Yang, H. and Zhang, W. (2017). The “inherent vice” in the anti-angiogenic theory may cause the highly metastatic cancer to spread more aggressively. *Scientific reports* 7, 1–14.
- Wang, H., Hu, W.-m., Xia, Z.-j., Liang, Y., Lu, Y., Lin, S.-x. and Tang, H. (2019). High numbers of CD163+ tumor-associated macrophages correlate with poor prognosis in multiple myeloma patients receiving bortezomib-based regimens. *Journal of Cancer* 10, 3239.
- Watanabe, Y., Tsukahara, T., Murata, K., Hamada, S., Kubo, T., Kanaseki, T., Hirohashi, Y., Emori, M., Teramoto, A., Nakatsugawa, M. et al. (2022). Development of CAR-T cells specifically targeting cancer stem cell antigen DNAJB8 against solid tumours. *British Journal of Cancer* 0, 1–10.
- Wculek, S. K. and Malanchi, I. (2015). Neutrophils support lung colonization of metastasis-initiating breast cancer cells. *Nature* 2015 528:7582 528, 413–417.
- Weavers, H. and Martin, P. (2020). The cell biology of inflammation: From common traits to remarkable immunological adaptations. *Journal of Cell Biology* 219.
- Weigt, S., Huebler, N., Strecker, R., Braunbeck, T. and Broschard, T. H. (2012). Developmental effects of coumarin and the anticoagulant coumarin derivative warfarin on zebrafish (*Danio rerio*) embryos. *Reproductive Toxicology* 33, 133–141.

- Weyrich, A. S., Elstad, M. R., McEver, R. P., McIntyre, T. M., Moore, K. L., Morrissey, J. H., Prescott, S. M. and Zimmerman, G. A. (1996). Activated platelets signal chemokine synthesis by human monocytes. *The Journal of Clinical Investigation* 97, 1525–1534.
- White, R. M., Sessa, A., Burke, C., Bowman, T., LeBlanc, J., Ceol, C., Bourque, C., Dovey, M., Goessling, W., Burns, C. E. and Zon, L. I. (2008). Transparent Adult Zebrafish as a Tool for In Vivo Transplantation Analysis. *Cancer Stem Cell* 2.
- Wienholds, E., Schulte-Merker, S., Walderich, B. and Plasterk, R. H. (2002). Target-selected inactivation of the zebrafish *rag1* gene. *Science* 297, 99–102.
- Williams, C. M., Li, Y., Brown, E. and Poole, A. W. (2018). Platelet-specific deletion of SNAP23 ablates granule secretion, substantially inhibiting arterial and venous thrombosis in mice. *Blood advances* 2, 3627–3636.
- Wojtukiewicz, M. Z., Rucinska, M., Zimnoch, L., Jaromin, J., Piotrowski, Z., Rózanska-Kudelska, M., Kisiel, W. and Kudryk, B. J. (2000). Expression of Prothrombin Fragment 1+2 in Cancer Tissue as an Indicator of Local Activation of Blood Coagulation. *Thrombosis Research* 97, 335–342.
- Xie, Y., Meijer, A. H. and Schaaf, M. J. (2020). Modeling Inflammation in Zebrafish for the Development of Anti-inflammatory Drugs. *Frontiers in Cell and Developmental Biology* 8, 620984.
- Xu, X., Zong, Y., Gao, Y., Sun, X., Zhao, H., Luo, W. and Jia, S. (2019). VEGF induce vasculogenic mimicry of choroidal melanoma through the PI3k signal pathway. *BioMed Research International* 2019.
- Yadav, S. S., Howell, D. N., Steeber, D. A., Harland, R. C., Tedder, T. F. and Clavien, P.-A. (1999). P-selectin mediates reperfusion injury through neutrophil and platelet sequestration in the warm ischemic mouse liver. *Hepatology* 29, 1494–1502.

- Yin, L., Maddison, L. A., Li, M., Kara, N., LaFave, M. C., Varshney, G. K., Burgess, S. M., Patton, J. G. and Chen, W. (2015). Multiplex Conditional Mutagenesis Using Transgenic Expression of Cas9 and sgRNAs. *Genetics* 200, 431–441.
- Yin, W., Li, Y., Song, Y., Zhang, J., Wu, C., Chen, Y., Miao, Y., Lin, C., Lin, Y., Yan, D., Chen, J. and He, R. (2021). CCRL2 promotes antitumor T-cell immunity via amplifying TLR4-mediated immunostimulatory macrophage activation. *Proceedings of the National Academy of Sciences* 118, e2024171118.
- Yun, S. H., Sim, E. H., Goh, R. Y., Park, J. I. and Han, J. Y. (2016). Platelet Activation: The Mechanisms and Potential Biomarkers. *BioMed Research International* 2016.
- Zander, R., Schauder, D., Xin, G., Nguyen, C., Wu, X., Zajac, A. and Cui, W. (2019). CD4+ T Cell Help Is Required for the Formation of a Cytolytic CD8+ T Cell Subset that Protects against Chronic Infection and Cancer. *Immunity* 51, 1028–1042.
- Zhang, J., Yin, C., Zhao, Q., Zhao, Z., Wang, J., Miron, R. J. and Zhang, Y. (2020). Anti-inflammation effects of injectable platelet-rich fibrin via macrophages and dendritic cells. *Journal of Biomedical Materials Research Part A* 108, 61–68.
- Zhang, R. L., Chopp, M., Chen, H. and Garcia, J. H. (1994). Temporal profile of ischemic tissue damage, neutrophil response, and vascular plugging following permanent and transient (2H) middle cerebral artery occlusion in the rat. *Journal of the Neurological Sciences* 125, 3–10.
- Zhao, H., Wu, L., Yan, G., Chen, Y., Zhou, M., Wu, Y. and Li, Y. (2021). Inflammation and tumor progression: signaling pathways and targeted intervention. *Signal Transduction and Targeted Therapy* 2021 6:1 6, 1–46.
- Zhou, J., Xu, Y., Wang, G., Mei, T., Yang, H. and Liu, Y. (2022). The TLR7/8 agonist R848 optimizes host and tumor immunity to improve therapeutic efficacy in murine lung cancer. *International Journal of Oncology* 61.
- Zhu, X. Y., Xia, B., Ye, T., Dai, M. Z., Yang, H., Li, C. Q. and Li, P. (2020). Ponatinib-induced ischemic stroke in larval zebrafish for drug screening. *European journal of pharmacology* 889.

- Zhu, Z., Khan, M. A., Weiler, M., Blaes, J., Jestaedt, L., Geibert, M., Zou, P., Gronych, J., Bernhardt, O., Korshunov, A. et al. (2014). Targeting self-renewal in high-grade brain tumors leads to loss of brain tumor stem cells and prolonged survival. *Cell stem cell* 15, 185–198.
- Zhuo, C., Zhang, J., Lee, J. H., Jiao, J., Cheng, D., Liu, L., Kim, H. W., Tao, Y. and Li, M. (2021). Spatiotemporal control of CRISPR/Cas9 gene editing. *Signal Transduction and Targeted Therapy* 2021 6:1 6, 1–18.
- Ziegler, C. G., Van Sloun, R., Gonzalez, S., Whitney, K. E., DePhillipo, N. N., Kennedy, M. I., Dornan, G. J., Evans, T. A., Huard, J. and LaPrade, R. F. (2019). Characterization of Growth Factors, Cytokines, and Chemokines in Bone Marrow Concentrate and Platelet-Rich Plasma: A Prospective Analysis. *American Journal of Sports Medicine* 47, 2174–2187.